Technical Report Documentation Page

1. Report No.	2. Government Accession No.	3. Recipient's Catalog No.
SWUTC/98/467312-1		

4. Title and Subtitle	5. Report Date
Fuel Consumption Estimation and Optimal Traffic Signal Timing	August 1998
	6. Performing Organization Code

7. Author(s)	8. Performing Organization Report No.
Tsai-Yun Liao and Randy B. Machemehl	Research Report 467312-1

9. Performing Organization Name and Address	10. Work Unit No. (TRAIS)
Center for Transportation Research University of Texas at Austin 3208 Red River, Suite 200 Austin, Texas 78705-2650	11. Contract or Grant No. 10727

12. Sponsoring Agency Name and Address	13. Type of Report and Period Covered
Southwest Region University Transportation Center Texas Transportation Institute The Texas A&M University System College Station, Texas 77843-3135	14. Sponsoring Agency Code

15. Supplementary Notes

Supported by general revenues from the State of Texas.

16. Abstract

Growing concern about environmental protection and energy conservation has led the Clean Air Act Amendments and a number of studies to increase fuel economy and reduce emissions. Since most of the United States fuel consumption is by the transportation sector and fuel consumed by vehicles is about 75% of all transportation energy used, developing ways to reduce vehicle fuel consumption in traffic systems has become an important task. Furthermore, high gasoline consumption worsens air quality in urban areas by emission of carbon monoxide (CO) and carbon dioxide (CO2), which makes these areas, especially in the vicinity of intersections, potentially dangerous to human health.

The objectives of this report are to develop an analytical model to estimate fuel consumption and to investigate the effects of signal timing on fuel consumption. Several numerical experiments, including a variety of geometric configurations, traffic conditions, and signal timing are conducted to test the AFCM estimation capability and to investigate the effects of signal timing on fuel consumption. The results from these experiments indicate that total fuel consumption, with respect to signal cycle time, possesses a convex pattern.

In order to analytically establish the relationship between fuel consumption and signal timing, a three-term form is reduced from the AFCM to represent major effects of vehicle characteristics, traffic behavior, and fuel consumption parameters on optimal cycle length. The first term represents vehicle idle fuel consumption, the second term describes vehicle fuel consumption during acceleration after a stop, and the third term accounts for stochastic effects. Numerical analysis and comparisons show that the optimal cycle lengths from the expression are rather close to those from the AFCM.

17. Key Words	18. Distribution Statement
Fuel Consumption Model, Signalized Intersections, Vehicle Speed, Signal Timing, Optimal Cycle Lengths, Acceleration, Deceleration	No Restrictions. This document is available to the public through NTIS: National Technical Information Service 5285 Port Royal Road Springfield, Virginia 22161

19. Security Classif.(of this report)	20. Security Classif.(of this page)	21. No. of Pages	22. Price
Unclassified	Unclassified	179	

Form DOT F 1700.7 (8-72) Reproduction of completed page authorized

FUEL CONSUMPTION ESTIMATION AND OPTIMAL TRAFFIC SIGNAL TIMING

by

Tsai-Yun Liao

Randy B. Machemehl

Research Report SWUTC/98/467312-1

Southwest Region University Transportation Center
Center for Transportation Research
The University of Texas at Austin
Austin, Texas 78712

August 1998

Disclaimer

The contents of this report reflect the views of the authors, who are responsible for the facts and the accuracy of the information presented herein. This document is disseminated under the sponsorship of the Department of Transportation, University Transportation Center s Program, in the interest of information exchange. The U.S. Government assumes no liability for the contents or use thereof.

ABSTRACT

Growing concern about environmental protection and energy conservation has led the Clean Air Act Amendments and a number of studies to increase fuel economy and reduce emissions. Since most of the United States fuel consumption is by the transportation sector and fuel consumed by vehicles is about 75% of all transportation energy used, developing ways to reduce vehicle fuel consumption in traffic systems has become an important task. Furthermore, high gasoline consumption worsens air quality in urban areas by emission of carbon monoxide (CO) and carbon dioxide (CO_2), which make these areas, especially in the vicinity of intersections, potentially dangerous to human health.

The objectives of this report are to develop an analytical model to estimate fuel consumption and to investigate the effects of signal timing on fuel consumption. In order to achieve these objectives, a conceptual framework is proposed to identify interrelationships among traffic characteristics, signal control strategies, and roadway geometric conditions. Based on the framework, an Analytical Fuel Consumption Model (AFCM) is developed to estimate fuel consumption at signalized intersections.

In order to capture vehicle operating conditions, experimental data are collected to develop vehicle speed and acceleration/deceleration profile models which are used to establish fuel consumption profile and cumulative fuel consumption models. The calibrated parameters from the fuel consumption models are then applied in the AFCM. Several numerical experiments, including a variety of geometric configurations, traffic conditions, and signal timing are conducted to test the AFCM estimation capability and to investigate the effects of signal timing on fuel consumption. The results from these experiments indicate that total fuel consumption, with respect to signal cycle time, possesses a convex pattern.

In order to analytically establish the relationship between fuel consumption and signal timing, a three-term form is reduced from the AFCM to represent major effects of vehicle characteristics, traffic behavior, and fuel consumption parameters on optimal cycle length. The first term represents vehicle idle fuel consumption, the second term describes vehicle fuel consumption during acceleration after a stop, and the third term accounts for stochastic effects. Numerical analysis and comparisons show that the optimal cycle lengths from the expression are rather close to those from the AFCM.

ACKNOWLEDGMENTS

This publication was developed as part of the University Transportation Centers Program which is funded 50% with general revenue funds from the State of Texas.

EXECUTIVE SUMMARY

The objectives of this research are to develop a fuel consumption model for signalized intersections and to explore the effects of signal timing on fuel consumption. In order to achieve these objectives, a conceptual framework is proposed which considers interrelationships among three major elements; traffic characteristics, signal control strategies, and roadway geometric conditions. Based on these processes, a fuel consumption model, AFCM, is developed for estimating fuel consumption in the intersection influence area. This is the first attempt to tackle the problem by considering the three elements simultaneously.

The AFCM, permitting application in undersaturated and oversaturated traffic conditions, includes basic model development and model extensions considering queue probability and overflow queues. The AFCM describes different vehicle operating conditions consuming fuel on the inbound approach, the intersection itself, and the outbound leg for three signal cycle stages (the effective red time, queue discharge green time t_0, and time from t_0 to the effective green time end). The basic model development assumes that vehicle arrivals are uniform and deterministic, and the model extension has included stochastic effects and overflow conditions. The overflow conditions have major impacts on fuel consumption for the inbound approach. The analysis of queue probability and overflow queues proposed by Cronje has been applied to characterize queue probability and overflow queue sizes in the AFCM (Cronje, 1983).

As previously mentioned, the AFCM aims to analyze impacts of three elements: traffic characteristics, signal control strategies, and roadway geometric configurations. Traffic characteristics such as traffic flow rates, vehicle movements, and overflow queues have major impacts on fuel consumption. Pretimed signal control is assumed, and fuel consumption is affected by signal cycle time and green split. Geometric configurations are basic elements in describing the conditions of the intersection influence area. The three elements, therefore, are investigated comprehensively by conducting experimental data collection and numerical tests to enrich the AFCM capability.

Experimental data collection is conducted to develop vehicle speed, acceleration/deceleration profile models which are then used to establish fuel consumption profile models and associated parameters. Data was collected by videotaping traffic on Congress Avenue between 1st Street and Barton Springs Blvd. in Austin, TX. Vehicle speed and acceleration/deceleration rates, calibrated from the data reduction and analysis, are used to establish speed and acceleration/deceleration profile models. The speed, acceleration/deceleration profile models are polynomials of elapsed cycle time which satisfy the

real traffic conditions that acceleration rate is zero at the start and end of acceleration. From the speed, acceleration/deceleration profile models, and corresponding fuel consumption data obtained from USEPA which describe fuel consumption in terms of vehicle speed and acceleration/deceleration rates, fuel consumption profile models are calibrated to capture fuel consumption behavior in the intersection influence area. The acceleration fuel consumption profile model is a function of vehicle speed and acceleration, and the deceleration profile model is a function of vehicle speed. Since speed and acceleration/deceleration profile models are functions of elapsed cycle time, and fuel consumption profile models are functions of speed and acceleration, the cumulative fuel consumption models are functions of elapsed cycle time. Therefore, average vehicular fuel consumption rates are estimated from cumulative fuel consumption differences divided by elapsed travel time.

The objective of deriving average fuel consumption rates integrated into the three major AFCM elements is to develop an aggregate fuel consumption model which is at least as good as instantaneous models and can estimate fuel consumption in a simple and broad way. The average fuel consumption rates are then included as AFCM fuel consumption parameters.

The AFCM is implemented and tested through hypothetical intersection configurations, various traffic conditions, and signal cycle times to explore AFCM estimation capability and to investigate the effects of signal timing on fuel consumption. Results from the AFCM are compared with the results from the TEXAS model. The comparisons show that elapsed fuel consumption from the two models are highly correlated and that the elapsed fuel consumption estimated from the AFCM provides representative trajectories of fuel consumption variation along the intersection influence area. Moreover, total fuel consumption can be represented as a convex function of signal cycle time, revealing that the optimal cycle length is obtainable for fuel consumption minimization.

In addition, numerical experiments are conducted to compare optimal cycle lengths for fuel consumption and delay minimization. Various cases are analyzed and compared, indicating optimal cycle lengths for fuel consumption minimization are generally higher than for delay minimization.

Through these experiments, it has been shown that signal timing could be optimized by minimizing fuel consumption. Due to the complicated forms of the AFCM, a simple form reduced from the AFCM is used to derive an expression to estimate optimal cycle lengths. The reduced form describes the major effects of vehicle characteristics, traffic behavior, and fuel consumption parameters on optimal cycle length. It includes three terms: the first term represents stopped vehicles with idle fuel consumption rates, the second term describes fuel consumption for

vehicles accelerating from a stop, and the third term represents stochastic effects of vehicle movements which consume excess fuel. The test results and the comparisons between the original AFCM form and the streamlined expression indicate that optimal cycle lengths from the expression are rather close to those from the AFCM. Optimal cycle lengths for fuel consumption minimization can be easily predicting using the reduced form.

TABLE OF CONTENTS

LIST OF FIGURES

LIST OF TABLES

CHAPTER 1. INTRODUCTION

MOTIVATION AND PROBLEM STATEMENT

Growing concern about environmental protection and energy conservation has led the Clean Air Act Amendments and a number of regulations to increase fuel economy and reduce emissions. Since most of the United States fuel consumption is by the transportation sector (65.1%) and fuel consumed by vehicles is about 75% of all transportation energy use [37], developing ways to reduce automobile fuel consumption in traffic systems has become an important task. Furthermore, high gasoline consumption worsens air quality in urban areas by emissions of carbon monoxide (CO) and carbon dioxide (CO_2), which make these areas, especially the vicinity of intersections, potentially dangerous to human health. Therefore, motivated by the Clean Air Act Amendments [56], the Environmental Protection Agency (EPA) has initiated a number of studies to reduce automobile emissions and fuel consumption .

Fuel consumption in traffic systems can be reduced by increasing fuel economy of new vehicles and optimizing traffic control measures. Fuel economy can be improved by improving new vehicle technology and design. Several regulations aiming at increasing the fuel economy of new vehicles in the United States have been proposed and ratified in response to increasing gasoline demand, such as the Energy Policy and Conservation Act of 1975 and Corporate Average Fuel Economies Act (CAFE) [56]. Since 1975, fuel economy of new cars has been propelled from 14 miles per gallon per car (mpgpc) to 28 mpgpc by joint government and private sector efforts. However, because of the growth of the use of automobiles and the number of old vehicles (more than 60% of the vehicles in use are over five years old), improved new vehicle fuel economy is not sufficient to reduce fuel consumption. Therefore, traffic control measures aimed at minimizing fuel consumption in traffic networks must be developed.

Several criteria have been defined and applied to evaluate the effectiveness of traffic control measures in traffic networks, including minimizing delay, minimizing a combination of delay and numbers of stops, and minimizing fuel consumption. Among all these criteria, delay is probably most widely used, but fuel consumption has become an important measure of effectiveness (MOE) in urban networks where fuel consumption and emissions may be more critical than delay.

Two primary means to estimate fuel consumption have been applied, namely, on-road measurement and the use of fuel consumption models. On-road measurement of fuel consumption requires a fuel meter equipped chase car. The use of fuel consumption models is

easier and cheaper than on-road measurement; however, the accuracy of the estimation highly depends on the basic fuel consumption models.

A number of studies have tackled the problem of estimating vehicle fuel consumption in traffic systems. Several existing fuel consumption models for signalized intersections are developed based on instantaneous data, in which vehicle speed, and acceleration/deceleration profiles are used to estimate fuel consumption. The instantaneous information is usually obtained through micro-simulation traffic models, such as NETSIM (a microscopic network simulation model) and the TEXAS model (Traffic EXperimental and Analytical Simulation model).

Several intersection fuel consumption models, based on vehicle types, vehicle engines, roadway geometric conditions, and/or traffic situations, have been developed and applied. However, several shortcomings of these models are: 1) the impact of traffic control measures is not explicitly modeled, 2) changes of traffic characteristics, such as arrival patterns and flow rates, cannot be reflected in the model, and 3) the fuel consumption model in the traffic model cannot respond exactly to traffic situation changes. In order to improve fuel consumption estimation for a signalized intersection, an alternative model is proposed in this research, and related analysis approaches.

OBJECTIVES

In this study, the relationship among fuel consumption, traffic characteristics, and signal parameters is analyzed and explicitly considered in the development of an alternative model called the Analytical Fuel Consumption Model (AFCM). The model, based on roadway geometric configuration, traffic flow characteristics and signal settings, could improve the fuel consumption estimation by considering the impact of both traffic control measures and traffic flow characteristics on fuel consumption. At-grade intersections are usually network "hotspots" for both fuel consumption and emissions. The model deals specifically with intersections by treating them and the upstream and downstream areas as three roadway segments, inbound, intersection, and outbound, which are separately analyzed according to three different signal cycle stages, red, the start of green, and green time. The methodology includes a basic model which assumes vehicle arrivals are uniform and deterministic, and model extensions include stochastic effects and overflow conditions. The objectives of this research are summarized as follows:

1. Analyze the relationship between fuel consumption and predictive factors, such as roadway geometric configurations, traffic characteristics, and traffic

signal parameters, and develop an Analytical Fuel Consumption Model (AFCM) for signalized intersections.

2. Calibrate fuel consumption parameters to be applied to the AFCM development. This task is accomplished by collecting traffic flow and vehicle movement data, developing speed, acceleration/deceleration, and fuel consumption profile models, and calibrating fuel consumption parameters from the cumulative fuel consumption model.
3. Implement and test the AFCM through hypothetical intersection configurations, various traffic conditions, and signal cycle times to explore the model capability and to investigate the effects of signal timing on fuel consumption.
4. Compare the fuel consumption model results with those of the TEXAS simulation model and verify the effects of fuel consumption at different intersection segments, namely the inbound approach, the intersection itself, and the outbound leg.
5. Derive an expression to formulate the optimal cycle time for minimizing fuel consumption and compare with the AFCM. The expression, reduced from the AFCM, represents major effects of vehicle characteristics, traffic behavior, and fuel consumption parameters on optimal cycle lengths.

RESEARCH OVERVIEW

This research first proposes a conceptual framework which identifies the intersection fuel consumption modeling process with regard to traffic characteristics, signal control strategies, and roadway geometric conditions. An analytical fuel consumption model AFCM which is an aggregate model is then developed for estimating intersection fuel consumption. The intersection, described as the "intersection influence area", includes three segments: the inbound approach, the intersection itself, and the outbound leg.

The AFCM model is first developed based on the assumption that vehicle arrivals are uniform and deterministic. Traffic characteristics, signal control strategies, and roadway geometric conditions are integrated to formulate the model describing fuel consumption in the three intersection segments during the effective green and red time. In order to reflect real traffic conditions, the basic model is extended to consider stochastic effects and overflow queues. Thus, the AFCM can be applied to both undersaturated and oversaturated conditions. The

analysis of queue probability and overflow queues proposed by Cronje is applied to identify overflow queues in the AFCM [33, 34, 35].

In order to enrich the development of the AFCM, experimental data are collected describing traffic flow and vehicle data which are used to calibrate vehicle speed, acceleration/deceleration, fuel consumption profile models, and associated fuel consumption parameters. Vehicle speed and acceleration/deceleration profile models are polynomial models, and are expressed as functions of elapsed time. Fuel consumption profile models are regression models which represents fuel consumption data from EPA as functions of vehicle speed and acceleration/deceleration rates. Fuel consumption parameters are then derived from the speed, acceleration/deceleration, and corresponded fuel consumption models, and are applied to the AFCM development.

The next part of the research deals with the implementation of the AFCM and the analysis of the model estimation capability. First, the AFCM formulation is implemented on a DEC Alpha machine and tested through hypothetical intersection configurations, various traffic conditions, and signal cycle times to explore the AFCM capability and to investigate the effects of signal timing on fuel consumption. What are the information and importance reveal in the estimation of intersection fuel consumption? What are the critical variables in the fuel consumption modeling? How are the trajectories of vehicle and fuel consumption related to elapsed signal cycle time? How does signal control affect vehicle fuel consumption? A number of numerical experiments are performed to test and compare to TEXAS model simulation.

In addition, delay and fuel consumption representing different traffic system management objectives are compared through numerical analysis.

The next part of the work specifically addresses the search for a fuel consumption based signal timing optimization relationship. An optimization expression representing major effects of vehicle characteristics, traffic behavior, and fuel consumption parameters on signal timing is formulated. The expression consists of a reduced form of the AFCM and is simplified through certain assumptions.

ORGANIZATION OF THE REPORT

The report includes eight chapters. Chapter 2 reviews different fuel consumption models and categorizes these models according to an hierarchy proposed by Akcelik et al. [3]. These models include speed-type, delay-type, and instantaneous fuel consumption models.

Chapter 3 proposes a conceptual framework for identifying the intersection fuel consumption modeling process with regarding to traffic characteristics, signal control strategies,

and roadway geometric configurations. The critical factors for the fuel consumption model are then synthesized to develop an analytical fuel consumption model.

Chapter 4 describes the modeling procedure and develops the Analytical Fuel Consumption Model (AFCM). The AFCM includes a basic model which assumes vehicle arrivals are uniform and deterministic arrival flow patterns and a model extensions which consider stochastic effects and overflow queues. In the AFCM development, geometric configurations, traffic characteristics such as flow rates, arrival patterns, and overflow queues, as well as signal control parameters such as cycle length and green split are explicitly considered. In Chapter 5, fuel consumption parameters are investigated and discussed.

Chapter 5 describes experimental data collection to investigate vehicle behavior and corresponded fuel consumption behavior, and to establish vehicle speed, acceleration/deceleration, and fuel consumption profile models to calibrate fuel consumption parameters. Speed and acceleration/deceleration profile models are functions of elapsed signal cycle time. Fuel consumption profile models are functions of speed and acceleration/deceleration. Cumulative fuel consumption models are thus established as functions of elapsed signal cycle time.

Numerical analysis and comparisons are conducted in Chapter 6 to evaluate the AFCM estimation capability and to investigate the effects of signal timing on fuel consumption. The AFCM is implemented and tested through several case studies particularly examining fuel consumption time histories through the intersection influence area and fuel consumption reduction through optimum signal control.

Chapter 7 derives an expression for optimal cycle lengths to minimize fuel consumption. A three-term form reduced from the AFCM is developed representing major effects of vehicle characteristics, traffic behavior, and fuel consumption parameters on optimal cycle lengths.

Chapter 8 discusses the overall research conclusions, identifies significant research contributions, and recommends desirable future research.

CHAPTER 2. LITERATURE REVIEW

INTRODUCTION

This chapter reviews approaches that have been applied to develop fuel consumption models for describing urban network fuel economy and consumption. Since different approaches and models have been developed and tested, a fuel-consumption model hierarchy proposed by Akcelik et al. [3] is first presented, followed by a detailed discussion of models. The hierarchy consists of a classification of fuel consumption models, including four levels: an instantaneous model, an elemental model, a running speed model, and an average travel speed model. This classification could be used to illustrate fuel consumption model development.

Based on the hierarchy and characteristics of different fuel consumption models, a wide variety of fuel consumption models developed are reviewed and described in three types: (1) instantaneous fuel consumption models, (2) delay-type fuel consumption models, and (3) speed-type fuel consumption models.

Instantaneous fuel consumption models that consider second-by-second individual vehicle data, vehicle types, and roadway conditions are described in Section 2.3. Section 2.4 presents delay-type fuel consumption models based on traffic measures of effectiveness, such as delay and stops. Speed-type fuel consumption models, which capture the relationship between fuel consumption and aggregate average travel speed, travel time, or travel distance, are reviewed in Section 2.5. Section 2.6 summarizes fuel consumption models that are embedded within traffic models, such as NETSIM and the TEXAS model. Section 2.7 discusses the possible impacts of traffic control measures on fuel consumption. A brief summary is given in Section 2.8.

FUEL CONSUMPTION MODEL HIERARCHY

Fuel consumption varies with vehicle types, roadway geometric conditions, traffic control measures, and traffic demand. Fuel consumption models must describe how fuel is consumed under a variety of roadway design and traffic control changes. The fuel economy problem has motivated researchers to develop comprehensive models in order to understand the relationship between fuel consumption and traffic control measures. Since a variety of mathematical models have been developed to estimate fuel consumption, it is important to understand their concepts and prediction capability.

Akcelik et al. [3] proposed an hierarchy that differentiate fuel consumption models into four levels. Figure 2.1 illustrates the proposed hierarchy and the interrelationships among these

four levels of fuel consumption models. These four levels of consumption models are briefly described hereafter.

(1) Level 0: Basic Models

Basic models consider fuel economy of individual vehicles which might be affected by vehicle components, such as engines, transmissions, and other vehicle characteristics. This level of fuel consumption models aims at providing a vehicle design aid.

(2) Level 1: Micro Models

Micro levels have the form of an instantaneous fuel consumption function as defined by speed and acceleration/deceleration profiles. Several simulation models, such as NETSIM and the TEXAS model, have the ability to generate speed-time profiles and use this information in fuel consumption estimates. This approach provides detailed insights to estimate fuel consumption in response to traffic conditions in terms of speed and speed change.

(3) Level 2: Micro/Macro Models

These models consider micro and macro variables. They provide a simpler form to estimate fuel consumption, but are capable of responding to small traffic condition changes. Therefore, these models could provide accurate approximation for traffic and transport management purposes.

(4) Level 3: Macro Models

Macro level models, aiming at providing network-level traffic system analysis, are characterized by regression models that include two major variables, travel time and travel distance.

According to the hierarchy, three different approaches, including instantaneous fuel consumption models, delay-type fuel consumption models, and speed-type fuel consumption models, can be applied to derive the fuel consumption. The first approach considers fuel consumption as a function of instantaneous speed, acceleration/deceleration, and individual vehicle data that aims at capturing speed change effects through kinetic energy or inertial power. Instantaneous fuel consumption models include basic and micro level models in the hierarchy. Delay-type fuel consumption models, micro/macro level models in the hierarchy, are mainly based on some traffic measures of effectiveness, such as delay and stops. The last approach uses aggregate data from network-wide parameters, such as average travel speed, travel time, and travel distance to estimate fuel consumption. The models developed under this approach are defined as speed-type models.

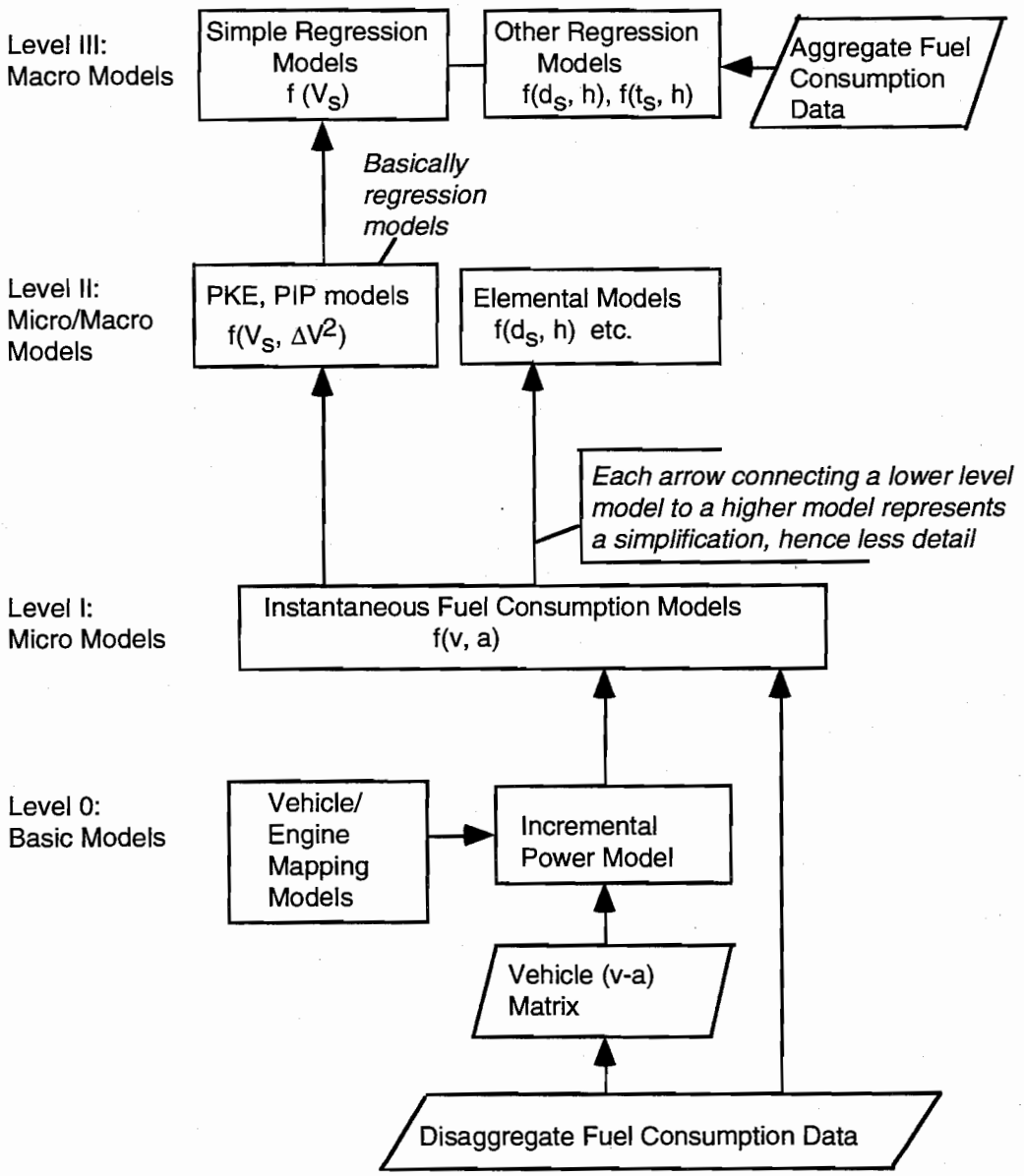

Figure 2.1 Hierarchy of vehicle fuel consumption models

Source: Akcelik et al. [3]

INSTANTANEOUS FUEL CONSUMPTION MODELS

This section discusses instantaneous fuel consumption models which include basic model and micro level model. Basically, the basic model is an engine-type model which considers vehicle design such as vehicle engine and torque as model parameters. The micro level model is a non engine-type model which requires second-by-second individual vehicle data. The engine of a moving vehicle must overcome resistance due to rolling, air, and gradients. It is obvious that pavement type affects fuel consumption through rolling resistance and roadway geometric design affects it through rolling resistance and gradient resistance. Vehicle design affects rolling, air, and gradient resistance. Therefore, fuel economy savings can be reached by improving vehicle design [55, 13).

An instantaneous fuel consumption model requires second-by-second individual vehicle data. The data include speed, acceleration/deceleration, vehicle engine speed, and time and location along road sections for an individual vehicle. Therefore, it is suitable for estimating fuel consumption in an urban traffic system where instantaneous traffic data are available [23].

An instantaneous model developed in ARRB is a detailed engine-map based model [19, 25, 18]. The engine-map based model is extended from the original power demand model [71] and is related to engine power, engine drag and efficiency, and engine speed. The model form is expressed as:

$$f = \beta (P_{out} + P_{eng}) \quad \text{or} \quad \alpha, \quad \text{whichever is greater} \qquad [2.1]$$

where,

f: the fuel consumption rate per unit time (ml/s),

α: the idle fuel consumption rate with accessories operating (ml/s),

β: the fuel-to-power efficiency factor (ml/s/kW),

P_{eng}: the power to overcome internal engine drag (KW), and

P_{out}: the total external engine power (KW) required to overcome rolling and air resistance, inertia and grade forces and provide power to run accessories.

The instantaneous model requires detailed individual vehicle design factors and is suitable for microscopic traffic models. Various fuel consumption models can be derived from the instantaneous model [19, 23, 18].

Lee et al. [58] developed a set of fuel consumption models used in the EMPRO simulation process which is a component of the TEXAS model. These models include non-

engine type models for passenger cars and engine-type models for trucks. The non-engine type models use emissions parameters as predictor variables which consist of carbon monoxide (CO), hydrocarbons (HC), and carbon dioxide (CO_2). The non-engine type models are expressed as:

$$FF = a_1 HC + a_2 CO + a_3 CO_2 \quad [2.2]$$

The emissions parameters are calibrated from instantaneous emissions models including steady state model and transient state model. The steady state model is modeled as a function of speed, and the transient state model is modeled as a function of speed and acceleration/deceleration. The emissions models are expressed as:

Steady state model: $$L(V) = \alpha_1 + \alpha_2 V + \alpha_3 V^2 \quad [2.3]$$

Transient state model: $$L(V, A) = \beta_1 + \beta_2 V + \beta_3 A + \beta_4 VA + \beta_5 V^2 + \beta_6 A^2 + \beta_7 V^2A + \beta_8 VA^2 + \beta_9 V^2 A^2 \quad [2.4]$$

where,

L = instantaneous emissions rate (gram/second),

V = speed (mile/hr),

A = acceleration or deceleration (mile/hr^2), and

α_i (i = 1, ..., 3) and β_j (j = 1, ..., 9) = model coefficients.

Basically, the models require second-by-second vehicle speed and acceleration/deceleration data obtained from the TEXAS simulation process.

The engine-type models use engine speed and torque as predictor variables. Typical engine-type fuel consumption models are expressed as:

$$FF_g = \alpha_1 + \alpha_2 |TRQ| RPM + \alpha_3 |RPM|^{1/2} + \alpha_4 (TRQ)^4 \quad [2.5]$$

$$FF_d = \beta_1 + \beta_2 |TRQ| + \beta_3 (RPM) |TRQ| + \beta_4 (|TRQ| + RPM) - \beta_5 |TRQ|^{1/2} \quad [2.6]$$

where,

FF_g: fuel consumption for gasoline trucks (grams/second),

FF_d: fuel consumption for diesel trucks (grams/second),

RPM: engine speed in revolutions per minute,

TRQ: engine torque in foot-pounds, and

α_i (i = 1, ..., 4) and β_j (j = 1, ..., 5) = model coefficients.

Since model parameters for engine-type models vary widely for different truck types, these models are primarily used for vehicle design analysis.

DELAY-TYPE FUEL CONSUMPTION MODELS

This type of fuel consumption model aims at establishing the relationship between fuel consumption and commonly used traffic measures of effectiveness, such as delay and stops. Since delay is a very popular measure of effectiveness in traffic analysis work, its use in a fuel consumption model is advantageous.

A fuel consumption model that was developed by stepwise multiple regression analysis is incorporated into the TRANSYT-7F model [79]. The model can be expressed as:

$$f = \sum_{i=1}^{N} [k_{i1} T + k_{i2} D + k_{i3} S] \qquad [2.7]$$

where,

f: fuel consumption in gallons per hour,

T: total travel time in vehicle-miles per hour,

D: total delay in vehicle-hours per hour,

S: total stops in stops per hour, and

k_{ij}: model coefficients which are functions of cruise speed on each link i:

Several studies [14, 32, 72] have focused on the study of traffic signal timing and fuel consumption. Bauer used an incremental fuel consumption model to analyze the change in fuel consumption due to signal cycle time. The form is expressed as:

$$\Delta E(c) = (E_{idle}) \sum_{j=1}^{N} d_j q_j + (E_{start}) \sum_{j=1}^{N} p_j q_j \qquad [2.8]$$

where

$\Delta E(c)$: total incremental energy consumption resulting from one hour of intersection operation at a cycle time c,

E_{idle}: idling energy consumption of an average vehicle in the traffic mix using the intersection (gallons/hour),

E_{start}: energy consumption of an average vehicle in the mix using the intersection during a 0 to 30 mph acceleration maneuver (gallons),

N: number of approaches to the intersection,

d_j: delay in vehicle-hours for vehicle-hours for vehicles on the j^{th} approach (Webster's equation) [84],

p_j: average number of stops per vehicle for vehicles on the j^{th} approach (Webster's equation) [84],

q_j: flow in vehicles/hour on the jth approach, and

c: cycle length used for signal timing.

Incremental fuel consumption based on different cycle lengths is related to idling energy consumption, acceleration energy consumption, vehicle flow rates, vehicle delay, and number of stops. The vehicle delay and number of stops are obtained from Webster's equation [84].

Courage and Parapar studied factors which affect fuel consumption and proposed a fuel consumption model consisting of two main model parameters delay and number of stops. The form of the model is:

$$E = \alpha D + \beta S \qquad [2.9]$$

where,

E: fuel consumed due to the signal timing plan in gallons of gasoline;

α: conversion coefficient in gallons per vehicle-hour of delay;

D: stopped delay in vehicle-hours;

β: conversion coefficient in gallons per vehicle-stop; and

S: number of stops for all vehicles.

Reljic et al. [72] proposed an optimization procedure for calculating the signal plan for the minimization of fuel consumption at an intersection. In addition to delay and number of stops, vehicle speed is considered in the fuel consumption model. The model is expressed as:

$$F = \sum_{j=1}^{n} (\beta_j^d q_j d_j + \beta_j^z V_j^2 q_j z_j) \qquad [2.10]$$

where,

F: total fuel consumption;

β_j^d: the coefficient of fuel consumption for one hour of delay on approach j;

β_j^z: the coefficient of fuel consumption for one stop on approach j;

V_j: flow speed;

d_j: average delay/vehicle at approach j; and

z_j: average number of stops at approach j.

SPEED-TYPE AGGREGATE FUEL CONSUMPTION MODELS

Speed-type fuel consumption models, generally, use regression analysis to derive a relationship between fuel consumption and network-wide variables, such as average travel speed, travel time, travel distance, and number of stops. Because these models do not consider

second-by-second speed change in the fuel consumption estimation, they are insensitive to small traffic condition changes.

Research conducted at General Motors Corporation was among the most well-known to establish macro level fuel consumption models. Herman and his colleagues [43, 44, 29, 30, 45, 41, 42, 52, 27, 28, 51] have conducted a series of experiments and studies in urban fuel economy and fuel consumption. Evans, Herman, and Lam [43] investigated 17 variables describing the effects of fuel consumption , including average trip speed, largest instantaneous deceleration and acceleration, average trip time per unit distance, and number of complete vehicle stops, and found that fuel consumption estimation F, can be estimated using average distance D, and average travel time T, i.e., $F = k_1 D + k_2 T$. Thus the fuel consumed per unit distance can be described as:

$$f = k_1 + k_2 t \qquad [2.11]$$

or

$$f = k_1 + k_2 / V \qquad [2.12]$$

where,

f: fuel consumption per unit distance,

t: average trip time per unit distance,

V: average trip speed,

k_1: a parameter associated with fuel consumption per unit distance to overcome rolling resistance and is approximately proportional to vehicle mass, and

k_2: a parameter that is approximately proportional to the idle fuel flow rate.

Parameters k_1 (gallons per mile) and k_2 (gallons per hour) are coefficients related to vehicle characteristics. Post et al. [71] examined parameter k_1 and showed that k_1 is related to power demand which accounts for inertial, drag, and gradient fuel consumption components. Using the model, fuel consumption can be estimated appropriately where vehicle speed is less than 35 mph.

Chang and Herman [28] used two instrumented vehicles to estimate fuel consumption on two routes under different traffic conditions in Milwaukee. The results show that fuel consumption is independent of metropolitan areas and is approximately linearly related to average trip time. The impact of speed change on fuel consumption was described by Chang and Herman [27] and Evans et al. [44]. The results show that conservative driving behavior and proper traffic maneuvers, which usually have fewer speed changes, can reduce fuel consumption. The fuel

consumption model was improved by considering the influence of vehicle stops in urban traffic systems by Herman and Ardekani [51]:

$$f = k_1 + k_2 t + k_3 \Delta N_S \qquad [2.13]$$

where,

f, k_1, k_2, and t: the same definitions as Equation 2.11,

ΔN_S: the difference between N_S and $N_S(t)$,

N_S: number of stops for a given datum point, and

$N_S(t)$: average number of stops associated with the trip time interval in which the datum point falls.

The results from regression analysis show that t and ΔN_S are independent; therefore, the model, including the additional variable ΔN_S, is more appropriate to estimate fuel consumption in urban traffic systems.

Results from several other studies [46, 67, 40, 82, 61, 83, 68, 17, 47] are consistent with the models described previously and have a similar fuel consumption model form. Pelensky et al. [67] used three test cars to investigate petrol consumption in Sydney and Melbourne, Australia. They examined fuel consumption factors including travel time, number of stops, stopped time, and grade and found that fuel consumption can be predicted by average travel speed. Watson et al. [82] used an instrumented vehicle to investigate variation of fuel consumption with average speed change in Melbourne traffic. Pienaar [68] examined car fuel consumption in South African cities and found that fuel consumption rate is a linear function of travel time (the reciprocal of speed) and minimum fuel consumption occurred at an average journey speed of about 64 km/hr.

The quadratic speed term incorporated into the simple speed-type models was proposed by Everall [46], Al-Nuami [8], and Al-Omishy et al. [9]. Everall [46] described the relationship between the variation of average fuel consumption and traffic speed in urban and rural roads as:

$$f = k_1 + k_2 / V + k_3 V^2 \qquad [2.14]$$

Al-Omishy [9] performed regression analyses to relate fuel consumption to vehicle speeds for different vehicle loads and developed a computer-simulation model to predict fuel consumption for gasoline and diesel vehicles. The model is expressed as:

$$F = a + b (1/V) + c V + d V^2 \qquad [2.15]$$

where,

F: 1/100 km fuel consumption,

V: speed in km/h, and

a, b, c, and d: coefficients.

Later in 1993, Al-Omishy et al. [9] used the model to evaluate fuel consumption in Iraq under various conditions and found that fuel consumption is high at very low and high speeds.

A number of studies [83, 17, 19, 12, 47] extended simple average speed fuel consumption model to combine with other variables that describe vehicle characteristics. Watson [83] derived a fuel consumption model as a function of speed and energy changes. The function can be described as:

$$f = k_1 + k_2 / V + k_3 V + k_4 PKE \qquad [2.16]$$

where k_1 to k_4 are coefficients, V is average speed, and PKE (Positive Kinetic Energy) is the sum of positive acceleration kinetic energy changes. The PKE term aims at capturing the dynamic effect of acceleration upon additional fuel consumption. One of the major shortcomings in this model is the difficulty to measure PKE, and thus a meaningful regression analysis is difficult.

A fuel consumption model based upon resistance to motion was derived by Bester [17], and the model form is:

$$f = P_1 + P_2 / V + P_3 V_2 + P_4 G \qquad [2.17]$$

where,

V: speed,

G: gradient,

P_2: a constant that is related to idling fuel consumption, and

P_1, P_3, and P_4: constants derived from the rolling, air, and gradient resistance.

Bester used the model to investigate the effect of pavement type and condition on fuel consumption and found that pavement type has a minor effect on fuel consumption, yet pavement condition has a strong fuel consumption effect.

Fwa and Ang [47] conducted an experiment to develop a fuel consumption model for passenger cars in Singapore. The model was developed following other studies [46, 19, 57]. The model form is:

$$F = a_0 + a_1 / V + a_2 K \qquad [2.18]$$

where coefficient a_0 and a_1 correspond to k_1 and k_2 in Equation 2.11 and coefficient a_2 and variable K represent the effect of vehicle operational characteristics.

HDM-III fuel consumption model was developed based on an experimental study in Brazil. It describes fuel consumed for an individual vehicle on any section of a specified geometric alignment. The fuel consumption is defined as:

$$F_L = 500\ \alpha_1\ \alpha_2\ (UFC_u / V_u + UFC_d / V_d) \quad [2.19]$$

where,

F_L: average round trip fuel consumption (liters/1000 vehicle-km),

α_1: relative energy-efficiency factor,

α_2: fuel adjustment factor,

UFC_u: the predicted unit fuel consumption for the uphill segment (ml/s),

UFC_d: the predicted unit fuel consumption for the downhill segment (ml/s),

V_u: predicted steady-state speed for the uphill segment (m/s), and

V_d: predicted steady-state speed for the downhill segment (m/s).

ARRB (Australian Road Research Board) has conducted a series of experiments where fuel consumption models were developed for each level of the hierarchy shown in Figure 2.1. The ARFCOM (ARRB Road Fuel Consumption Model) [18] includes four sub-models: an instantaneous model, a four mode elemental model, a running speed model, and an average speed model.

The four mode elemental models of ARFCOM, derived from an instantaneous model, require detailed but more aggregate data to estimate fuel consumption. They include fuel consumption models describing idle, cruise, acceleration, and deceleration. Idle fuel consumption is a function of the idle fuel consumption rate and idling time. Cruise fuel consumed depends on the cruise speed and speed fluctuation impacts. Acceleration fuel consumption mainly depends on vehicle power components and deceleration fuel consumption is related to deceleration time and idle fuel consumption rate. The expressions of the four mode elemental models in ARFCOM are:

Idle fuel consumption model:

$$F_i = \alpha\ t_i \quad [2.20]$$

Cruise fuel consumption model:

$$F_c = \beta_b\ (1 + e_{hp}\ k_2\ P_{out} / P_{max})\ (P_{out} + P_{eng})\ 3600 / V_c$$

$$\text{or} \quad 3600\ \alpha / V_c, \text{ whichever is greater} \quad [2.21]$$

Acceleration fuel consumption model:

$$F_a = \beta_b\ (1 + e_{hp}\ k_2\ P_{out} / P_{max})\ (P_{out} + P_{eng})\ t_a$$

$$\text{or} \quad \alpha, \text{ whichever is greater} \quad [2.22]$$

Deceleration fuel consumption model:

$$F_d = \beta_b\ (1 + e_{hp}\ k_2\ P_{out} / P_{max})\ (P_{out} + P_{eng})\ t_d \quad [2.23]$$

where,

F_i: idle fuel consumption (ml),

F_c: cruise fuel consumption (ml),

F_a: acceleration fuel consumption (ml),

F_d: deceleration fuel consumption (ml),

α: idle fuel consumption rate with accessories operating (ml/s),

t_i: idle (stopped) time (s),

β_b: base engine fuel efficiency factor (ml/s/kW),

e_{hp}: proportionate decrease in engine fuel efficiency at maximum power,

P_{max}: maximum rated engine power (kW),

P_{out}: total output power of the engine (kW),

P_{eng}: power required to overcome engine drag (kW),

V_c: cruise speed (km/h),

t_a: acceleration time (s), and

t_d: deceleration time (s).

Luk and Akcelik [59] evaluated the predicting capability of the elemental fuel consumption model and reported that the model can accurately predict fuel consumption changes in the CBD.

The ARFCOM running speed model [19, 23, 18], derived from an instantaneous fuel consumption model, is a macro level expression. It requires average running speed, idle time (stopped time), and travel distance. The model is expressed as:

$$F_S = \alpha t_i + f_r x_S \qquad [2.24]$$

where,

f_r: the fuel consumption per unit distance (ml/km) for a given average running speed, V_r, and sum of positive kinetic energy changes, denoted as E_{k+},

x_S: the section distance (km),

t_i: the idle (stopped) time (s), and

α: the idle fuel consumption rate (ml/s).

The running speed model is similar to Equation 2.11.

An average travel speed model developed in ARRB requires vehicle travel distance and average travel speed data. The model is expressed as:

$$F_S = f_X x_S \qquad [2.25]$$

where f_x is fuel consumption rate given average travel speed and x_s is vehicle travel distance. The model is accurate only for average travel speeds less than 50 km/h, and it is suitable for estimation of total fuel consumption in large urban traffic systems.

A family of fuel consumption models developed by Taylor and Young [76, 77] improves the IMPAECT (Impact Model for the Prediction and Assessment of the Environmental Consequences of Traffic) model capability. Fuel consumption models are developed based on collected fuel consumption data from a Toyota Camry sedan with a 2.0 litre four cylinder EFI engine, both on-road and in the laboratory, and from a Ford Falcon station wagon with a 4.0 litre six cylinder EFI engine, on-road. Cruise and acceleration fuel consumption models are developed respectively, and the models are expressed as:

$$f_c = \alpha_1 + \alpha_2 V_c + \alpha_3 V_c^3 \qquad [2.26]$$

$$f_a = \beta_1 V_f + \beta_2 V_f^2 \qquad [2.27]$$

where,

f_c = cruise fuel consumption,

f_a = acceleration fuel consumption,

V_c = vehicle cruise speed,

V_f = final speed of acceleration, and

α_i (i = 1, ..., 3) and β_j (j = 1, 2) = model coefficients.

FUEL CONSUMPTION MODELS WITHIN TRAFFIC MODELS

Fuel consumption estimation, generally, requires traffic variables as input data; therefore, it is practical to incorporate fuel consumption models with traffic models which are a primary ways to estimate traffic variables [24]. For example, EMPRO [58], includes instantaneous fuel consumption models for passenger cars and trucks, is an emissions and fuel consumption processor for the TEXAS simulation model. It needs instantaneous vehicle speed and acceleration/deceleration with respect to time and location along the road section through the simulation process (SIMPRO) of the TEXAS model. EMPRO, therefore, is more functional by incorporating into a traffic model the TEXAS model.

A number of traffic models have been developed and applied all over the world. Since the objectives of traffic management vary from city to city and from country to country, the choice of traffic model and associated fuel consumption model is essential to the success of traffic management. Table 2.1 summaries traffic models and associated fuel consumption models.

Also, traffic variables required in these models are specified. Fuel consumption models within traffic model the TEXAS, NETSIM, and INSECT models are instantaneous models which require second-by-second individual vehicle data. Speed-type models are embedded in traffic models UTPS, SATURN, and IMPAECT and a delay-type model is applied in TRANSYT. Since SATURN also utilizes delay and number of stops in fuel consumption estimation, the model is called as a hybrid (speed-type and delay-type) model.

TABLE 2.1 TRAFFIC MODELS AND FUEL CONSUMPTION MODELS

Traffic Model	Fuel Consumption Model	Basic Required Variables
TEXAS	Instantaneous Model	speed, acceleration/deceleration, and vehicle engine speed for each second
NETSIM	Instantaneous Model	speed and acceleration/deceleration for each second
INSECT	Instantaneous Model	distance and grade for each second over a road section
UTPS	Speed-type Model	average speed, travel time, and stopped time
SATURN	Hybrid (Speed-type and Delay-type) Model	average speed, cruise speed, delay, and stops
TRANSYT	Delay-type Model	average speed, travel distance, delay, and stops
IMPAECT	Speed-type Model	cruise speed, final speed over a travel distance

FUEL CONSUMPTION ESTIMATION AND TRAFFIC CONTROL MEASURES

Fuel economy saving is an important issue because of both energy conservation and environmental concerns. Although fuel economy can be improved by improving new vehicle design, fuel savings still need traffic control management to reduce fuel consumption [14, 32, 31, 82, 15, 2, 62, 8, 70, 7, 24, 26, 69, 80, 65, 85, 48, 63, 72].

A number of studies [14, 32, 31, 8, 7, 26, 72] have focused on the impact of traffic signal to fuel consumption. In 1980s, a fund was approved for California's Fuel Efficient Traffic Signal Management (FETSIM) program to work on reducing fuel consumption through traffic signal timing. California local governments have conducted a series of studies [26] by using TRANSYT to investigate impact of traffic signals on traffic control measures. They suggested that fuel savings can be improved by signal improvement. Cohen and Euler [31] used NETSIM to evaluate fuel consumption for different signal timing plans and found that the optimal cycle lengths for

minimizing delay and for minimizing fuel consumption are the same. However, the result is different from the studies of Bauer [14] and Courage and Parapar [32] where the results show that the optimum cycle length for minimizing fuel consumption is much longer than the cycle length for minimizing isolated intersection delay. Al-Khalili and El-Hakeem [8] designed a computer control system incorporated with a fuel consumption model for fuel consumption minimization in urban traffic network and presented that minimization of fuel consumption can be achieved by optimal signal control. Later in 1985, Al-Khalili examined optimal green split of a cycle length on traffic management measures and commented that minimum of a traffic management measure is obtainable by giving optimum green split. Reljic et al. [72] presented an optimization procedure for calculating the signal plan which minimizes the selected optimization criterion such as total delay, total number of stops, total cost of losses, and total fuel consumption at an intersection subject to certain constraints.

Different approaches related to traffic signal timing are conducted to investigate fuel consumption and traffic control measures. Watson et al. [82] investigated the impact of vehicle driving pattern and traffic characteristics on fuel consumption in Melbourne traffic and deduced that fuel consumption can be reduced by increasing average speed, smoothing vehicle maneuvers, and co-ordinating traffic signals. Bayley [15] evaluated fuel consumption can be reduced through reducing speed fluctuations and smoothing driving pattern. Hence, optimal traffic signal control is important for fuel consumption reduction. Akcelik [2] examined the ARFCOM elemental model and concluded that three traffic control measures, cruise speed distance, average stopped delay time, and number of stops, are main factors in fuel consumption estimation. Therefore, optimal signal control which can affect the three traffic control measures is required to reduce fuel consumption. Polanis [70] and Matsuura and Liu [60] concluded that co-ordinated signals can reduce fuel consumption by applying the fuel consumption model derived from General Motors' research.

The accuracy of fuel consumption estimation is a critical traffic control measure where fuel economy and consumption is important to traffic system management. A wide range of fuel consumption models, include aggregate speed-type, delay-type, and instantaneous fuel consumption models, are developed and implemented in a variety of traffic considerations for different level of analyses. Therefore, the correct choice of an appropriate fuel consumption model for predicting and evaluating fuel consumption in an urban traffic system is required.

SUMMARY

In this chapter, various fuel consumption models have been reviewed based on a model hierarchy proposed by Akcelik et al. [3]. These models, including instantaneous, delay-type, and speed-type fuel consumption models have been developed to estimate fuel consumption according to different traffic situations and roadway conditions. The instantaneous models, including engine type and non-engine type models, utilize second-by-second vehicle data. Delay-type models consider parameters related to traffic measures of effectiveness, such as delay and number of stops. In speed-type models, fuel consumption is estimated as functions of average travel speed, travel time, or travel distance. Most of fuel consumption models can be applied in traffic models to accurately estimate fuel consumption. Furthermore, the impacts of traffic control measures on fuel consumption have been discussed to highlight the importance of traffic system management in terms of fuel consumption.

However, most of the fuel consumption models are used in specific traffic situations. Several shortcoming of most intersection fuel consumption models are : 1) the impact of traffic control measures is not explicitly modeled, which is very important in the intersections, 2) changes of traffic characteristics, such as arrival patterns and flow rates, cannot be reflected in the model, and 3) the fuel consumption models cannot respond exactly to traffic situation changes.

In the following chapters, a modeling framework for developing fuel consumption model is proposed, a new fuel consumption model called the Analytical Fuel Consumption Model (AFCM) is developed, and experimental design and numerical analysis are conducted to explore the fuel consumption estimation and other related characteristics.

CHAPTER 3. MODELING FRAMEWORK

INTRODUCTION

Based on the previous discussion, several shortcomings of existing intersection fuel consumption models are: 1) the impact of traffic control measures is not explicitly modeled, 2) changes of traffic characteristics, such as arrival patterns and flow rates, cannot be reflected, and 3) the models cannot respond exactly to traffic situation changes. In order to overcome these shortcomings, an alternative approach is proposed to estimate fuel consumption from an aggregate view point. In this approach, signal control strategies, geometric configurations, and traffic characteristics are all explicitly represented by appropriate variables. Due to the complexity of this problem, the interrelationships among signal control strategies, geometric configurations, and traffic characteristics need to be further clarified.

In this chapter, a conceptual framework for an alternative fuel consumption model is presented and discussed. The conceptual framework describes three major elements (signal control strategies, geometric configurations, and traffic characteristics), other important factors (vehicle travel time, speed and acceleration/deceleration profiles, and fuel consumption rates), and their interrelationships. Based on the framework, a modeling approach, which considers aggregate vehicle behavior and fuel consumption rate, is described. The relationships between vehicles and associated fuel consumption are then described and illustrated to provide an overall picture for the proposed modeling approach. The conceptual idea of the approach is discussed in this chapter and mathematical formulations are presented in Chapter 4.

Section 3.2 describes the conceptual framework for an alternative fuel consumption model. Section 3.3 describes the conceptual idea of the aggregate modeling, including the relationship between vehicles and fuel consumption, average fuel consumption rate, and total fuel consumption estimation. A brief summary is given in Section 3.4.

MODELING FRAMEWORK FOR INTERSECTION FUEL CONSUMPTION ESTIMATION

Introduction

Fuel consumption near or within signalized intersections could be described by different variables, depending upon the applied approach. Possible predictor variables and their relationships, which might be critical to fuel consumption, are depicted in Figure 3.1.

In Figure 3.1, three fundamental elements signal control strategies, geometric configurations, and traffic characteristics describe the basic intersection characteristics. These elements have direct impacts on vehicle travel time and how vehicles travel through the intersection. Vehicle trajectories can be represented by vehicle speed and acceleration/deceleration profiles. Based on the three elements, instantaneous vehicle speed and acceleration/deceleration profiles can be calibrated, and vehicle travel time can be estimated. Fuel consumption rates can be obtained from the vehicle speed and acceleration/deceleration profiles and the corresponding EPA fuel consumption data which are collected through on-road measurement [50]. Basically, for fuel consumption estimation due to changing vehicle trajectory characteristics, the intersection can be divided into three segments, namely, the inbound approach, the intersection itself, and the outbound leg. Fuel consumption for each intersection segment, thus, can be estimated incorporating signal control strategies, traffic characteristics, travel time, and fuel consumption rates. Individual elements and factors are described in the following sections.

The modeling framework only considers pretimed signalized intersections; however, the approach could be easily extended to other traffic control types.

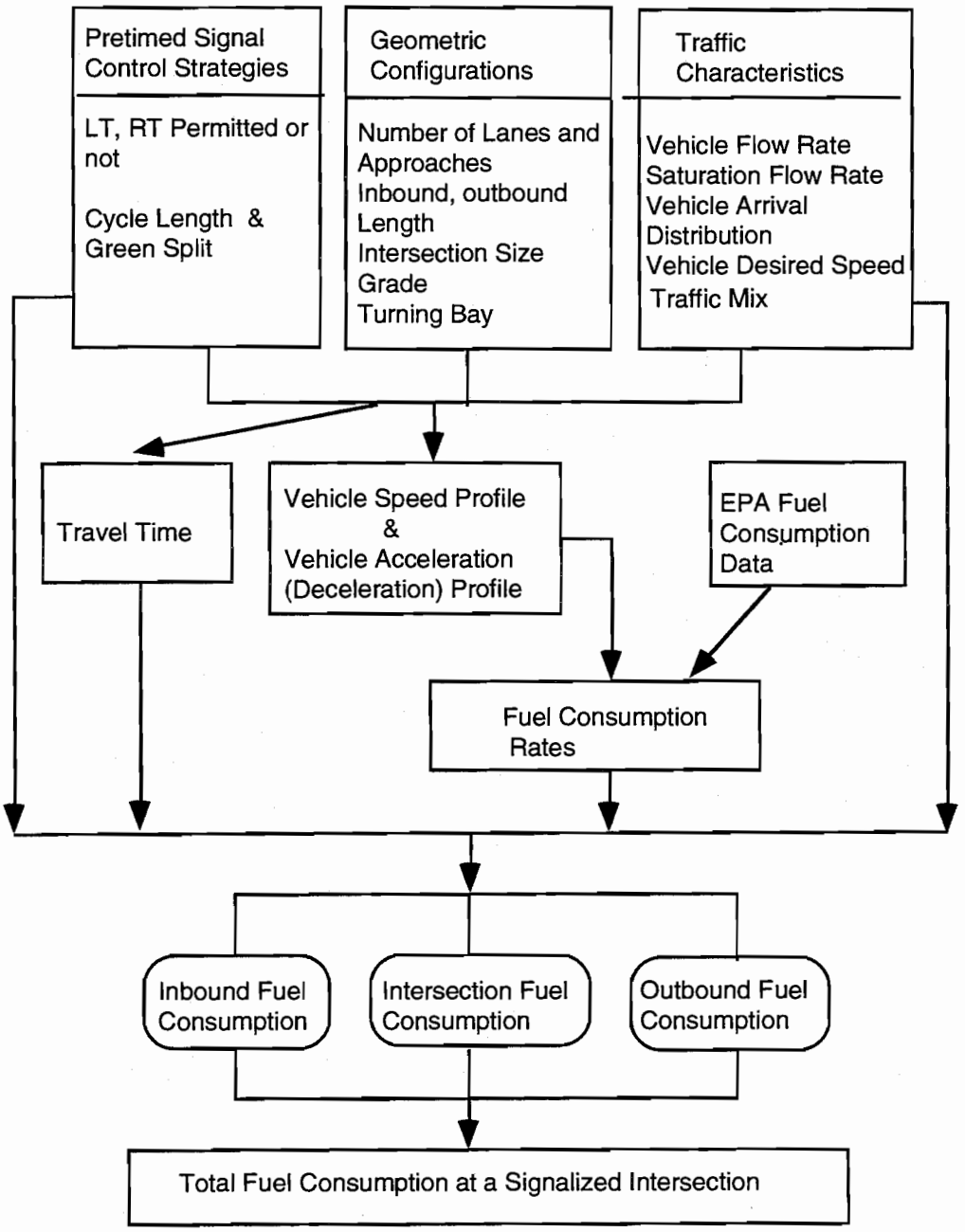

Figure 3.1 Modeling Framework

Elements in Fuel Consumption Estimation Process

Traffic Characteristics. In practice, traffic characteristics include traffic flow rate, saturation flow rate, vehicle desired speed, turning movements, and vehicle arrival process type.

Traffic flow rates, usually addressed as passenger car units (pcu), must be specified for each movement on each approach. Traffic flow rates are critical in determining cycle split and traffic conditions, and thus are important for estimating total intersection fuel consumption. Saturation flow rate is the flow in vehicles per hour assuming all green time is given to only one approach and it allows an infinite queue. The vehicle arrival process type has a major impact on fuel consumption, especially at the beginning of the green signal time when vehicles accelerate at high fuel consumption rates to cross the stop line. Mixed traffic generally consumes more fuel than passenger cars only. Turning movements consume more fuel than straight movements due to the conflicts with movements on other approaches. Especially, left-turn movements can cause more traffic fluctuations and interruption, and thus can have major effects on fuel consumption estimation. Vehicle desired speed is associated with the speed limit on each approach and affects vehicle maximum speed and acceleration/deceleration rates, and thus directly affects fuel consumption. Generally, higher desired speeds consume more fuel.

Other factors such as pedestrian flow rates and parking activity are also important in estimating fuel consumption. Although pedestrians flows interfere with right-turn and left-turn movements, they are not currently considered in this research.

Signal Control Strategies. Signal control strategies assign right-of-way to each intersection approach. They include actuated or pretimed signal controllers providing phase sequences, cycle lengths, and green splits. This research is concentrated on pretimed signal control characterized by a phase plan, cycle length, and green splits, which are based on roadway geometric conditions and traffic demands. The following terms defined in HCM describing signal operation are used in this study [54]:

cycle: any complete sequence of signal indications,

cycle length: the total time for the signal to complete one cycle, stated in seconds and given the symbol C,

interval: a period of time during which all signal indications remain constant,

phase: the part of a cycle allocated to any combination of traffic movements receiving the right-of-way simultaneously during one or more intervals,

change interval: the "yellow" plus "all-red" intervals that occur between phases to provide for clearance of the intersection before conflicting movements are released,

green time: the time within a given phase during which the green indication is shown,

lost time: time during which the intersection is not effectively used by any movements,

effective green time: the time during a given phase that is effectively available to the permitted movements, generally taken to be the green time plus the change interval minus the lost time for the designated phase, stated in seconds and given the symbol g,

effective green ratio: the ratio of effective green time to the cycle length,

effective red time: the time during which a given movement or set of movements is effectively not permitted to occur, the cycle length minus the effective green time for a specified phase, stated in seconds and given the symbol r, and

pretimed operation: the cycle length, phases, green times, and change intervals are all preset in pretimed operation.

The number of signal phases varies with traffic flow characteristics which are described by vehicle composition, turn movement volumes, and other parameters. Higher volumes generally require longer cycle lengths, and larger green time fractions. A two-phase sequence pattern is the most basic scheme and it is extended to more than two phases when there is a large left turn volume. The cycle length can be divided into what may be called the effective green time and the effective red time. Within this work, the number of phases is defined as P; cycle length is defined as C; and the effective green ratio for phase i is defined as g_i/C, $\forall\ i \in P$. Thus, the effective green time and effective red time for an approach given phase i can be defined as

$$g_i = \frac{g_i}{C} C \qquad [3.1]$$

$$r_i = C - \sum_{j \in P \setminus \{i\}} g_j \qquad [3.2]$$

Another important factor in signal design is the vehicle clearance interval. The clearance interval is the duration of amber signal indication provided for vehicles to clear the intersection before cross traffic starts moving. The Traffic Engineering Handbook suggests that the following formula be used to estimate the clearance interval duration [78].

$$Y = t + \frac{1}{2}\frac{v}{a} + \frac{(w+l)}{v} \qquad [3.3]$$

where,

Y = vehicle clearance interval, in seconds,

t = perception-reaction time, in seconds,

v = vehicle approach speed, in feet per second,

a = vehicle deceleration rate, in feet per second^2,

w = intersection width, in feet, and

l = length of vehicle, in feet.

A clearance interval follows every green interval, and it is counted as part of the effective green time in estimating fuel consumption.

The other important factor is the lost time which is defined as queue start-up plus all red time. During the all red time, all vehicles are stopped and consume fuel at an idle fuel consumption rate. During the start-up time, vehicles have low or zero speed. In order to describe fuel consumption behavior within the lost time, one half the lost time is assigned to the effective red time and the other half is assigned to the effective green time.

In current practice, signal control parameters are often based on the objective of minimizing a combination of delay and number of stops. However, this does not guarantee fuel consumption minimization. A fuel consumption model should be able to reflect the impact of these parameters and use them to obtain the optimal signal setting which minimizes fuel consumption.

Roadway Geometric Configurations. Roadway geometric configuration factors include area type, number of lanes, lane width, lane length, existence of exclusive left-turn or right-turn lanes, storage bay length, grades, and parking conditions.

Major factors included in this research are numbers of approaches and lanes, length of inbound and outbound lanes, existence of turning bays, and bay length. These factors are considered within the *intersection influence area* which includes the inbound approach, the intersection itself, and the outbound leg. The intersection influence area is further described in Chapter 4. All other factors are absorbed into the characterization of the saturation flow rate.

Generally, the intersection can have different lane groups using different phases. Vehicles of the same approach move in the same phase are defined as the same lane group, i.e., all straight and turning vehicles are analyzed as the same group if they operate in the same phase, but they will be taken as different groups if the turning vehicles operate in different phase.

The lengths of inbound and outbound leg are critical factors in describing the intersection influence area. It may be the criterion for identifying isolated intersections and determining total

intersection fuel consumption. Lengths of storage bays are important factors when turning movements are high volume.

Other Factors for Fuel Consumption Estimation

In addition to the basic elements described in the previous sections, other factors such as travel time, vehicle speed and acceleration/deceleration profiles, and fuel consumption rates are also important in developing fuel consumption models. These factors are described as follows.

Vehicle Travel Time. As discussed in the literature review, common intersection fuel consumption models are instantaneous models requiring second-by-second data. However, the fuel consumption model proposed in this study is an aggregate model which considers fuel consumption to be dependent upon average travel time. The average travel time T_i for an individual vehicle in the intersection influence area can be expressed as:

$$T_i = \frac{TL_i}{v_i} + D_i \qquad [3.4]$$

where v_i is the average speed without signal delay; Di is the delay caused by signal control; and TL_i is the total traversed roadway length, which is expressed as:

$$TL_i = LIB_j + LOB_k + LINT_{jk} \quad \forall\, i \in N_{jk} \qquad [3.5]$$

where,

N_{jk} = is the set of vehicles traveling from inbound approach j to outbound approach k,

LIB_j = inbound approach length,

LOB_k = outbound leg length, and

$LINT_{jk}$ = intersection width.

Vehicle Speed and Acceleration/Deceleration Profiles. Changes in vehicle speed and acceleration/deceleration have direct effects on fuel consumption. Generally, the higher the speed, the more fuel is consumed. Especially, high fuel consumption is produced when vehicles travel at high speeds with high acceleration rates.

Individual vehicle speed and acceleration/deceleration histories can be obtained through on-road measurement or micro-simulation models, such as the TEXAS model and NETSIM. Several intersection fuel consumption models, described in Chapter 2, are formulated as functions of speed, or speed and acceleration/deceleration. In this research, vehicle speed and

acceleration/deceleration profile models are developed in Chapter 5, and are used to generate AFCM fuel consumption parameters.

Fuel Consumption Rates. Fuel consumption rates corresponding to vehicle speed and acceleration/deceleration could be determined through fuel measurement using instrumental techniques or laboratory experiments. Total fuel consumption depends upon vehicle speed, acceleration/deceleration, and fuel consumption rates. If V_{nt} and a_{nt} represent speed and acceleration/deceleration of vehicle n at time t, ideally, total fuel consumption for the intersection can be expressed as:

$$\sum_{n=1}^{N} \sum_{t=1}^{T_n} f_{nt}(V_{nt}, a_{nt}) \qquad [3.6]$$

where f_{nt} is the fuel consumption rate for vehicle n at time t, T_n is the total time for vehicle n in the intersection influence area, and N is the total number of vehicles.

In this research, fuel consumption rates f_{nt} are obtained from vehicle speed and acceleration/deceleration profiles and their corresponding EPA fuel consumption data. Consequently, fuel consumption at a signalized intersection can be estimated incorporating signal control strategies, traffic characteristics, travel time, and the fuel consumption rates.

MODELING APPROACH

Based on the above discussion, a conceptual idea of the modeling approach is discussed in this section. Effects of the factors discussed in the previous section are illustrated and their contributions to fuel consumption are discussed. Three fundamental relationships are described in this section to illustrate the modeling approach. First, fuel consumption for each individual vehicle within the intersection influence area is investigated. Secondly, average fuel consumption rate is described. The average fuel consumption rate is defined as the average rate for a group of vehicles with similar vehicle maneuvers. Finally, total fuel consumption in the intersection influence area is estimated.

Vehicles and Associated Fuel Consumption

Fuel consumption trajectories represent how vehicles consume fuel within the intersection influence area. Vehicles decelerate to stop before the stop line during a red signal, or continue to move during a green signal. The intersection stop line is a critical factor in differentiating vehicle behavior along the intersection segments; therefore, it is used as a

reference point describing individual vehicle fuel consumption behavior. Figure 3.2 illustrates typical vehicle time-distance trajectories. Each line represents each vehicle movement in the intersection influence area. The inbound approach, the area before the stop line, is depicted on the bottom, and the intersection and outbound leg, the areas beyond the stop line, are depicted on the top. For subsequent cycles, vehicle time-distance and fuel consumption trajectories are considered identical. Therefore, fuel consumption at the end of effective green time in the n^{th} cycle is the same as at the start of effective red time in the $(n+1)^{th}$ cycle.

In Figure 3.2, vehicle 1 stops at the stop line at the start of red time, and vehicles 2 to 9 decelerate to stop and join the stopped queue. After the green starts, these vehicles accelerate crossing the stop line, continue to accelerate to reach their desired speeds on the outbound leg, and travel at desired speeds until they leave the area. This group of vehicles consumes fuel as a function of its trajectory which includes deceleration, idling, acceleration and constant speed operation. Vehicles 10 to 13 decelerate during the red signal, but they might or might not stop depending on whether or not the queued vehicles ahead of them have moved when they approach the stop line. Vehicles 14 to 21 enter the inbound approach after the start of green. They travel at higher speeds than vehicles 1 to 13, but they might decelerate due to the queued vehicles or continue traveling at their desired speeds. Vehicles 16 to 21 cannot cross the stop line before the end of the green time; therefore, they decelerate to a stop. Practically, the trajectories of vehicles 16 to 21 are assumed to be the same as those of vehicles 1 to 6, and the trajectories of vehicles 22 to 27 are assumed to be the same as those of vehicles 7 to 12.

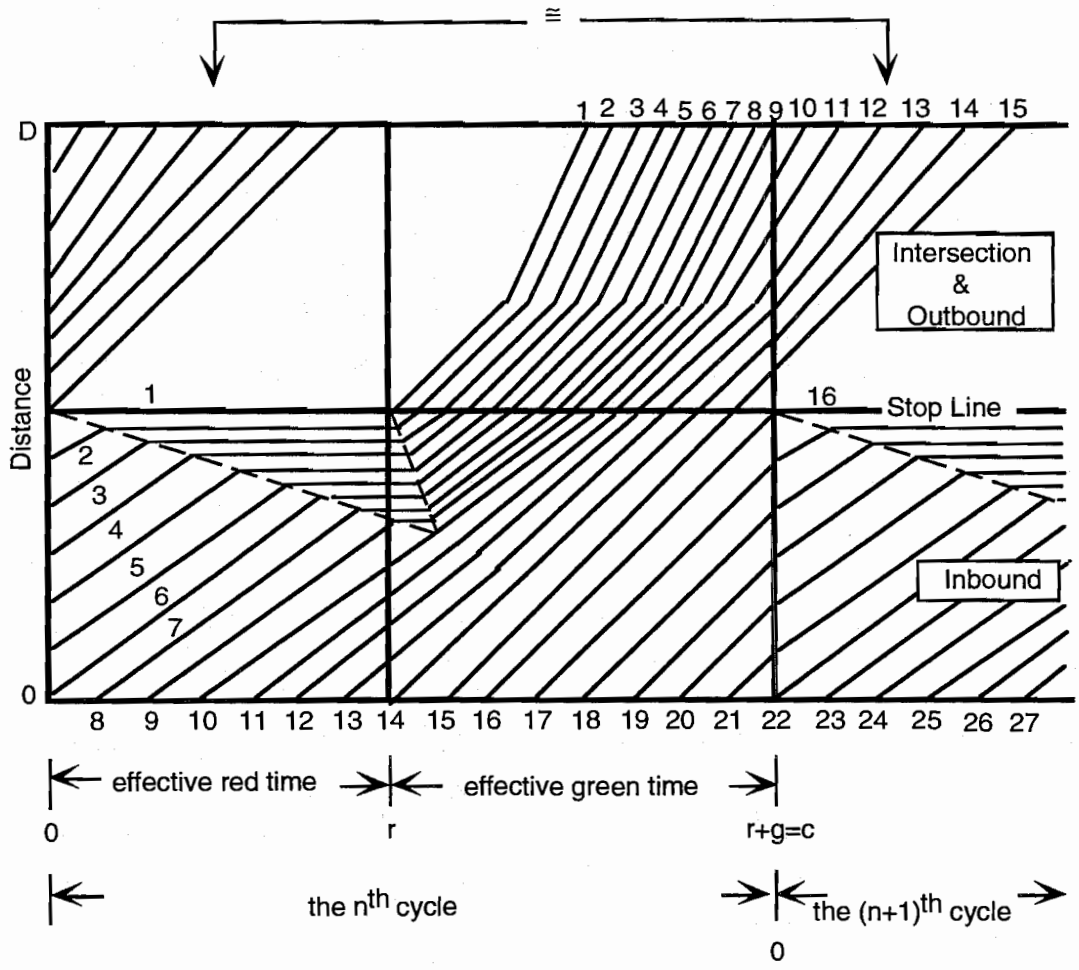

Figure 3.2 Time-distance trajectories of vehicles in the intersection influence area

Based on the above discussion, fuel consumption trajectories for individual vehicles are shown in Figure 3.3. Vehicles 1 to 13 enter the inbound approach during the effective red time. Vehicles 1 to 9 have deceleration fuel consumption and idle fuel consumption after they stop. Vehicles 10 to 13 have deceleration fuel consumption as they approach the stop line, and might have idle fuel consumption due to the queued vehicles ahead of them. After the signal indication turns green, all vehicles accelerate and have acceleration fuel consumption rates as they cross the stop line until they reach their desired speeds and have constant speed fuel consumption rates. Vehicles 14 to 21 enter the inbound approach during the effective green time. They are assumed to have deceleration fuel consumption rates during the first a few seconds of green time, and constant fuel consumption rates after they reach their desired speeds. Vehicles 14 and 15 cross the stop line and continue to have constant speed fuel consumption rates on the outbound leg. However, vehicles 16 to 21 will have deceleration fuel consumption rates after they recognize they cannot cross the stop line within the effective green time.

Fuel consumption trajectories can be investigated in more detail. For example, due to the queued vehicles, vehicle 9 might travel slowly but not completely stop in front of the stop line; vehicle 16 might speed up and enter the outbound leg before the end of green. Moreover, various acceleration/deceleration rates can be investigated in different street segments. Theoretically, the more detailed the fuel consumption behavior that is captured, the more likely the instantaneous fuel consumption trajectories can be developed. As mentioned above, the objective of this research is to define a mathematical function which is able to capture aggregate fuel consumption behavior in the AFCM. Therefore, fuel consumption trajectories for groups of vehicles are investigated and described as follows.

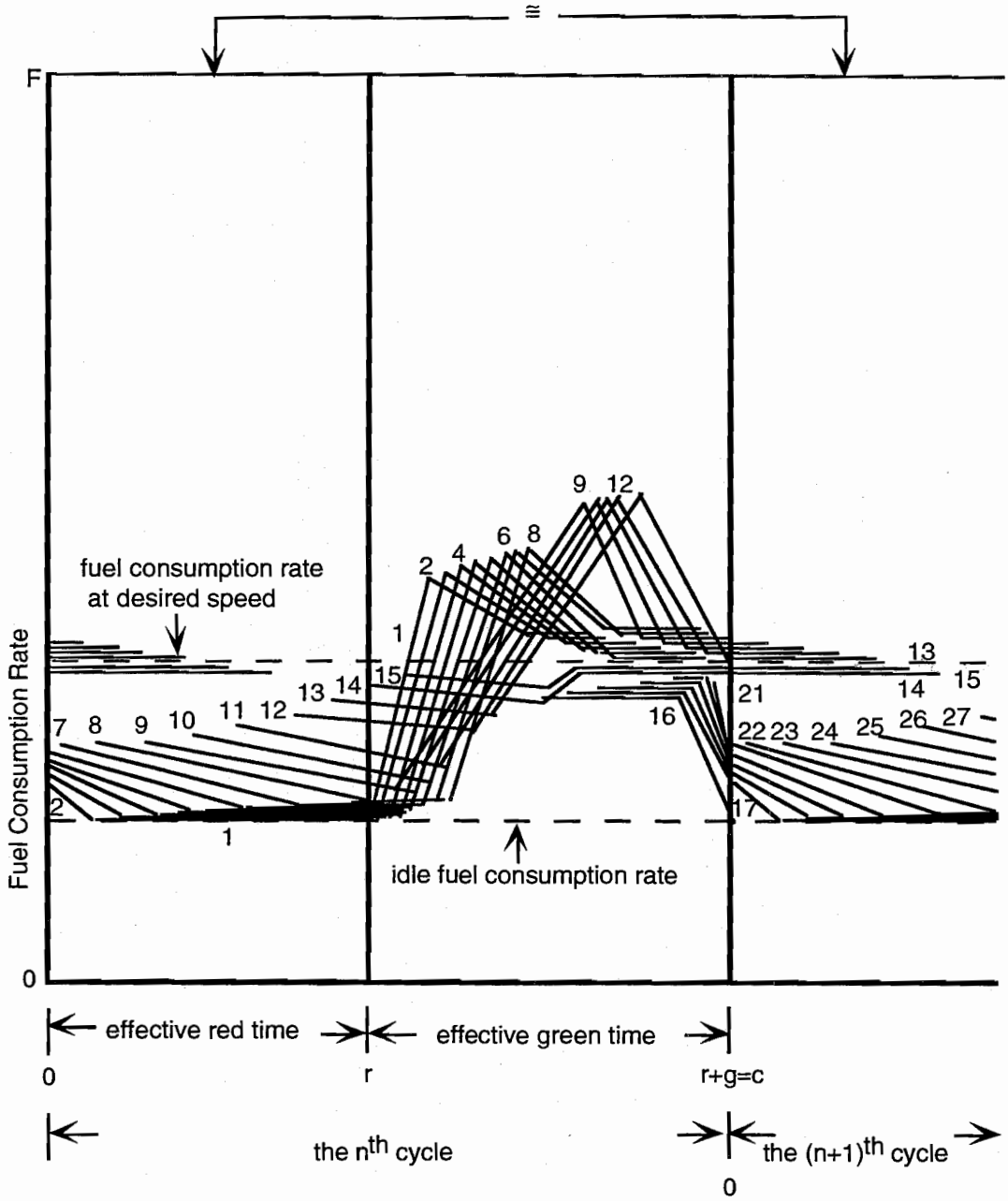

Figure 3.3 Individual fuel consumption trajectories of vehicles in the intersection influence area

Average Fuel Consumption Rate

Since the objective of the AFCM development aims at using an aggregate approach to estimate fuel consumption, aggregate fuel consumption trajectories are investigated to describe fuel consumption for vehicle groups. Figures 3.4 and 3.5, follow the description of Figure 3.3, depict aggregate fuel consumption trajectories before and beyond the stop line, respectively.

In Figure 3.4, lines A, B, C, and D depict fuel consumption trajectories for vehicles entering the inbound approach during the effective red time. Line A represents idle fuel consumption for vehicles 1 to 9, and line C represents a deceleration fuel consumption trajectory for vehicles 2 to 13 as they approach the stop line. After vehicles start to move, fuel consumption rates dramatically increase, and the results can be observed from line B and D in the effective green time. Line E and F depict fuel consumption trajectories for vehicles 14 to 21 entering the inbound approach after the start of green. Line E and F are assumed to be different because vehicles will move smoothly after desired speeds have been reached.

In practice, due to different traffic situations, fuel consumption trajectories are not necessarily identical to those depicted in Figure 3.4. At certain times, line A might be higher than line C, and line E might be lower than line A. Furthermore, these lines might not be straight but could be complex curves.

In Figure 3.5, lines G and J are respectively connected to lines B and D in Figure 3.4. Generally, lines B, G, and H represent fuel consumption trajectories for vehicles which have been stopped during the effective red time, and lines D, J, and K depict fuel consumption trajectories for vehicles which join moving queues. After vehicles have reached their desired speeds, their fuel consumption trajectories are represented as line I. Line I should be similar to line F in Figure 3.4.

Since vehicles accelerate as they enter the outbound leg, the fuel consumption trajectories are higher than those on the inbound approach. Also, like the situations described on the inbound approach, the fuel consumption trajectories are not necessarily equal to those depicted in Figure 3.5.

From the above discussion, the critical factors for differentiating aggregate fuel consumption behavior are the effective red time, the effective green time, and the time and position of vehicles in the intersection influence area. By following vehicle time-distance and fuel consumption trajectories, the AFCM can be developed and total fuel consumption can be estimated.

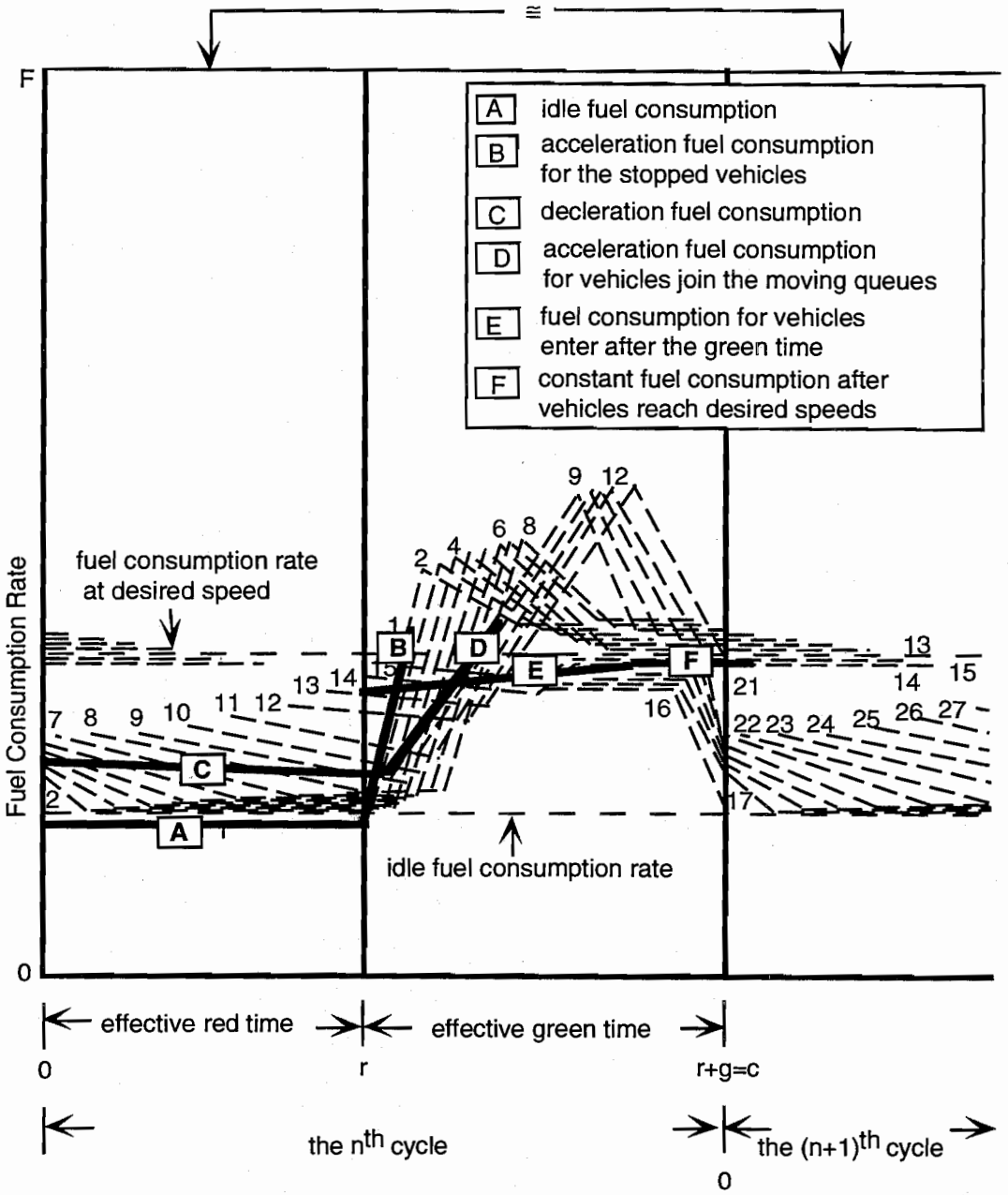

Figure 3.4 Aggregate fuel consumption trajectories of vehiclesbefore the stop line (inbound approach)

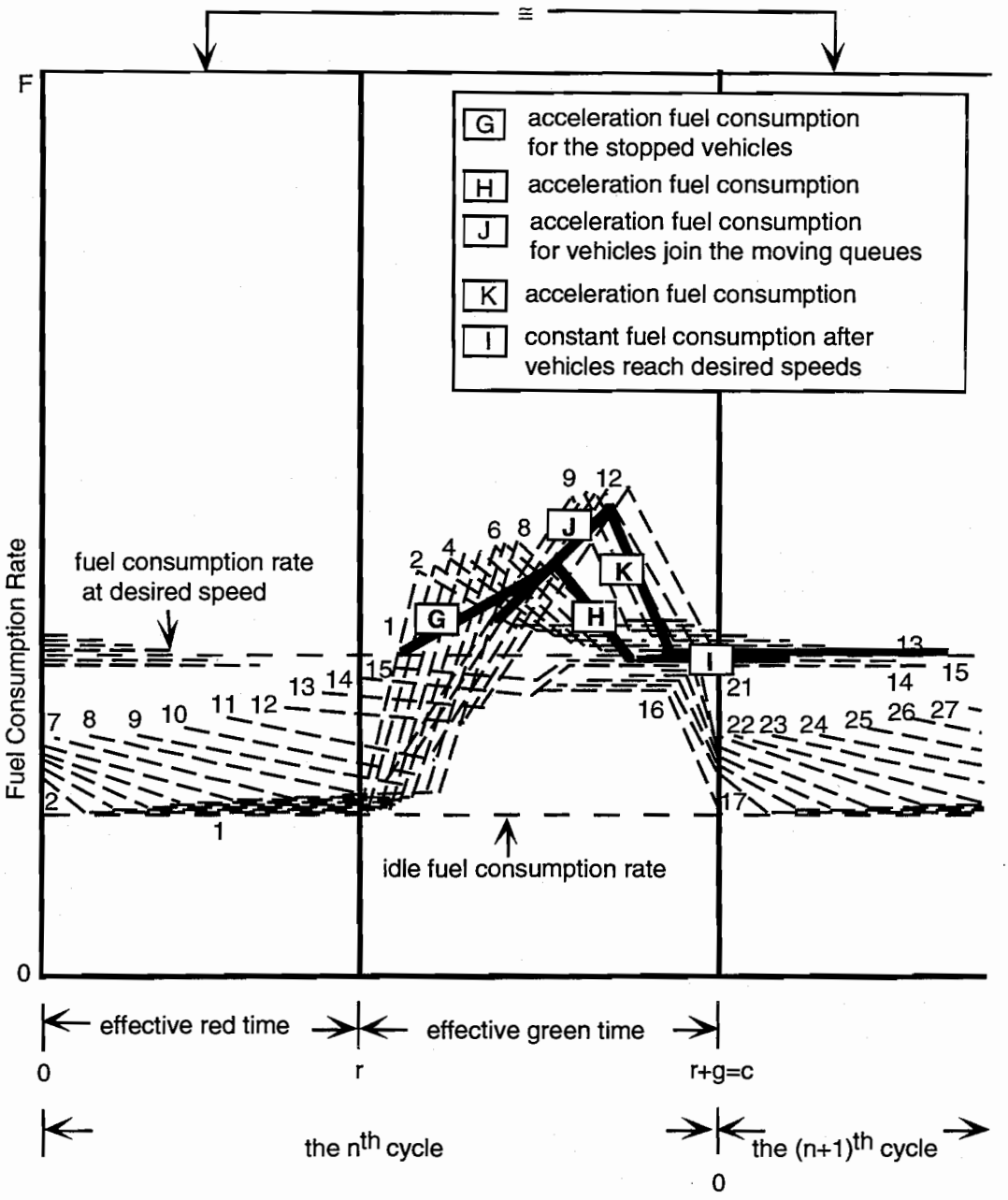

Figure 3.5 Aggregate fuel consumption trajectories of vehiclesbeyond the stop line (intersection and outbound leg)

Total Fuel Consumption Estimation

Since fuel consumption trajectories vary with time in the intersection influence area, the AFCM development and total fuel consumption estimation are based on the critical factors "time" and "position" in the intersection influence area.

The "time" in a pretimed signal cycle is initially separated into two cycle stages: the effective red time and the effective green time. Since fuel consumption rates are different during different parts of the effective green time, it is divided into two parts: the time from green onset to time t_0, during which vehicles cross the stop line at saturation flow rates, and the time from t_0 to the end of the effective green. The "position" in the intersection influence area is first divided into two segments: the area before the stop line (inbound approach) and the area after the stop line (intersection and outbound leg). However, the area after the stop line is separated into the intersection itself and the outbound leg due to the effects of turning movements. Vehicle operations and representative fuel consumption trajectories for each cycle stage and intersection segment are summarized in Table 3.1. Two intersection segments, one before the stop line and the other after the stop line, are illustrated as two tables. Within each table, vehicle maneuvers and associated fuel consumption trajectory lines are differentiated by three cycle stages.

On the inbound approach, vehicles decelerate to stop with fuel consumption trajectory C and consume idle fuel consumption rate A after stopping during the effective red time. After the start of green, vehicles use either B or D depending on their acceleration situations; however, arriving vehicles might have fuel consumption trajectory E due to queued vehicles ahead of them. After time t_0, all queued vehicles have been dissipated, and vehicles travel at desired speeds with fuel consumption trajectory F.

Vehicle fuel consumption rates after the stop line are usually higher than those on the inbound approach because vehicles accelerate crossing the stop line, i.e., fuel consumption trajectories G, H, J, and K should be higher than B and D. After time t_0, some vehicles reach their desired speeds with fuel consumption trajectory I which is assumed to be equal to F in Figure 3.4, but some vehicles might still try to reach their desired speeds with fuel consumption rates from H or K. No vehicle can cross the stop line during the red signal; however, remaining vehicles continue to move on the outbound leg with fuel consumption trajectory I, H, or K.

Fuel consumption on each street segment for each cycle stage, therefore, can be estimated from the number of vehicles, the travel time, and the fuel consumption rate from the corresponded trajectories, i.e.,

$$FC_{ij} = q_{ij}\, t_{ij}\, FF_{ij} \qquad [3.7]$$

and total fuel consumption in the intersection influence area can be obtained from:

$$\sum_i \sum_j FC_{ij} = \sum_i \sum_j q_{ij}\, t_{ij}\, FF_{ij} \qquad [3.8]$$

where,

FC_{ij} = fuel consumption on street segment i for cycle stage j with average fuel consumption rate FF_{ij},

q_{ij} = number of vehicles on street segment i for cycle stage j,

t_{ij} = vehicle travel time on street segment i for cycle stage j, and

FF_{ij} = average fuel consumption rate on street segment i for cycle stage j.

The values of FF_{ij} can be estimated from the average of the instantaneous fuel consumption rate $f_{nt}(V_{nt}, a_{nt})$, which is described in Section 3.2.3.

$$FF_{ij} = \left[\sum_{n=1}^{q_{ij}} \sum_{t=1}^{t_{ij}} f_{nt}(V_{nt}, a_{nt}) \right] / q_{ij}\, t_{ij} \qquad [3.9]$$

However, due to the nature of the aggregate model, the fuel consumption rates FF_{ij} are obtained from the aggregate fuel consumption trajectories A to I.

Based on the above discussion, the aggregate model AFCM can be developed and total fuel consumption can be estimated. Detailed descriptions of the AFCM and fuel consumption estimation are discussed in the following chapters.

TABLE 3.1 VEHICLE BEHAVIOR AND FUEL CONSUMPTION TRAJECTORIES ON EACH STREET SEGMENT FOR DIFFERENT CYCLE STAGES

		Fuel Consumed Before the Stop Line (Inbound)		
		Traffic Characteristics	Fuel Consumption Trajectory	
The Effective Red Time		Vehicles stop	A	
		Vehicles decelerate to stop	C	
The Effective Green Time	Green Onset to Time t0	Stopped vehicles start to move	B	
		Non-stopped vehicles accelerate	D	
		Vehicles enter after the green time	E	
	Time t0 to the Effective Green End	Vehicles reach desired speeds	F	
		Fuel Consumed After the Stop Line		
		Traffic Characteristics	Fuel Consumption Trajectory	
			Intersection	Outbound
The Effective Red Time		No vehicle cross the intersection	None	None
		Remaining vehicles is leaving	None	I
The Effective Green Time	Green Onset to Time t0	Vehicles accelerate	G	G or H
		Vehicles accelerate to reach desired speeds	J	J or K
	Time t0 to the Effective Green End	Vehicles reach desired speeds or continue to reach desired speeds	I	I (or H, K)

CHAPTER 4. DEVELOPMENT OF THE ANALYTICAL FUEL CONSUMPTION MODEL (AFCM)

INTRODUCTION

As discussed in Chapter 2, most existing intersection fuel consumption models are developed based on instantaneous data. In these models, vehicle speed-acceleration-deceleration profiles are utilized, and Monte Carlo simulation is applied to estimate fuel consumption. However, fuel consumption is not directly considered in the models, but reflected through vehicle movement due to the traffic signals.

In this study, an alternative fuel consumption model, the Analytical Fuel Consumption Model (AFCM), is proposed to estimate fuel consumed at the intersection in order to encompass two important features. First, the relationship among fuel consumption, traffic characteristics, and traffic signal parameters is explicitly considered; therefore, this model directly considers impacts of both traffic control measures and traffic flow characteristics on fuel consumption. Second, the process yields a direct fuel consumption estimate that does not require simulation or solutions of complex mathematical formulations. Therefore, the AFCM focuses on the underlying processes of how signal control parameters affect fuel consumption and how vehicles consume fuel while approaching and leaving intersections. In order to explain these processes, the AFCM development is based on three street segments (inbound approach, intersection itself, and outbound leg) for three cycle stages (the effective red time, time from green onset to time t_0, and time from t_0 to the effective green time end). A uniform and deterministic arrival flow pattern is assumed for development of the basic AFCM, then AFCM is extended to include stochastic effects.

Basic assumptions and definitions, including terminology and notations used in this study, are defined and explained in Section 4.2. The AFCM is discussed in Section 4.3 and the extension of the AFCM to include overflow queues is described in Section 4.4. A brief summary is given in Section 4.5.

BASIC ASSUMPTIONS AND DEFINITIONS

Basic assumptions on geometric configurations, signal control strategies, and traffic conditions are discussed in Sections 4.2.1 to 4.2.3, and notations used in this study are defined in Section 4.2.4.

Geometric Configurations

The AFCM is developed for isolated traffic intersections. The confines of the intersection area include the inbound approaches, the intersection itself, and the outbound legs of all intersection legs. This area, called the *intersection influence area*, is depicted in Figure 4.1 which shows an isolated intersection with four legs and one inbound and outbound lane on each leg. The beginning of each inbound approach is the point where most vehicles start to decelerate upon seeing a red signal and the terminus of the outbound leg is the point where most vehicles complete their accelerations after they pass the stop line. Therefore, the lengths of inbound and outbound legs are based on speed limits, traffic characteristics, and signal controls.

The isolated intersections considered can have any configuration within the intersection influence area. However, approach grades are not considered, and parking in the intersection vicinity is not explicitly considered.

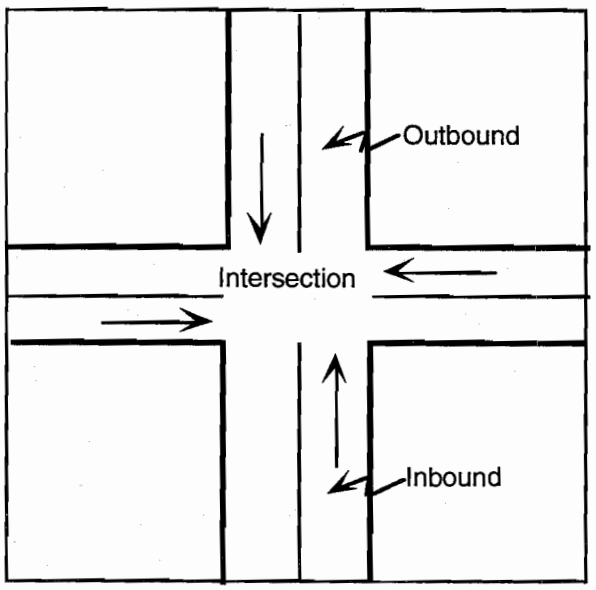

Figure 4.1 Intersection influence area for the AFCM development

Signal Control Strategies

Pretimed signal control is assumed for AFCM development. The pretimed signal cycle is separated into three stages: effective red time ($0 \le t \le r$), time from green onset to time t_0 ($r < t \le r+t_0$) (t_0 is the time from the start of green until the queue is dissipated), and time from t_0 to the end

of the effective green ($r+t_0 < t \leq r+g = C$). Vehicle operations for each cycle stage are briefly described as follows:

1 Effective red time ($0 \leq t \leq r$)

Vehicles on the inbound approach decelerate to stop before the stop line and the number of queued vehicles increases as vehicles arrive. Vehicles in the intersection and on the legs continue to move until they leave the system.

2 Time from green onset to time t_0 ($r < t \leq r+t_0$)

On the inbound approach, queued vehicles start to move, accelerating across the stop line, being discharged at the saturation flow rate until the queue is dissipated. Concurrently, some vehicles enter the system traveling into the intersection influence area.

3 Time from t_0 to the end of the effective green ($r+t_0 < t \leq r+g = C$)

After time t_0, all queued vehicles have been discharged; therefore, vehicles are assumed to travel at desired speeds passing through the intersection and the outbound leg.

Traffic Conditions

Traffic characteristics are described using an arrival flow rate and an arrival flow distribution. The major effect of the arrival flow rate in fuel consumption estimation is the number of vehicles considered in the estimation process. On the other hand, the arrival flow pattern affects how queues are formed and discharged. Section 4.3 focuses on the AFCM with the assumption of a uniform, deterministic arrival flow pattern. Extensions of the AFCM to include stochastic effects are discussed in Section 4.4. The arrival flow rate is expressed in terms of passenger car units (pcu's), and there are no particularly conservative or aggressive drivers.

Definitions and Terms

Variables and notation used throughout this study are defined and explained in this section. The estimation of fuel consumption for a vehicle through the intersection influence area involves how the vehicle moves in the intersection influence area, and how signal control affects the movements. Thus, the total fuel consumed by a vehicle includes the aggregation of fuel consumed through the inbound approach, intersection, and outbound leg. Vehicles can be

either moving or stopped. Stopped vehicles have decelerated to zero speed in response to a red signal. They begin moving as they accelerate passing the stop line in response to the green signal. If moving vehicles do not receive a red signal they move continuously without stopping. Vehicles approaching the stop line with speeds less than 5 mph are considered as stopped vehicles.

Notations used in the AFCM are defined as follows:

N_S: Number of stopped vehicles

N_m: Number of moving vehicles

q: average flow rate on the approach (vehicle/sec)

s: saturation flow rate on the approach (vehicle/sec)

y: q / s (flow ratio of the approach)

x: qc / gs (degree of saturation of the approach)

C: cycle time (sec), C = r + g

r: effective red time (sec)

g: effective green time (sec)

t_0: after the green time starts, at time t_0 the arrivals equal the discharge

D_{ib}: length of inbound approach

D_{ob}: length of outbound leg

T_{ij}: average travel time for vehicles moving on street segment i in cycle stage j

T_{11}: average travel time on the inbound approach in the effective red time

T_{13}: average travel time on the inbound approach from time t_0 to the end of the effective green

t: average time for vehicles to traverse the outbound leg

k: time for the first vehicle to enter the outbound leg from the stop line

r_1: elapsed time required for all vehicles to leave the outbound leg after the end of green

V_i: vehicle speed i

f_{ij}: average fuel consumption rate for vehicles moving from speed V_i to V_j

f_0: idle fuel consumption rate

f_r: vehicle fuel consumption rate for desired speed V_r

F_{ij}: fuel consumption at any instant on street segment i in cycle stage j

F_{ij}^{q}: fuel consumption at any instant on street segment i in cycle stage j (consider queue distribution and queue length under the condition that queue departure time is less than the green time)

F_{ij}^{qd}: fuel consumption at any instant on street segment i in cycle stage j (consider queue distribution and queue length under the condition that queue departure time is equal to green time and all queued vehicles are discharged)

F_{ij}^{qq}: fuel consumption at any instant on street segment i in cycle stage j (consider queue distribution and queue length under the condition that queue departure time is equal to green time and queued vehicles are not discharged completely)

TF_{ij}: total fuel consumption on street segment i in cycle stage j

TF_{ij}^{q}: total fuel consumption on street segment i in cycle stage j (consider queue distribution and queue length under the condition that queue departure time is less than the green time)

TF_{ij}^{qd}: total fuel consumption on street segment i in cycle stage j (consider queue distribution and queue length under the condition that queue departure time is equal to green time and all queued vehicles are discharged)

TF_{ij}^{qq}: total fuel consumption on street segment i in cycle stage j (consider queue distribution and queue length under the condition that queue departure time is equal to green time and queued vehicles are not discharged completely)

STF: total fuel consumption during a cycle in the intersection influence area

THE ANALYTICAL FUEL CONSUMPTION MODEL (AFCM) WITH DETERMINISTIC ARRIVALS

Basic Idea

In this section, a simple example is used to illustrate how to describe vehicle movements at signalized intersections. Figure 4.2 shows how a queue is formed and discharged, assuming continuous arrival flow. This figure represents the behavior when the capacity of the green interval exceeds the number of arriving vehicles during the green plus red time. The vertical axis represents the cumulative number of vehicles, and the horizontal axis represents the time.

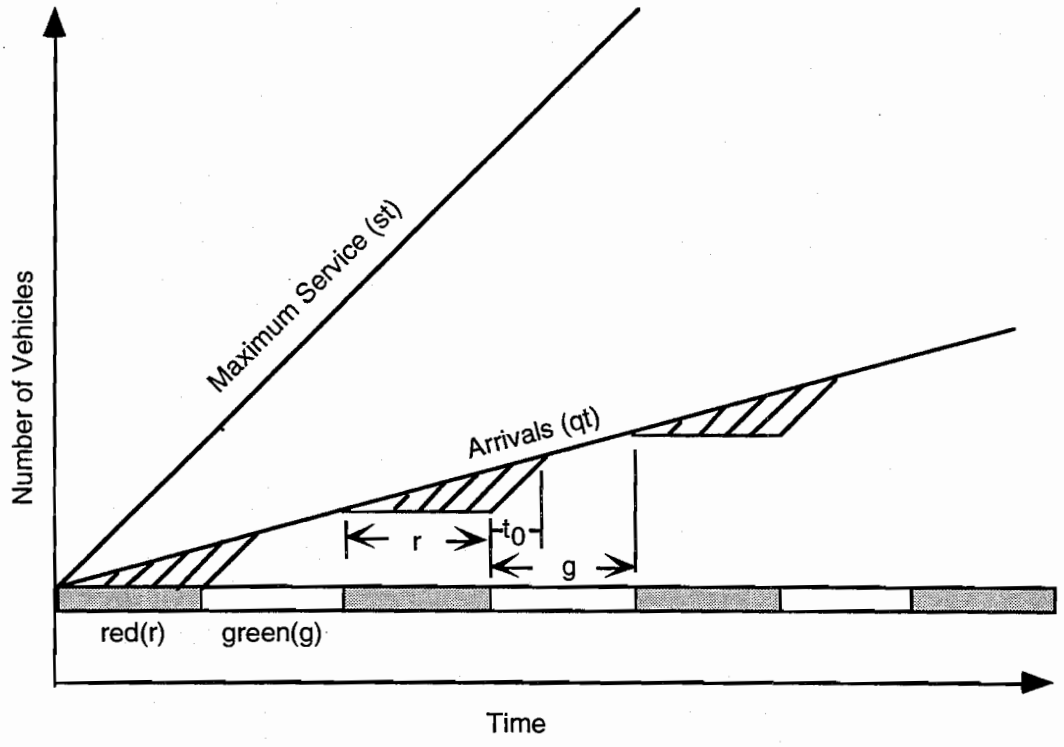

Figure 4.2 Representation of queuing at a signalized intersection (87)

Formulas could be developed to express simple relationships between signals and arrival flow in Figure 4.2. For any given cycle, during the time t_0 after the start of green the accumulated number of vehicles plus new arrivals equals the total discharge, i.e., $q(r+t_0) = st_0$ and $t_0 = \frac{q}{s}r/(1-\frac{q}{s}) = yr/(1-y)$. The average number of vehicles in the queue during a cycle is:

$$\overline{Q} = \frac{(qr/2)r + (qr/2)t_0 + 0(g-t_0)}{r+t_0+g-t_0} = [(r+t_0)/c]\,(qr/2) \qquad [4.1]$$

The total vehicle-time of delay is given by the area of the triangle and is defined as:

$$D = \frac{1}{2}(r+t_0)\,qr = \frac{qr^2}{2(1-y)} \qquad [4.2]$$

The average individual delay is given by dividing the total delay by the number of vehicles:

$$d = \frac{D}{qc} = \frac{r^2}{2c(1-y)} \qquad [4.3]$$

In these simple formulas, the number of vehicles in a queue and vehicle delay could be calculated; however, fuel consumption and delay characteristics are different due to the high fuel

consumption rate during acceleration. Therefore, the inbound approach as well as the intersection and outbound leg must be considered as a whole.

The Analytical Fuel Consumption Model (AFCM) considers three intersection street segments (inbound approach, intersection itself, and outbound leg) and three cycle stages. In this section, the arrival pattern is assumed to be uniform, with deterministic arrivals [64]. Note that the basic model considers only undersaturated flow conditions, and no overflow queues exists in any cycle. In an ideal undersaturated flow situation, queued vehicles are cleared during the next available green. However, this condition will be relaxed in a more general model described in Section 4.4 which considers overflow queues for both undersaturated and oversaturated conditions. Table 4.1 shows the symbols and notations used in AFCM for the three street segments and cycle stages.

TABLE 4.1 SYMBOLS USED IN THE AFCM

	Inbound	Intersection	Outbound
Effective Red time	F_{ib-1} TF_{ib-1}	F_{int-1} TF_{int-1}	F_{ob-1} TF_{ob-1}
Time from Green Onset to Time t_0	F_{ib-2} TF_{ib-2}	F_{int-2} TF_{int-2}	F_{ob-2} TF_{ob-2}
Time from t_0 to the End of Green	F_{ib-3} TF_{ib-3}	F_{int-3} TF_{int-3}	F_{ob-3} TF_{ob-3}

Inbound Approach Fuel Consumption Model

On the inbound approach, vehicles arriving during the effective red time must decelerate and stop; therefore, two different vehicle maneuvers are considered in the model, namely, deceleration and idling. From the green onset to time t_0, queued vehicles are discharged at the saturation flow rate. In the last cycle stage from time t_0 to the end of green, all queued vehicles have been discharged; therefore, vehicles are assumed to travel at their desired speeds. Vehicle inbound approach fuel consumption can be estimated based on the vehicle maneuvers during the cycle stages and corresponding fuel consumption rates. Detailed descriptions of the AFCM development and fuel consumption estimation on the inbound approach are discussed according to three cycle stages.

(1) The effective red time ($0 \leq t \leq r$)

During the effective red time, arriving vehicles decelerate and stop on the inbound approach. The number of queued vehicles increases with the elapsed red time. These queued vehicles have zero speed V_0 with corresponding idle fuel consumption rate f_0. Moving vehicles continue to enter the inbound approach. traveling at desired speeds, V_r, and decelerate to stop joining the vehicle queue. The average fuel consumption rate for speeds changing from V_r to V_0 is f_{r0}. Fuel consumption $F_{ib\text{-}1}$ at any time can be expressed as:

$$\begin{aligned} F_{ib\text{-}1} &= (\text{queued vehicles})f_0 + (\text{arriving vehicles})f_{r0} \\ &= N_s f_0 + N_m f_{r0} \\ &= qt f_0 + qT_{11} f_{r0} \end{aligned} \qquad [4.4]$$

In Equation 4.4, the total number of vehicles on the inbound approach is expressed as N_s queued vehicles and N_m moving vehicles, and corresponding fuel consumption rates are f_0 and f_{r0}. Assuming the arrival flow rate (vehicles/second) is q, N_s can be calculated as qt. T_{11} is defined as the free flow travel time for a vehicle traveling from the start of the inbound approach to the stop line and is used to characterize the inbound approach geometric configuration. Therefore, qT_{11} can be used to represent the number of moving vehicles currently on the inbound approach preparing to join the queue. During the first seconds of effective red time, there may be no queued vehicles, but there will usually be moving vehicles approaching the intersection. T_{11} can be estimated by:

$$\begin{aligned} T_{11} &= \frac{D_{ib} - (\frac{N_s \bullet L}{n})}{D_{ib}} T_{ib} \\ &= (1 - \frac{N_s \bullet L}{S}) T_{ib} \end{aligned} \qquad [4.5]$$

where,

D_{ib}= inbound approach length,

n = number of lanes,

L= average queue space per vehicle, and

$T_{ib} = \frac{D}{V}$, free flow travel time for the inbound approach.

The total fuel consumption $TF_{ib\text{-}1}$ can thus be estimated by the following:

$$TF_{ib\text{-}1} = \int_0^r [qt f_0 + qT_{11} f_{r0}]\, dt$$

$$= \int_0^r [qt\, f_0 + q\,(1 - \frac{N_S \bullet L}{S})\, T_{ib}\, f_{r0}]\, dt$$

$$= \frac{1}{2} qr^2 f_0 + [q\,(r - \frac{qr^2 \bullet L}{2S})\, T_{ib}]\, f_{r0}$$

$$= \frac{1}{2} qr^2 f_0 + [q\, r\,(1 - \frac{qr \bullet L}{2S})\, T_{ib}]\, f_{r0} \qquad [4.6]$$

Equation 4.6 expresses the integration of Equation 4.4 with respect to the time period, 0 to r. In this presentation, the total fuel consumption during this cycle stage on the inbound approach is estimated through the arrival flow rate q, signal control strategies r, fuel consumption rate f, and the geometric configuration indicator T_{ib}. The first term indicates that fuel consumption of stopped vehicles increases proportionally with respect to flow rate q, the effective red time r, and idle fuel consumption rate f_0. The second term indicates that fuel consumption of moving vehicles is composed of the number of moving vehicles, the effective red time r, average travel time T_{ib}, and fuel consumption rate f_{r0} for the deceleration process from speed V_r to idle V_0. In order to obtain reasonable results, the condition $(1 - \frac{qr \bullet L}{2S})$ needs to be positive and it indicates the condition, $2S \geq qr \bullet L$, must hold. Detailed experimental analysis is discussed in Chapter 6.

(2) Time from green onset to time t_0 $(r < t \leq r+t_0)$

In this cycle stage, queued vehicles and newly arriving vehicles are discharged at the saturation flow rate. Queued vehicles are assumed to accelerate to average speed V_2 when they cross the stop line with corresponding average fuel consumption rate f_{02}. Arriving vehicles, discharged at the saturation flow rate, travel at higher speeds on the inbound approach. These vehicles have initial speed V_r and either decelerate when they recognize the existence of queued vehicles, or travel at their desired speeds after the queues have been discharged. These arriving vehicles are assumed to pass the stop line at speed V_3. Therefore, fuel consumption $F_{ib\text{-}2}$ at any instant in time is:

$$F_{ib\text{-}2} = (\text{queued vehicles})\, f_{02} + (\text{arriving vehicles})\, f_{r3}$$

$$= (qr + qt - st)\, f_{02} + qT_{12}\, f_{r3} \qquad [4.7]$$

Total fuel consumption is:

$$TF_{ib\text{-}2} = \int_0^{t_0} F_{ib\text{-}2}\, dt \qquad [4.8]$$

According to the definition of t_0, at time t_0 the arrivals equal the discharge, i.e., $qr + qt_0 = st_0$ and $t_0 = qr/(s-q)$. However, the queued vehicles from the effective red time and queuing

vehicles from the start of green onset might have different fuel consumption behavior. A variable t_q, defined as the time for queued vehicles to discharge, i.e., $qr = st_q$ and $t_q = qr/s$, is introduced to differentiate vehicle fuel consumption behavior from green onset to time t_q and from time t_q to time t_0. Therefore, $F_{ib\text{-}2}$ is modified as:

$$\begin{aligned} F_{ib\text{-}2} &= \text{(queued vehicles) } f_{02} + \text{(arriving vehicles within } t_q) f_{r2} + \\ &\quad \text{(queuing vehicles) } f_{03} + \text{(arriving vehicles after } t_q) f_{r3} \\ &= (qr\text{-}st)\, f_{02} + qt\, f_{r2} + qT_{12}\, f_{r2} \qquad \text{if } r \le t \le r+t_q \\ &= (qt_q+qt\text{-}st)\, f_{03} + qT_{12}\, f_{r3} \qquad \text{if } r+t_q < t \le r+t_0 \end{aligned} \qquad [4.9]$$

where,

$$T_{12} = \begin{cases} \dfrac{[D_{ib} - (qr + qt - st)L/n]\, T_{ib}}{D_{ib}} & \text{if } r \le t \le r+t_q \\ \dfrac{[D_{ib} - (qt_q + qt - st)L/n]\, T_{ib}}{D_{ib}} & \text{if } r+t_q < t \le r+t_0 \end{cases} \qquad [4.10]$$

In Equation 4.9, (qr-st) describes the queued vehicles which discharge with speeds changing from V_0 to V_2 within time t_q and have fuel consumption rate f_{02}; and (qt_q+qt-st) indicates the queuing vehicles which discharge with speeds changing from V_0 to V_3 after time t_q and have fuel consumption rate f_{03}. The arriving vehicles have initial speed V_r and either decelerate to join the moving queue or continue to move with fuel consumption rates f_{r2} before t_q and f_{r3} after t_q. In this expression, the total fuel consumption depends significantly upon t_q and t_0. Also, average fuel consumption rates at this stage are usually high because vehicles are accelerating as they pass the stop line.

(3) Time from t_0 to the end of the effective green ($r+t_0 < t \le r+g = c$).

During this cycle stage, arriving vehicles are not interrupted by signal control; thus these vehicles are assumed to travel according to their desired speeds V_r. At any instant during this cycle stage, fuel consumption $F_{ib\text{-}3}$ can be expressed as:

$$\begin{aligned} F_{ib\text{-}3} &= \text{(moving vehicles) } f_r \\ &= qT_{13}\, f_r \end{aligned} \qquad [4.11]$$

In order to estimate fuel consumption by all vehicles, a geometric configuration indicator T_{13} is used to count the possible number of vehicles on the outbound leg. T_{13} is estimated as the traversed distance divided by V_r; thus the total fuel consumption can be expressed as:

$$TF_{ib-3} = \int_{t_0}^{g} qT_{13} f_r \, dt$$

$$= q T_{13} f_r (g - t_0) \qquad [4.12]$$

In Equation 4.12, the fuel consumption is evaluated by flow rate, a geometric indicator, a fuel consumption rate for running vehicles, and a signal timing parameter ($g - t_0$). The whole term must be greater than 0, so the condition $g \geq t_0$ is imposed. This constraint identifies an undersaturation situation. Although possible speed fluctuations might occur, the model could still estimate the fuel consumption without loss of generality.

Intersection Fuel Consumption Model

In this section, the fuel consumption model for the intersection is developed. Major considerations include how vehicles accelerate and speeds with which they pass through the intersection. When the signal changes to green, queued vehicles on the inbound approach accelerate and enter the intersection. From green onset to time t_0, vehicles enter the intersection at the saturation flow rate and follow certain acceleration trajectories. Although the length of the intersection is relatively short compared to the inbound and outbound legs, the total fuel consumption is important because of the high fuel-consumption rate during the acceleration process.

(1) The effective red time ($0 \leq t \leq r$)

During this cycle stage, vehicles cannot enter the intersection, thus total fuel consumption due to vehicles from the considered approach in the intersection itself TF_{int-1} is zero.

(2) Time from green onset to time t_0 ($r < t \leq r+t_0$)

Vehicles are discharged from the stop line according to the saturation flow rate after the start of green, and fuel consumption is estimated through corresponding fuel consumption trajectories. Queued vehicles and arriving vehicles might have different speeds when crossing the stop line, thus these two vehicle trajectories are differentiated in order to accurately capture acceleration profiles. It is assumed that queued vehicles enter the intersection with initial average speed V_2 and accelerate to speed V_4 until they reach the beginning of the outbound leg. Similarly, arriving vehicles have an initial average speed V_3 and accelerate to speed V_5.

Vehicles in the intersection include those accelerating from a queue and those that did not stop before entering. Fuel consumption at any instant in time in this stage F_{int-2} is given by:

F_{int-2} = (queued vehicles) f_{24} + (moving vehicles) f_{35}

$$= st\, f_{24} \qquad \text{if } r < t \le r+k$$

$$= sk\, f_{24} \qquad \text{if } r+k < t \le r+t_q$$

$$= sk\, f_{35} \qquad \text{if } r+t_q < t < r+t_0 \qquad [4.13]$$

where k is a time lag to indicate the travel time for the first vehicle from the stop line to the beginning of the outbound leg, and is used to describe the geometric intersection configuration. The total fuel consumption is:

$$TF_{int\text{-}2} = \int_0^{t_0} F_{int\text{-}2}\, dt$$

$$= \int_0^{k} st\, f_{24}\, dt + \int_k^{t_q} sk\, f_{24}\, dt + \int_{t_q}^{t_0} sk\, f_{35}\, dt$$

$$= \frac{1}{2} sk^2 f_{24} + sk\, f_{24} (t_q - k) + sk\, f_{35} (t_0 - t_q) \qquad [4.14]$$

The three terms in Equation 4.14 represent fuel consumption during three time intervals from time zero to time equal t_0. The first integral shows fuel consumption while the first few vehicles cross the intersection. The second term shows fuel consumption while the intersection is filled with vehicles (saturated). The third term is similar to the second, but with a different fuel consumption rate since vehicles leave in contributing to fuel consumption during this time.

(3) Time from t_0 to the end of the effective green ($r+t_0 < t \le r+g = c$)

After t_0, queued vehicles and vehicles arriving within t_0 have been discharged. Arriving vehicles are not affected by signal operation, and are assumed to travel at desired speeds V_r and to have fuel consumption rate f_r. Fuel consumption at the intersection itself $F_{int\text{-}3}$ at any time instant is:

$$F_{int\text{-}3} = (\text{moving vehicles})\, f_r$$

$$= qk\, f_r \qquad [4.15]$$

and total fuel consumption is:

$$TF_{int\text{-}3} = \int_{t_0}^{g} qk\, f_r\, dt$$

$$= qk\, f_r\, (g - t_0) \qquad [4.16]$$

In this representation, arriving vehicles are assumed to travel at their desired speed, and the number of vehicles in the intersection is estimated by qk. The variable k represents the average travel time across the intersection and might be a little greater than the k described earlier; however, the same notation is still used to maintain consistency.

Outbound Leg Fuel Consumption Model

The number of vehicles on the outbound leg depends on the length of the outbound leg, and the numbers of vehicles entering and leaving the outbound leg. Vehicles that have not exited the outbound leg by the end of the green time will affect the fuel consumption during the effective red time of the next cycle. The discussion of fuel consumption estimation in this section begins with the time from green onset to time t_0 ($r < t \leq r+ t_0$).

Since most fuel is consumed during the period when vehicles accelerate to reach their desired speeds, the analysis of the outbound leg is critical to fuel consumption estimation.

(1) Time from green onset to time t_0 ($r < t \leq r+t_0$)

In this cycle stage, vehicles try to reach their desired speed V_r after being stopped by signal control. The number of vehicles at any time on the outbound leg is the difference between the number of entering and exiting vehicles. In this discussion, t is used to indicate the average travel time for the outbound leg, and is estimated by D_{ob}/V. Fuel consumption on the outbound leg at any time instant in this stage F_{ob-2} is described as:

$$
\begin{aligned}
F_{ob-2} &= \text{(queued vehicles) } f_{4r} + \text{(moving vehicles) } f_{5r} \\
&= 0 && \text{if } r < t \leq r+k \\
&= \{\min(st, qr) - \max(0, s(t - t))\} f_{4r} + \\
&\quad \max\{[st - qr - \max(0, s(t - t))], 0\} f_{5r} && \text{if } r+k < t \leq r+ t_0 \qquad [4.17]
\end{aligned}
$$

The first expression considers the saturation flow st and the maximum of vehicles for this group, qr. The term, max(0, s(t- t)) is used to indicate the number of vehicles in the system, and is dependent of the relative magnitude of t and t. If t is less than t, the whole term should be equal to 0. The values of f_{4r} and f_{5r} represent two different fuel consumption rates, one for vehicles that have been stopped, and the other for vehicles which are delayed by signals. The total fuel consumption TF_{ob-2} can be estimated from:

$$
\begin{aligned}
TF_{ob-2} &= 0 && \text{if } r < t < r+k \\
&= \int_k^{t_0} (\{\min(st, qr) - \max(0, s(t - t))\} f_{4r} + \\
&\quad \max\{[st - qr - \max(0, s(t - t))], 0\} f_{5r}) \, dt && \text{if } r+k < t \leq r+ t_0 \qquad [4.18]
\end{aligned}
$$

In this equation, the solution could be estimated by assuming different time intervals.

(2) Time from t_0 to the end of the effective green ($r+t_0 < t \leq r+g = c$)

In this cycle stage, vehicles are assumed to travel at their desired speeds V_r and to move onto the outbound leg with fuel consumption rate f_r. However, some vehicles remaining on the outbound leg from the last cycle stage are still trying to reach their desired speeds. These

vehicles follow the fuel consumption trajectory from the last cycle and have fuel consumption f_{5r}. Therefore, fuel consumption F_{ob-3} at any time instant is:

$$\begin{aligned} F_{ob-3} &= \text{(moving vehicles with acceleration) } f_{5r} + \\ &\quad \text{(moving vehicles at desired speed) } f_r \\ &= (s\,t_0 - \min\{s\,t_0, \max\{0, s(t-t)\}\})\, f_{5r} + \\ &\quad (q\,(t-t_0) - \max\{0, q(t-t_0-t)\})\, f_r \end{aligned} \qquad [4.19]$$

and total fuel consumption TF_{ob-3} is defined as:

$$\begin{aligned} TF_{ob-3} = \int_{t_0}^{g} &((s\,t_0 - \min\{s\,t_0, \max\{0, s(t-t)\}\})\, f_{5r} + \\ &(q\,(t-t_0) - \max\{0, q(t-t_0-t)\})\, f_r)\, dt \end{aligned} \qquad [4.20]$$

In this expression, the total number of vehicles that have entered the outbound leg is st_0, and the number of vehicles is decreasing due to the limited outbound leg length.

(3) The effective red time ($0 \le t \le r$)

Since the vehicular flow has been interrupted by signals, the number of vehicles on the outbound leg is decreasing with respect to time. The total fuel consumption is thus estimated through these remaining vehicles. The fuel consumption F_{ob-1} at any time instant is:

$$\begin{aligned} F_{ob-1} &= \text{(moving vehicles with acceleration) } f_{5r} + \\ &\quad \text{(moving vehicles at desired speed) } f_r \\ &= (s\,t_0 - \min\{s\,t_0, \max\{0, s(t-t)\}\})\, f_{5r} + \\ &\quad (q\,(g-t_0) - \max\{0, q(t-t_0-t)\})\, f_r \end{aligned} \qquad [4.21]$$

Total fuel consumption TF_{ob-1} is:

$$\begin{aligned} TF_{ob-1} = \int_{g}^{g+r_1} &((s\,t_0 - \min\{s\,t_0, \max\{0, s(t-t)\}\})\, f_{5r} + \\ &(q\,(g-t_0) - \max\{0, q(t-t_0-t)\})\, f_r)\, dt \end{aligned} \qquad [4.22]$$

The magnitude of r_1 is the elapsed time required for all vehicles to leave the system, and is equal to "t" for the isolated intersection.

AFCM WITH OVERFLOW QUEUES

AFCM, developed under ideal situations, has been discussed in detail in the previous sections. In order to be more general and realistic, the assumptions of deterministic and undersaturated flow conditions are relaxed to include overflow queues. An *Overflow queue*, defined as a non-zero number of queued vehicles at the start of the effective red time, complicates the development but represents a more realistic situation. Therefore, the AFCM is

extended to consider overflow queues for both undersaturated and oversaturated conditions. In this section, basic ideas of the developments are first introduced in Section 4.4.1, queue length and distribution calculations are discussed in Section 4.4.2, and discussions of the improvement are in Sections 4.4.3 and 4.4.4.

Basic Idea

Queue lengths play an important role in evaluating intersection performance. In a realistic situation, queues might exist when traffic lights turn red indicating an overflow situation. Not only is the queue length itself a performance index, but it can also be used to estimate delay. There are considerable amounts of literature on this issue, For example, Webster [84] derived mean queue lengths and delay. Several authors [33, 35, 36, 66, 6] proposed queue probability distributions instead of mean values. Among these studies, the results from Cronje [33,35,36], Olszewski [66], and Akcelik and Rouphail [6] are used to improve the AFCM in queue and flow behavior.

Queue formation and discharge directly impacts inbound approach fuel consumption estimation. Some vehicles might stop more than twice and consume excess fuel due to stochastic effects or oversaturation situations. Therefore, the AFCM improvement focuses on the inbound approach. Fuel consumption models at the intersection itself and the outbound leg are also improved to consider the impacts of overflow queues. Table 4-2 shows the symbols and notations used in the AFCM with overflow queues.

TABLE 4.2 NOTATIONS USED IN THE AFCM WITH OVERFLOW QUEUES

		The Saturation Condition		
		Case I	Case II	Case III
		If $g > t_0$	If $g <= t_0$	
			queued vehicles discharged	some queued vehicles not discharged
Inbound	Red Time	F_{ib-1}^{q}	F_{ib-1}^{q}	F_{ib-1}^{q}
	Green Time	F_{ib-2}^{q} F_{ib-3}^{q}	F_{ib-2}^{qd}	F_{ib-2}^{qq}
Intersection	Red Time	0	0	0
	Green Time	F_{int-2}^{q} F_{int-3}^{q}	F_{int-2}^{qd}	F_{int-2}^{qq}
Outbound	Red Time	F_{ob-1}^{q}	F_{ob-1}^{qd}	F_{ob-1}^{qq}
	Green Time	F_{ob-2}^{q} F_{ob-3}^{q}	F_{ob-2}^{qd}	F_{ob-2}^{qq}

Analysis of Queue Distribution and Queue Length at Signalized Intersections

Since an overflow queue is defined as a non-zero number of queued vehicles at the end of the effective green time, then the queue length at the start of the following effective red time in the next cycle is

$$Q_i = Q_{i-1} + A_i - B_i \qquad Q_i \geq 0 \qquad [4.23]$$

where,

Q_i = overflow queues in the cycle i,

Q_{i-1} = overflow queues in the previous cycle i-1,

A_i = number of vehicles arriving in the cycle i, and

B_i = sg, product of saturation flow rate and effective green time, or capacity in cycle i.

The estimation of overflow queues is a Markov process based on the following assumptions [66]:

1. Number of vehicle arrivals A in each cycle is a random variable with a known probability distribution and independent of queue length in the previous cycle.
2 Capacity in each cycle is either a constant or random variable with a known probability distribution. It is independent of queue length.

The calibration of Equation 4.23 requires a sequential calculation regarding probability of transition from Q_{i-1} to Q_i. Several authors [33,35, 66] formulated the transition probability matrix to analyze the queue length probability. This study followed Cronje's [33,35] method to derive overflow queues at intersections. The vehicle arrivals are assumed to be Poisson or Binomial distributed, and the capacity is assumed to be constant.

Queue Probability Distribution and Queue Length. The derivation of queue probability and queue length follows Cronje's study [33,34,35] and is applicable for undersaturated and oversaturated conditions. As stated by Cronje [35], the probability of an overflow queue Q_i in this cycle, given overflow queues Q_{i-1} in the previous cycle, is represented as:

$$P(Q_i)=P(Q_{i-1})\cdot P(A_i)\cdot P(B_i)$$

It is assumed that $P(A_i)$ is the probability distribution of arriving vehicles with stationary arrivals, and capacity B_i is a constant per cycle; therefore,

$$\begin{aligned} P(Q_i) &= P(Q_{i-1})\cdot P(A_i)\cdot P(B_i) \\ &= P(Q_{i-1})\cdot P(qc)\cdot P(sg) \\ &= P(Q_{i-1})\cdot P(qc) \end{aligned} \qquad [4.24]$$

where,

$P(Q_i)$ = probability of overflow queue Q_i,

qc = number of vehicles arriving in cycle c, and

sg = departures per cycle.

It is assumed that there is no flow in the initial cycle; therefore, there are no overflow queues at the end of the cycle, i.e., $Q_0=0$. It is obvious that $P(Q_0=0)=1$ and $P(Q_0>0)=0$. The

probability P(qc) is obtained from the arrival distribution. Therefore, $P(Q_i)$ can be obtained from the following algorithm:

Let Q_i^e = overflow queue size at the end of cycle i, and Q_i^s = overflow queue size at the start of cycle i. Therefore, $Q_{i-1}^e = Q_i^s$.

Step 1: i = 0, initial flow is zero, $Q_0^e = Q_0^s = 0$, $P(Q_0^s = 0) = 1$.

Step 2: i=1, $Q_1^s = Q_0^e$

Vary vehicle arrivals qc from zero to k and let $\sum_{j=0}^{k} P(qc = j) \geq 0.9999$.

Vary vehicle arrivals qc from zero to k and estimate $Q_1^e = Q_1^s + qc - sg$ and $P(Q_1^e) = P(Q_1^s) \cdot P(qc) \cdot P(sg)$, where $P(Q_1^e = 0) = \sum P(Q_1^e \leq 0)$.

Step 3: Let i = i+1, $Q_{i+1}^s = Q_i^e$.

Step 4: Vary vehicle arrivals qc from zero to k and estimate $Q_{i+1}^e = Q_{i+1}^s + qc - sg$ and $P(Q_{i+1}^e)$

$$= \sum_{Q_{i+1}^s} P(Q_{i+1}^s) \cdot P(qc) \cdot P(sg).$$

$$E(Q_{i+1}^e) = \sum Q_{i+1}^e P(Q_{i+1}^e)$$

Step 5: Estimate total delay D_i and average delay $d_i = \frac{D_i}{m}$, where m is the mean number of arrivals.

Estimate $\Delta d_i = (d_i - d_{i-1})$.

Step 6: If this is an undersaturated condition and $\Delta d_i < 0.001$, then stop; expected overflow queues $E(Q_i^e)$ can be estimated. Otherwise, go to Step 3. If this is an oversaturated condition and $\Delta d_i - \Delta d_{i-1} < 0.001$, then stop; overflow queues $E(Q_i^e)$ can be estimated. Otherwise, go to Step 3.

The total delay in cycle i is:

$$D_i = [(2 Q_i^s + qr)\frac{r}{2}] + [(qr + Q_i^s + Q_i^e)\frac{g}{2}] \qquad [4.25]$$

Approximating Macroscopic Queue Probability and Queue Length. Since the transition probability of overflow queues is a Markov process and requires complex matrix

calculation, Cronje [35] proposed the geometric probability distribution as an approximating macroscopic model to calibrate the probability of overflow queues. The general form of the geometric distribution is:

$$P(x) = (1-p)^x p \quad x=0, 1, 2,... \qquad [4.26]$$

where,

P(x) = probability of the number of necessary trials (x) to obtain the first success,

p = the probability of success, and

(1-p) = the probability of failure.

Let p be the probability of a queue at the start of the cycle, thus the probability of queue length Q at the start of the cycle is:

$$P(Q) = p^Q(1-p), \qquad [4.27]$$

where,

$$p = E(Q^S)/(1+E(Q^S)).$$

From the properties of the geometric probability distribution and the relationship of $Q^e=Q^S+qc-sg$, the expected overflow queue value $E(Q^e)$ at the end of cycle is:

$$E(Q^e) = E(Q^S)+E(qc)-E(sg)- \sum_{sg} P(sg) \sum_{qc=0}^{sg-1} P(qc) \sum_{Q^S=0}^{sg-qc-1} (Q^S+qc-sg)P(Q^S) \qquad [4.28]$$

Thus, the expected overflow queue value is applied in AFCM to estimate the total fuel consumed by overflow queues.

Inbound Approach Fuel Consumption Model

The original AFCM is extended to consider the impact of overflow queues on fuel consumption. The first term in Equation 4.4 must be modified to include stopped vehicles due to both red signals and overflow queues. The number of moving vehicles (or arriving vehicles) depends on the arrival rates and cycle length. Since there is limited space within the intersection influence area, the number of queued vehicles cannot exceed maximum queue length Q_m.

$$Q_m=D_{ib}/L \qquad [4.29]$$

where D_{ib} is the inbound approach length and L is the average queue length consumed by one vehicle. Since the estimation of fuel consumption on the inbound approach depends on the intersection influence area length which is assumed to be sufficient to accommodate all arriving vehicles.

One major factor to be considered is the value of t_0. Due to the traffic demand and

overflow queues, the value of t_0 might be greater than the effective green time. In subsequent discussions, cycle length is divided into two cycle stages: the effective red time and the effective green time. The effective green time is further divided into two parts if the value of t_0 is less than the effective green time.

(1) The effective red time ($0 \le t \le r$)

During the effective red time, queued vehicles potentially include overflow from an earlier cycle and newly arriving vehicles. The number of moving vehicles is estimated by arrival rates and travel time. The fuel consumption $F_{ib\text{-}1}{}^{q}$ at any instant of time t can be expressed as:

$$\begin{aligned} F_{ib\text{-}1}{}^{q} &= (\text{queued vehicles})\, f_0 + (\text{arriving vehicles})\, f_{r0} \\ &= N_S f_0 + N_m f_{r0} \\ &= [Q^S + qt] f_0 + qT_{11}{}' f_{r0} \end{aligned} \qquad [4.30]$$

where,

Q^S = overflow queues from the previous cycle.

By comparing with Equation 4.4 in Section 4.3, Equation 4.30 includes an additional term, Q^S, which represents the initial queue size at the start of red time. During fuel consumption estimation, these vehicles are idling and contribute to fuel consumption with rate f_0. Overflow queues affect not only the number of queued vehicles but also the moving vehicles traveling distance which is shorter due to a longer stopped queue. Therefore, the moving vehicles are estimated by $qT_{11}{}'$, where $T_{11}{}'$ is equal to:

$$T_{11}{}' = \frac{[D_{ib} - (Q^S + qt)L/n]\, T_{ib}}{D_{ib}} \qquad [4.31]$$

$T_{11}{}'$ is the estimated travel time on the inbound approach during the effective red time. It represents a geometric configuration indicator and describes the relationship between vehicles and the inbound approach. Thus, the total fuel consumption $TF_{ib\text{-}1}{}^{q}$ in the effective red time is:

$$\begin{aligned} TF_{ib\text{-}1}{}^{q} &= \int_0^r F_{ib\text{-}1}{}^{q}\, dt \\ &= \int_0^r \{(Q^S + qt) f_0 + q \frac{[D_{ib} - (Q^S + qt)L/n]\, T_{ib}}{D_{ib}} f_{r0}\}\, dt \end{aligned} \qquad [4.32]$$

The first term represents the effect of the initial queue with idle fuel consumption during the effective red time. The second term is similar to Equation 4.6, and is not described again.

(2) The effective green time ($r < t <= r+g = c$)

During this cycle stage, vehicles start to move from the idle status The model modification described below considers the situation that vehicles may or may not be discharged within the effective green time.

(2.a) If the effective green time is greater than t_0 ($g > t_0$) [Queue departure time is less than green time]

Obviously, an undersaturated condition exists if the effective green time is greater than t_0. In an undersaturated operation, overflow queues are the results of random arrivals. For fuel consumption estimation, the effective green time is still divided into time from green onset to time t_0 ($r < t \leq r+t_0$) and time from t_0 to the end of the effective green ($r+t_0 < t \leq r+g = c$).

(2.a.1) Time from green onset to time t_0 ($r < t \leq r+t_0$)

In this cycle stage, vehicles are discharged at the saturation flow rate. Since there are overflow queues from the previous cycle, the value of t_0 is changed. According to the t_0 definition, at time t_0 the queue has been discharged, i.e., $Q^s + q(r+t_0) = st_0$ and $t_0 = (Q^s+qr) / (s-q)$. In a more general sense t_q is defined as the time for queued vehicles to discharge, i.e., $Q^s+qr = st_q$, and $t_q = (Q^s+qr)/s$. Therefore, the magnitude of t_0 with overflow queues is greater than without overflow queues, and $t_q \leq t_0$.

Fuel consumption $F_{ib\text{-}2}^q$ at any instant, similar to the definition of Equation 4.7, is estimated from both queued and arriving vehicles:

$$\begin{aligned} F_{ib\text{-}2}^q &= \text{(queued vehicles) } f_{02} + \text{(arriving vehicles within } t_q) f_{r2} + \\ &\quad \text{(queuing vehicles) } f_{03} + \text{(arriving vehicles after } t_q) f_{r3} \\ &= (Q^s+qr-st) f_{02} + qt f_{r2} + q T_{12}' f_{r2} \qquad \text{if } r \leq t \leq r+t_q \\ &= (qt_q+qt-st) f_{03} + q T_{12}' f_{r3} \qquad \text{if } r+t_q < t \leq r+t_0 \end{aligned} \qquad [4.33]$$

where,

$$\begin{aligned} T_{12}' &= \frac{[D_{ib} - (Q^s + qr + qt - st)L/n] T_{ib}}{D_{ib}} \qquad \text{if } r \leq t \leq r+t_q \\ &= \frac{[D_{ib} - (qt_q + qt - st)L/n] T_{ib}}{D_{ib}} \qquad \text{if } r+t_q < t \leq r+t_0 \end{aligned} \qquad [4.34]$$

Total fuel consumption $TF_{ib\text{-}2}^q$ is:

$$TF_{ib\text{-}2}^q = \int_0^{t_0} F_{ib\text{-}2}^q \, dt \qquad [4.35]$$

From Equation 4.35, total fuel consumption is affected by several factors: fuel

consumption rates, f_{02}, f_{03}, f_{r2} and f_{r3}, representing different vehicle movement states, signal timing, and geometric configuration indicators.

(2.a.2) Time from t_0 to the end of green ($r+t_0 < t \leq r+g = c$)

In the absence of overflow queues after t_0, all queued vehicles and vehicles arriving in time t_0 have been dissipated. Therefore, vehicles which still move on the inbound approach are assumed to travel at their desired speeds V_r with fuel consumption:

$$F_{ib\text{-}3}^{q} = \text{(moving vehicles) } f_r$$

$$= qT_{13} f_r \qquad [4.36]$$

and

$$TF_{ib\text{-}3}^{q} = \int_{t_0}^{g} F_{ib\text{-}3}^{q} \, dt \qquad [4.37]$$

where,

T_{13} = D_{ib}/V, estimated travel time on the inbound approach from t_0 to the end of the effective green.

Actually, $F_{ib\text{-}3}^{q}$ is equal to $F_{ib\text{-}3}$ at any time instant, yet $TF_{ib\text{-}3}^{q}$ is less than $TF_{ib\text{-}3}$ due to the change of t_0.

(2.b) If the effective green time is less than or equal to t_0 ($g \leq t_0$) [Queue departure time is equal to green time]

If the effective green time is less than time t_0, queued vehicles and vehicles arriving within the effective green are discharged at the saturation flow rate, but cannot be discharged completely. Therefore, only the time from green onset to the end of green ($r < t \leq r+g = c$) must be considered, and the remaining vehicles form the initial queue in the next cycle. Stopped vehicles, including the initial queue and the vehicles arriving during red time, might or might not be discharged completely, i.e., $t_q \leq g$ or $t_q > g$. Vehicles arriving during green time are affected by the overflow queues and either decelerate to stop when they recognize the existence of overflow queues, or continue to move after the queues have been discharged. Therefore, fuel consumption is estimated based on the condition of whether queued vehicles have been discharged ($t_q \leq g$) or not ($t_q > g$).

(2.b.1) If queued vehicles have been discharged ($t_q \leq g$)

Under this condition, all queued vehicles are discharged but arriving vehicles may not be dissipated completely. Queued and arriving vehicles have the same fuel consumption rates in Equation 4.33. Since some arriving vehicles cannot be discharged, an additional fuel

consumption rate f_{030} is imposed to describe their fuel consumption behavior from idle to speed V_3 and from speed V_3 to stop. These vehicles follow the moving vehicles ahead of them and try to move from idle to speed V_3; however, they are forced to stop again due to the end of the effective green. The fuel consumption $F_{ib\text{-}2}^{qd}$ at any time instant is:

$$\begin{aligned} F_{ib\text{-}2}^{qd} = & \text{ (queued vehicles) } f_{02} + \text{(arriving vehicles within } t_q) f_{r2} + \\ & \text{(queuing vehicles) } f_{03} + \text{(arriving vehicles after } t_q) f_{r3} + \\ & \text{(arriving vehicles cannot be discharged) } f_{030} \\ = & (Q^s + qr - st) f_{02} + qt f_{r2} + qT_{12}' f_{r2} \qquad \text{if } r \le t \le r+t_q \\ = & (qt_q + qt - st) f_{03} + qT_{12}' f_{r3} + Q^e f_{030} \qquad \text{if } r+t_q < t \le r+g \end{aligned} \qquad [4.38]$$

and total fuel consumption $TF_{ib\text{-}2}^{qd}$ is:

$$TF_{ib\text{-}2}^{qd} = \int_0^g F_{ib\text{-}2}^{qd}\, dt \qquad [4.39]$$

Where Q^e is the overflow queue at the end of effective green, expressed as:

$$Q^e = Q^s + qr + qg - sg$$

In these equations, five different fuel consumption rates are used, f_{02}, f_{r2}, f_{03}, f_{r3}, and f_{030}, which represent idle vehicles accelerating to speed V_2, running vehicles decelerating to speed V_2, idle vehicles accelerating to speed V_3, running vehicles decelerating to speed V_3, and idle vehicles accelerating and decelerating. The other terms are similar to the previous discussions.

(2.b.2) If queued vehicles have not been discharged ($t_q > g$)

If the queued vehicles have not been discharged completely, some of these vehicles must stop twice before they pass the stop line. These vehicles start to move by following the vehicles ahead and stop again due to a red signal. The stop-move-stop fuel consumption for these queued vehicles is cumbersome because vehicle maneuvers are extremely variable within the approach. Since the vehicles ahead of them pass the stop line at speed V_2, the average maximum speed they can reach is V_2. For simplification of the fuel consumption estimation, vehicles moving from stop to speed V_2 by following vehicles ahead of them and from V_2 to stop due to a red signal are assumed to have average fuel consumption rate f_{020}. The arriving vehicles have average fuel consumption rate f_{r0}.

Fuel consumption at any instant of the effective green time is expressed as:

$$F_{ib\text{-}2}^{qq} = \text{(queued vehicles) } f_{02} + \text{(arriving vehicles) } f_{r2} + \text{(queued vehicles which cannot be discharged) } f_{020}$$

$$= (Q^s+qr-st)f_{02} + qt\, f_{r2} + qT_{12}'f_{r2} + (Q^e)\, f_{020} \quad [4.40]$$

and total fuel consumption is:

$$TF_{ib\text{-}2}^{qq} = \int_0^g F_{ib\text{-}2}^{qq}\, dt \quad [4.41]$$

Where Q^e is the overflow queue at the end of effective green, expressed as:

$$Q^e = (Q^s+qr-sg)$$

Three fuel consumption rates, f_{02}, f_{r2}, and f_{020} are used to represent idle vehicles accelerating to speed V_2, running vehicles decelerating to speed V_2, and idle vehicles accelerating and decelerating.

Intersection and Outbound Leg Fuel Consumption Model

In this section, the overflow queue fuel consumption model for the intersection and outbound leg is discussed. Although the capacity (sg) in each cycle is independent of overflow queue length, queued and arriving vehicles may possess different trajectories which affect fuel consumption estimation beyond the stop line. Several factors are explored and used in the fuel consumption model improvement. However, it is possible that queued and arriving vehicles are unable to be discharged within a given cycle and create overflow queues. In order to differentiate the possible impact, the discussion will be separated into two parts, undersaturation and oversaturation conditions, defined as $t_0 \le g$ and $t_0 > g$. Since the basic AFCM is used as the model to be improved and the formulations are very similar to those discussed in Section 4.3; therefore, the discussion combines the intersection and outbound leg.

Undersaturation Flow Condition. In this section, the effective green time is assumed to be greater than t_0, i.e., $g \ge t_0$, which means that all arriving vehicles could be discharged. The fuel consumption model for the undersaturated flow condition is similar to the one in Section 4.3, but with the additional condition of existing a non-zero queue length.

(1) Time from green onset to time t_0 ($r < t \le r+t_0$)

The number of vehicles in the intersection itself is limited to the intersection width at any time instant. Therefore, the model has the same forms as given in Equations 4.13 and 4.14:

$$F_{int\text{-}2}^{q} = \text{(queued vehicles) } f_{24} + \text{(moving vehicles) } f_{35}$$

$= st\, f_{24}$ if $r < t \leq r+k$

$= sk\, f_{24}$ if $r+k < t \leq r+t_q$

$= sk\, f_{35}$ if $r+t_q < t < r+ t_0$ [4.42]

$TF_{int\text{-}2}{}^q = \int_0^{t_0} F_{int\text{-}2}{}^q\, dt$ [4.43]

Similarly, definitions of the outbound leg fuel consumption at time t ($F_{ob\text{-}2}{}^q$) and total fuel consumption ($TF_{ob\text{-}2}{}^q$) have similar forms as in Equations 4.17 and 4.18 and are given by:

$F_{ob\text{-}2}{}^q =$ (queued vehicles) f_{4r} + (moving vehicles) f_{5r}

$= 0$ if $r< t \leq r+k$

$= \{\min(st, Q^s+qr)- \max(0, (t-t)s)\}\, f_{4r} +$

$\max\{[st - (Q^s+qr) - \max(0, (t-t_q-t)s)], 0\} f_{5r}$ if $r+k < t \leq r+ t_0$ [4.44]

$TF_{ob\text{-}2}{}^q = 0$ if $r < t < r+k$

$= \int_k^{t_0} F_{ob\text{-}2}{}^q\, dt$ if $r+k < t \leq r+ t_0$ [4.45]

The difference between Equations 4.17 and 4.44 is in the estimation of queued and moving vehicles. The estimation of queued and moving vehicles in Equation 4.44 considers overflow queues and the arrival distribution.

(2) Time from t_0 to the end of green ($r+t_0 < t \leq r+g = c$)

After t_0, queued vehicles and vehicles arriving within t_0 have been discharged from the intersection. Since vehicles are not affected by the signal operation, fuel consumption estimation at the intersection and on the outbound leg is the same as the case without overflow queues, i.e.,

$F_{int\text{-}3}{}^q = F_{int\text{-}3}$ [4.46]

$F_{ob\text{-}3}{}^q = F_{ob\text{-}3}$ [4.47]

However, the magnitudes of total fuel consumption considering overflow queues ($TF_{int\text{-}3}{}^q$, $TF_{ob\text{-}3}{}^q$) are different from the case without overflow queues ($TF_{int\text{-}3}$, $TF_{ob\text{-}3}$) due to the change of t_0.

(3) The Effective Red Time ($0 < t \leq r$)

Since no vehicles enter the intersection within the effective red time, total fuel consumption in the intersection itself ($TF_{int\text{-}1}{}^q$) is zero. Nevertheless, some vehicles remain on the outbound leg and consume fuel after the end of green time. Since these vehicles consume fuel with rates greater than idle after the end of green time, fuel consumption estimation during

the red time must consider them. For these vehicles the definition of Equation 4.48, the same as Equations 4.21, describes fuel consumption at any time instant,

$$F_{ob\text{-}1}^{q} = F_{ob\text{-}1}$$
$$= \text{(moving vehicles with acceleration) } f_{5r} + \text{(moving vehicles at desired speed) } f_r$$
$$= (s\, t_0 - \min\{s\, t_0, \max\{0, s(t-t)\}\})\, f_{5r} + (q\,(g - t_0) - \max\{0, q(t - t_0 - t)\})\, f_r \qquad [4.48]$$

and the total fuel consumption $TF_{ob\text{-}1}^{q}$ is:

$$TF_{ob\text{-}1}^{q} = \int_{g}^{g+r_1} F_{ob\text{-}1}^{q}\, dt \qquad [4.49]$$

Overflow Condition. In the overflow condition, queued and arriving vehicles cannot all be discharged during the green time, i.e., $g \le t_0$. Thus, t_q is used to examine whether all of the queued vehicles could be discharged within the green time. If t_q is less than g, the queue may be discharged, but vehicles arriving after queue departure (still during green) may not be discharged.

(1) The effective green time ($0 < t < g$)

(1.a) If queued vehicles have been discharged ($t_q \le g < t_0$)

Under this condition, all queued vehicles are discharged but arriving vehicles may not be discharged completely. Although arriving vehicles which cannot be discharged at the end of green time have fuel consumption on the inbound approach, they do not consume fuel beyond the stop line. Therefore, the forms of intersection and outbound fuel consumption models are exactly the same as Equations 4.42-4.45 except that the estimation period is for the entire effective green time, i.e.,

$$F_{int\text{-}2}^{qd} = F_{int\text{-}2}^{q} \qquad [4.50]$$

$$TF_{int\text{-}2}^{qd} = \int_{0}^{g} F_{int\text{-}2}^{qd}\, dt \qquad [4.51]$$

$$F_{ob\text{-}2}^{qd} = F_{ob\text{-}2}^{q} \qquad [4.52]$$

$$TF_{ob\text{-}2}^{qd} = \int_{0}^{g} F_{ob\text{-}2}^{qd}\, dt \qquad [4.53]$$

(1.b) If queued vehicles have not been discharged ($g < t_q < t_0$)

If the queued vehicles have not been discharged completely, some of the queued vehicles and all arriving vehicles cannot enter the intersection and outbound leg. Therefore, only queued vehicles which are discharged consume fuel in the intersection itself and on the outbound leg. Fuel consumption in the intersection can be expressed as:

$F_{int\text{-}2}^{qq}$ = (queued vehicles which have been discharged) f_{24}

$= st\, f_{24}$ if $r < t < r+k$

$= sk\, f_{24}$ if $r+k < t < r+g$ [4.54]

$$TF_{int\text{-}2}^{qq} = \int_0^g F_{int\text{-}2}^{qq}\, dt \quad [4.55]$$

Fuel consumption on the outbound leg can be expressed as:

$F_{ob\text{-}2}^{qq}$ = (queued vehicles which have been discharged) f_{4r}

$= [st - \max(0, (t-t)s)]\, f_{4r}$ [4.56]

$$TF_{ob\text{-}2}^{qq} = \int_0^g F_{ob\text{-}2}^{qq}\, dt \quad [4.57]$$

(2) The effective red time ($0 < t \leq r$)

(2.a) If queued vehicles have been discharged ($t_q \leq g < t_0$)

Since no vehicles enter the intersection within the effective red time, total fuel consumption in the intersection itself ($TF_{int\text{-}1}^{q}$) is zero. Nevertheless, some vehicles remain on the outbound leg and have fuel consumption after the end of green time. Since vehicles follow fuel consumption trajectories after the end of green time, the estimation of fuel consumption during the red time must consider the effects of the effective green time.

By comparing with the above condition, vehicles arriving after t_0 will not be considered because the effective green time is less than t_0. Therefore, the value of t_0 is replaced by the value of g in Equation 4.48 and

$F_{ob\text{-}1}^{qd}$ = (moving vehicles with acceleration) f_{5r} +

(moving vehicles at desired speed) f_r

$= (sg - \min\{sg, \max\{0, (t-t)s\}\})f_{5r} +$

$(q(g-g) - \max\{0, q(t - g - t)\})f_r$

$= (sg - \min\{sg, \max\{0, (t - t)\, s\}\})\, f_{5r}$ [4.58]

(2.b) If queued vehicles have not been discharged ($g < t_q < t_0$)

By investigating the definition of Equation 4.58, only vehicles which pass the intersection at the saturation flow rate remain on the outbound leg after the effective green time. Therefore, fuel consumption at any instant during the effective red time is the same for both conditions, $t_q \leq g$ and $t_q > g$, i.e.,

$$F_{ob\text{-}1}^{qq} = F_{ob\text{-}1}^{qd} \quad [4.59]$$

and total fuel consumption is

$$TF_{ob\text{-}1}^{qq} = TF_{ob\text{-}1}^{qd}$$

$$= \int_{g}^{g+r_1} F_{ob\text{-}1}^{qd}\, dt \qquad [4.60]$$

SUMMARY

This chapter presents basic model development of the Analytical Fuel Consumption Model (AFCM) and a model extension which considers queue probability distribution and queue lengths. The model, aiming to include the impact of traffic characteristics, fuel consumption rates, and signal control variables, includes three different vehicle operating conditions describing fuel consumption on the inbound approach, the intersection itself, and the outbound leg for three signal cycle stages (the effective red time, time from green onset to time t_0, and time from t_0 to the effective green time end). Implementation of the model will be accomplished by estimating model parameters such as fuel consumption rates and average travel times. Calibration of the model parameters is discussed in Chapter 5.

The flexible design of this model permits application in undersaturated and oversaturated conditions. Furthermore, the model may consider various flow arrival patterns and traffic conditions. Two features of the AFCM demonstrate the model capability: (1) the consideration of traffic control measures and traffic flow characteristics on fuel consumption estimation, and (2) the direct method of estimating intersection fuel consumption without simulation or complex mathematical calculation. Experimental setups and fuel consumption estimation are described in the following chapters illustrating the model capability and the relationship between fuel consumption and signal control strategy.

CHAPTER 5. DATA COLLECTION AND CALIBRATION FOR VEHICULAR AND FUEL CONSUMPTION PARAMETERS

INTRODUCTION

In the previous chapter, traffic flow characteristics and traffic control measures as well as fuel consumption variables are employed in the development of fuel consumption models. In order to capture traffic behavior and its impact on fuel consumption, field experiments were conducted to analyze vehicle behavior near intersections. Since the main variables in the AFCM include change of vehicle speed with respect to time and distance to stop line, the experiment aims at collecting vehicle travel time, speed, and acceleration/deceleration with respect to time as well as distance between two signalized intersections. Fuel related variables are calibrated through the data obtained from extensive field experiments, conducted by the U.S. Environmental Protection Agency (USEPA).

Vehicular behavior in terms of vehicle speed-time histories is affected by control strategies and fuel consumption in urban networks is strongly affected by traffic control strategies implemented through signalized intersections. Statistical results show that vehicle type, signal timing, and travel distance from the intersection have significant effects on vehicle traffic behavior and how they consume fuel [58]. An explanatory variable representing the product of speed and acceleration is a robust fuel consumption predictor for estimating instantaneous fuel consumption.

This chapter investigates traffic behavior in terms of vehicle speed and acceleration/deceleration at signalized intersections and analyzes the impact of traffic behavior on fuel consumption modeling. Vehicle profile models are first developed as polynomial models based on the collected data. Mathematical formulations of fuel consumption profile models are developed and aggregate fuel consumption rates proposed in the AFCM are calibrated to estimate total fuel consumption at signalized intersections.

The field experiment is described in the next section, followed by the discussion of model calibration. Detailed data analysis is discussed in Section 5.3 to identify key parameters in the calibration process, including vehicle speed, acceleration/deceleration. Explanatory data analysis and results are described in Section 5.4 addressing the underlying effects of traffic behavior on fuel consumption. Fuel consumption profile models are defined in Section 5.5. The aggregate fuel consumption rates are calibrated in Section 5.6. A brief summary is given in the last section.

EXPERIMENTAL DESIGN

The experiment aims at finding the interrelationship among vehicles, traffic flow characteristics, and traffic control measures; therefore, data was collected near signalized intersections in an urban area. The section of Congress Avenue between 1st street and Barton Springs Blvd. in the City of Austin was chosen to collect related information, including vehicle movement and traffic control parameters.

Data Collection

The best way to collect vehicle speed-time histories might be through vehicles equipped with proper instruments to instantaneously measure vehicle speed, acceleration/deceleration, and fuel consumption. However, instrumented vehicle techniques could not be used due to funding constraints. An alternative to instrumented vehicles is videotaping which involves intensive data reduction effort. However, appropriately detailed traffic data can be extracted from video records.

The chosen site, Congress Avenue between 1st Street and Barton Springs Blvd. in Austin, TX, is a medium-volume six-lane urban street with a 30 mph speed limit. First Street is a one-way three-lane urban arterial street. The pretimed signal at Congress Avenue and 1st Street has a 90 second cycle time and three phases with a protected southbound left turn phase. The portion of Congress for which vehicle trajectories were measured starts at an intersection with a medium volume street (1st Street) and continues unconstrained by traffic control for approximately 1700 feet downstream. Parking, bus stops, and turn movements are not allowed between these two intersections. Data were collected by videotaping from the 32nd floor of a nearby building, approximately 1200 feet north of the test section.

Data were collected from 3:00pm to 5:00pm on weekdays with uncongested traffic operations and dry weather. Due to weather and traffic conditions, all data was not collected during one week. However, at least one data set was collected on Tuesday, Wednesday, and Thursday respectively to represent typical weekday traffic conditions. The weekday p.m. peak traffic is about 600 vehicles per hour (vph).

Figure 5.1 illustrates geometric configuration and signal phasing and timing data at the Congress Avenue and 1st Street intersection. For the outbound (OB) and inbound approach (IB), the road segment is divided into several smaller sections, differentiated by fiducial marks, which are identified by utility poles on both street sides. Although the lengths of these sections are slightly different, use of the poles as fiducial marks was very convenient.

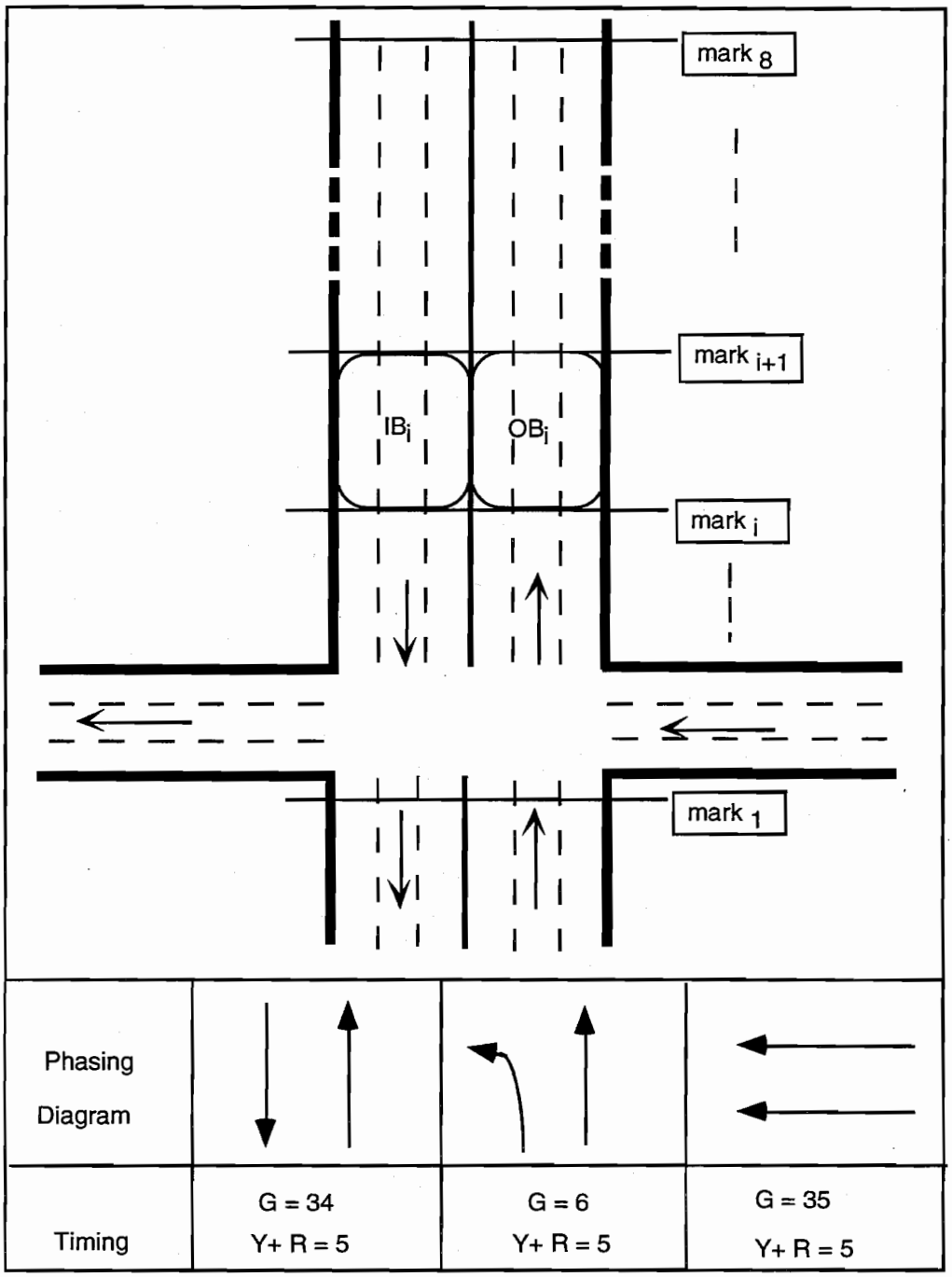

Figure 5.1. Geometry diagram at the signalized intersection

Data Reduction

Through the videotape, traffic movements were observed and recorded. Two data types termed primary and secondary data were obtained. Primary data refers to the data which could be obtained through videos directly; secondary data refers to the data which is obtained through the primary data. Table 5.1 shows the typical data reduction process.

The resolution of the videotape time base is 30 frames/sec and can track vehicles at intervals of 0.03 second. Primary data can be summarized as follows:

1) traffic counts

The number of vehicles passing a fiducial mark within a given time is counted by turning movement, including straight, right-turn, left-turns, and U-turns. The total number of vehicles for each videotaping period within the survey area is recorded.

2) vehicle movement

All vehicles are identified as moving or stopped. Moving vehicles are further described as decelerating, accelerating, or cruising.

3) vehicle maneuvers

Vehicle maneuvers noted include lane-changing and overtaken movements.

4) travel time

Vehicle travel time from fiducial mark to fiducial mark is obtained through the video time clock.

5) signal control parameters

Signal indication changes and phase durations are recorded.

Other necessary data such as vehicle types, vehicle stopped positions, and vehicle start-to-move positions are also recorded. For better quality control of the reduced data, an experimental procedure was developed to ensure the consistency and stability of manually reading data. Furthermore, a data check was performed by a second person.

Table 5.1 Data Reduction Form

Vehicle #:		Vehicle Type:					Date: / /
Fiducial Mark #	Time Code of Vehicle Traverse Fiducial Mark	Lane #	Position in Platoon	Maneuver			
				Stop	Move	Right Turn	Left Turn
1							
2							
3							
4							
5							
6							
7							
8							
9							
10							
11							

ESTIMATION OF SPEED AND ACCELERATION/DECELERATION

As discussed in the previous section, primary videotape data can directly produce certain vehicle related information. Other vehicle related attributes, such as vehicle speed and acceleration/deceleration, could not be measured directly, but must be estimated from the primary data. This section describes basic assumptions required to identify vehicle maneuvers and a procedure to estimate vehicle speed and acceleration/deceleration.

Basic Assumptions

Travel times and distances between fiducial marks are major primary data for speed and acceleration/deceleration estimation. Distances are measured manually. Vehicle traverse time between fiducial marks is the elapsed time for a vehicle passing successive fiducial marks. However, precise times of certain vehicle maneuvers, including stopping and starting-to-move are not clearly visible in the video data reduction process. For data tracking and analysis convenience, vehicles with speed less than 5 mph are termed stopped vehicles, and associated stopped time is the total time when the speed is less than 5 mph.

Therefore, vehicles approaching a stop with speed less than 5 mph are termed stopped vehicles, and all others are grouped as moving vehicles. Stopped vehicles decelerate to stop upon a red signal and accelerate to pass the stop line upon a green signal; moving vehicles travel along the intersection continuously without stopping. Vehicles that stop after passing the intersection stop line are counted but deleted from speed and acceleration/deceleration estimation. The stopped and moving vehicles have different traffic behavior and significant effects on fuel consumption.

The travel times between fiducial marks were averaged to represent necessary aggregate information within each road section. Although the data are not the second-by-second speeds and accelerations/decelerations required by instantaneous fuel consumption models, the aggregate data can explicitly represent traffic characteristics and vehicle behavior along the street segment. Thus an aggregate fuel consumption model can be developed.

Procedures for Speed and Acceleration/Deceleration Calibrations

Vehicle arrival time at each fiducial mark was obtained from the video screen. Vehicle speed, addressed as average travel speed within a section, is expressed as:

$$V_{ij} = \frac{D_j}{T_{i,j+1} - T_{ij}} \qquad [5.1]$$

where,

Vij: average speed for vehicle i in section j,

Dj: length of section j, and

Tij: recorded time code for vehicle i at fiducial mark j.

Thus, average speed $\bar{V}_{ij}$ for vehicle i crossing fiducial mark j can be approximately estimated by the following equation:

$$\bar{V}_{ij} = \frac{D_{j-1}+D_j}{(D_{j-1}/V_{i,j-1}+D_j/V_{ij})}$$

$$= \frac{(D_{j-1}+D_j)V_{i,j-1}V_{ij}}{D_{j-1}V_{ij}+D_jV_{i,j-1}} \qquad [5.2]$$

Acceleration/deceleration $\bar{A}_{ij}$ at fiducial mark j is estimated from average speed $\bar{V}_{ij}$ divided by the travel time:

$$\bar{A}_{ij} = \frac{\bar{V}_{ij}-\bar{V}_{i,j-1}}{T_{ij}-T_{i,j-1}} \qquad [5.3]$$

Individual vehicle average speed in each section, average speed and average acceleration/deceleration at each fiducial mark along the street segment are calculated by using Equations 5.1, 5.2, and 5.3.

Experimental Setups for Calibrating Fuel Consumption Rates

Fuel consumption data from the Federal Test Procedure (FTP) revised by USEPA are used to calibrate fuel consumption rates based on speed and acceleration/deceleration values. The EPA, the California Air Resources Board (CARB), and the Automotive Industry agreed to participate in the drive cycle testing program to certify whether new vehicles meet federal emission standards and to evaluate emissions from on-road vehicles [50]. Twenty-seven vehicles, including sixteen cars, seven light trucks, and four heavy light trucks were tested at the Vehicle Emissions Laboratory at the GM Milford Proving Ground from 1993 to 1994. Four test cycles LA4, REP05, HL07, and ARB02 were developed based on different drive patterns measured in real traffic conditions and were used to conduct the emissions testing program. The LA4 test cycle resulted from drive pattern measurements made in morning rush hour driving in LA and involved two 7.5 mile trips. The REP05 cycle is generated from actual measured micro-trips. The trips have distributions of speeds and accelerations that represents 15% of off-cycle driving and 28% of the miles traveled that are greater than contained in the LA4 cycle. HL07 is a test cycle designed to force vehicles into maximum accelerations at speeds up to 80 mph. The

ARB02 cycle was based on actual measured micro-trips, but the individual trips were selected to represent very stringent combinations of speed and accelerations.

The four test cycles have different speed and acceleration/deceleration combinations, and could produce different emissions and fuel consumption. Although the test is a chassis dynamometer laboratory test, fuel consumption and emissions data derived can reflect vehicles operating in real-world conditions. The fuel consumption and emissions data were represented as results of vehicle speed and acceleration/deceleration in the data base. Therefore, in this research, the fuel consumption rate for an individual vehicle traversing an intersection can be obtained as a function of vehicle speed and acceleration/deceleration rate.

VEHICLE SPEED AND ACCELERATION/DECELERATION PROFILE MODELS

One fundamental issue for characterizing traffic flow in urban areas is how vehicles move from one location to another location. The movement could be captured by vehicle speed and acceleration profiles, which delineate how vehicles travel in response to traffic conditions, roadway configurations, and traffic control measures. Although these profiles might vary widely according to driver behavior and vehicle types, several studies have established speed and acceleration profile models to capture the effect of traffic control measures [4, 86]. Among all these models, a polynomial model has been found to be best for estimating the acceleration rates and this model yields a good indication of the speed-time trajectory along the urban street. The polynomial model satisfies the real traffic condition that the acceleration rate is zero at the start and end of acceleration and can predict vehicle acceleration distance and determine signal offset at downstream intersections. Typical acceleration and speed profiles for vehicles passing the intersection with initial speed zero are depicted in Figures 5.2 and 5.3.

A general polynomial form for acceleration profile models, given by Akcelik and Biggs [4], is described in the following:

$$a(t)=r\, a_m\, \theta^n\, (1-\theta^m)^2 \qquad [5.4]$$

where

$a(t)$= acceleration rate at time t,

a_m= maximum acceleration,

θ= time rate, t/t_a,

t_a= acceleration time,

m, n= parameters to be determined, and

r= a parameter which depends on the values of m, n.

The values of m and n are very critical for fitting a good model based on the collected data. As a simple procedure, a value of n=1 is chosen to use in practice [4]. Other variables in the model can be defined as follows:

$$r = [(1+2m)^{2+1/m}] / 4m^2 \quad [5.5]$$

$$a_m = \bar{a}/rq = (v_f - v_i) / rqt_a \quad [5.6]$$

$$q = m^2 / [(2m+2)(m+2)] \quad [5.7]$$

$$\theta_m = t_m/t_a = (1+2m)^{-1/m} \quad [5.8]$$

where,

v_i = vehicle initial speed,

v_f = vehicle final speed (desired speed),

$\bar{a}$ = vehicle average acceleration rate, and

t_m = time of maximum acceleration rate.

In order to measure the goodness of fit between the collected acceleration data and the polynomial model, various values of m from 0 to 1.0 are chosen. A model with m=0.43 is found to be best to describe the collected data. Figure 5.4 shows the measured and predicted vehicle acceleration trajectories departing from the stop line at the signalized intersection. The vehicle increases acceleration rate dramatically in the first few seconds, reaches the maximum acceleration rate around the 4th to 7th second, and decreases from maximum acceleration to zero at the end of the acceleration time. The polynomial acceleration model represents a very good prediction of the acceleration rates (R^2=0.886). The average time for vehicles accelerating to a desired speed is about 20 seconds and the maximum acceleration rate is 5.1 ft/sec^2 at the 4th second after the start of green. Figure 5.5 shows that the accuracy of acceleration rate estimates is high although the acceleration rates are underestimated in the middle of the acceleration time.

Vehicles accelerate to reach their maximum acceleration rates and continue to reach their desired speeds. Vehicles are assumed to maintain constant speeds downstream after they reach desired speeds. The corresponding speed profile model could also be modeled as a polynomial:

$$v(t) = v_i + t_a\, r\, a_m\, \theta^{2n} (0.5 - 2\,\theta^m / (m+2) + \theta^{2m} / (2m+2)) \quad [5.9]$$

With the same parameters used in the acceleration model, the measured and predicted speed trajectories are depicted in Figure 5.6. The accuracy of speed estimates as shown in Figure 5.7 is very high (R^2=0.963).

The deceleration profile model is similar in shape to the acceleration profile model, except that the curve is reversed. The deceleration model also satisfies the real traffic conditions that the deceleration rate is zero at the start and end of deceleration. This model could be applied to determine stopping sight distance and signalized intersection clearance intervals.

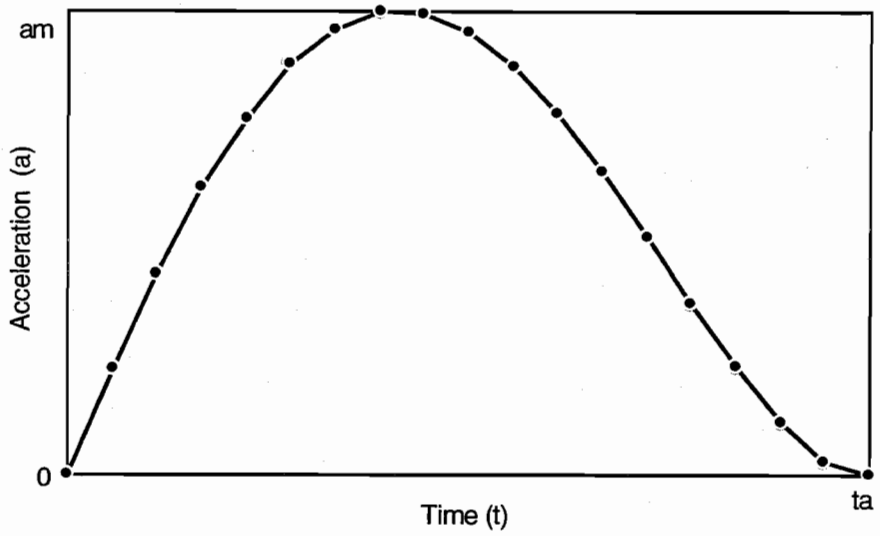

Figure 5.2. Typical acceleration profiles for vehicles passing through the intersection from the start of green time

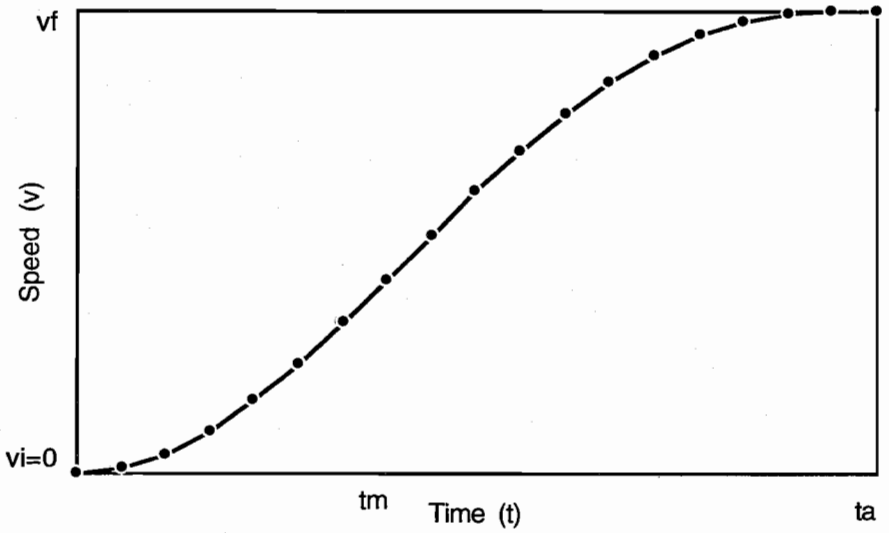

Figure 5.3. Typical speed profiles for vehicles passing through the intersection from the start of green time

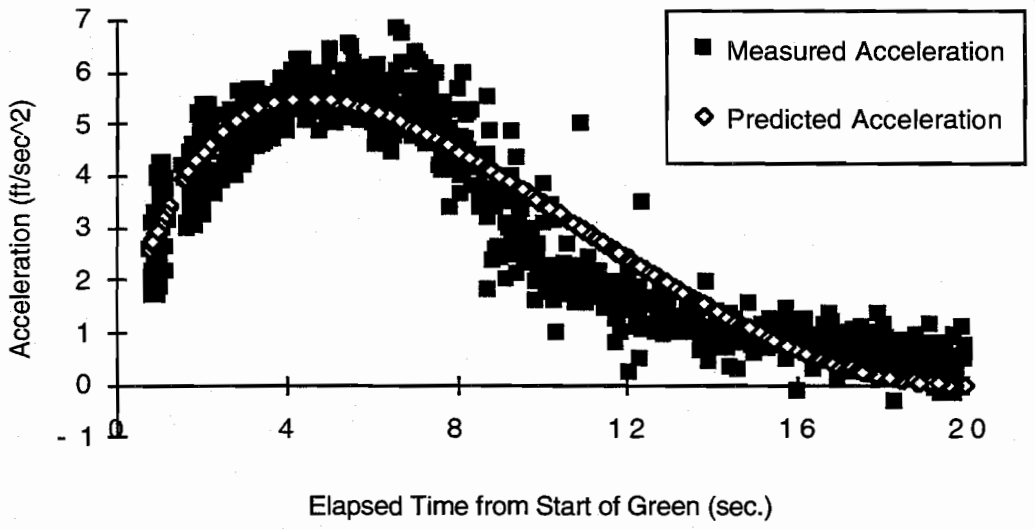

Figure 5.4. Measured and predicted vehicle acceleration trajectories

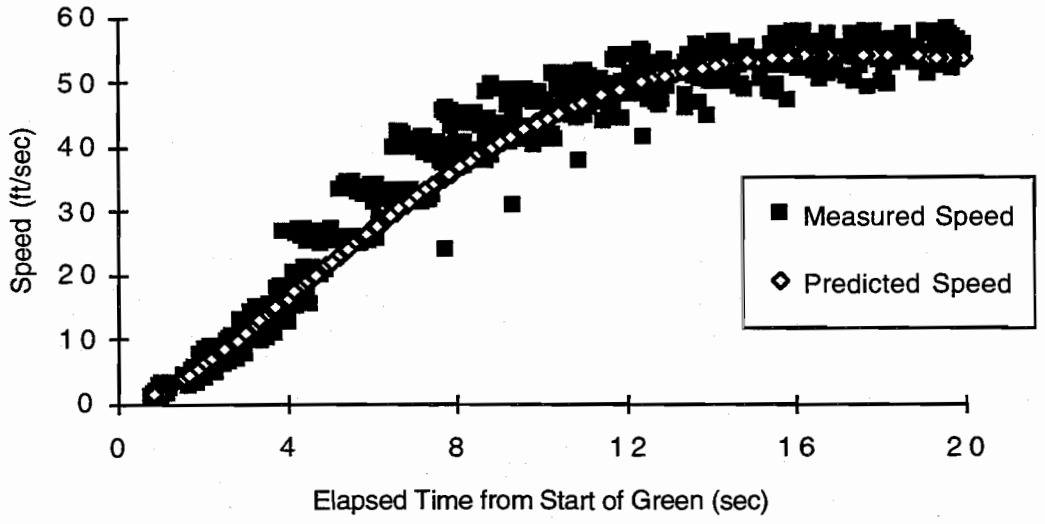

Figure 5.5. Measured and predicted vehicle speed trajectories

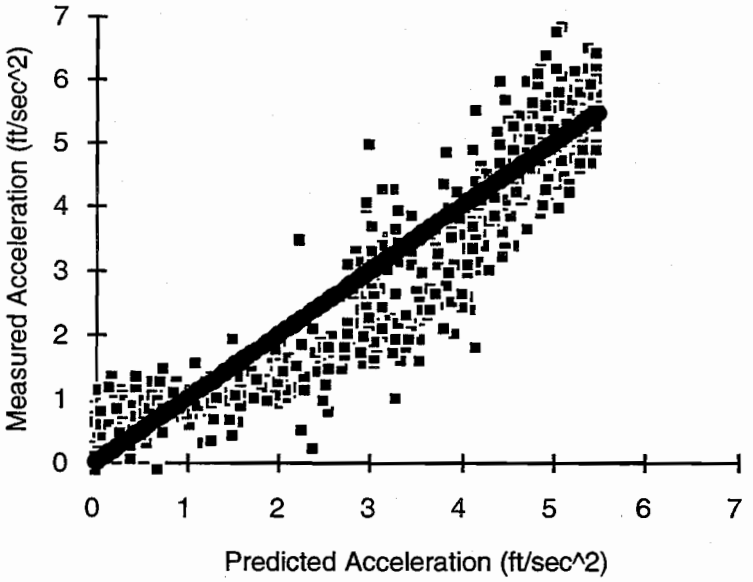

Figure 5.6. Predictive capability of the polynomial acceleration profile model

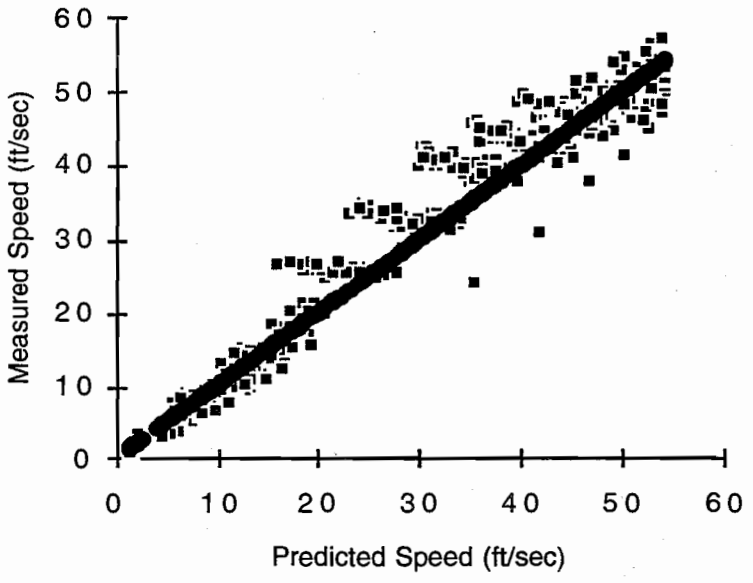

Figure 5.7. Predictive capability of the polynomial speed profile model

FUEL CONSUMPTION PROFILE MODELS

From the previous sections, vehicle movement is modeled through the speed and acceleration/deceleration profile model derived from observed traffic data. In order to utilize fuel consumption data from USEPA, fuel consumption models based on the speed, acceleration/deceleration profile models must be established. This section develops the procedure for estimating fuel consumption rates by first describing fuel consumption characteristics.

In general, fuel consumption in urban areas has the following characteristics:

1. Vehicles have the smallest fuel consumption rate during idling while stopped and consume more fuel after they start moving.
2. The most fuel is consumed when vehicles are at high speed with a high acceleration rate. However, due to signal control and speed limits, vehicles reach maximum acceleration rates after a few seconds of green time while the speeds are still low, and gradually decrease acceleration rates to zero upon reaching desired speeds.
3. Usually, vehicles have higher fuel consumption rates during the time of maximum acceleration.

From the observation, fuel consumption is highly related to vehicle speed and acceleration/deceleration. Let V_{nt} and a_{nt} represent the speed and acceleration/deceleration of vehicle n at time t, respectively. The fuel consumption rate at time t for a vehicle can thus be expressed as:

$$ff_{nt} = f(V_{nt}, a_{nt}) \qquad [5.10]$$

Since speed and acceleration/deceleration are functions of elapsed time from the start of signal green, fuel consumption rate could be related to signal timing. Fuel consumption profile models, therefore, can be obtained through the speed, acceleration/deceleration, and corresponding fuel consumption rate at any instant in time.

Fuel consumption profile models can be defined based on vehicle acceleration and speed profile models. Vehicles have idle fuel consumption during stopped time and consume more fuel after they start to move. Since acceleration and deceleration have different effects on fuel consumption, typical fuel consumption profile models are divided into two groups: (1) fuel consumption profile models characterizing acceleration which can be used to describe vehicles discharging from the stop line upon a green signal, and (2) fuel consumption profile models characterizing deceleration which are useful for describing fuel consumption for vehicles decelerating to a stop at a red signal.

Fuel Consumption Profile Model During Acceleration

An acceleration fuel consumption profile model describes vehicle fuel consumption after the vehicles pass the intersection stop line. Maximum fuel consumption occurs during high speed and high acceleration. However, due to signal control and speed limits, only 5% of the vehicles passing through an intersection are observed with high speed and high acceleration rates. From the EPA fuel consumption data base, fuel consumption rate is represented as a result of vehicle speeds and acceleration rates. Therefore, instantaneous vehicle fuel consumption rates can be calibrated from a function of vehicle speed and acceleration.

The fuel consumption rate at time t for a vehicle given in Equation 5.10 is $ff_{nt} = f(V_{nt}, a_{nt})$; therefore, a typical fuel consumption profile model used to estimate average vehicle fuel consumption rate can be expressed as:

$$ff = f(V, a) \qquad [5.11]$$

where V is average vehicle speed and a is average acceleration. From the regression analysis, the best model for describing fuel consumption during acceleration is:

$$ff_{acc} = \alpha + \beta V a \qquad [5.12]$$

where,

ff_{acc} = instantaneous fuel consumption rate during acceleration, and

α, β = coefficients,

The vehicle speed v and vehicle acceleration a with respect to time can be obtained from equations 5.4 and 5.9. The value of α is the idle fuel consumption rate and is equal to 13.0×10^{-5} gallon/second (0.3310 grams/second). The magnitude of β is 0.8434 and from the collected data the adjusted R^2 is 0.929. Figure 5.8 depicts the instantaneous fuel consumption trajectory after the start of green on the outbound leg. The figure shows the EPA fuel consumption data and predicted values from the regression model. It indicates that vehicle fuel consumption rates strongly depend on the linear interaction of vehicle speed and acceleration (product of v and a). Therefore, for energy conservation, the best strategy is to accelerate rapidly at the start of green and slowly as the desired speed is reached.

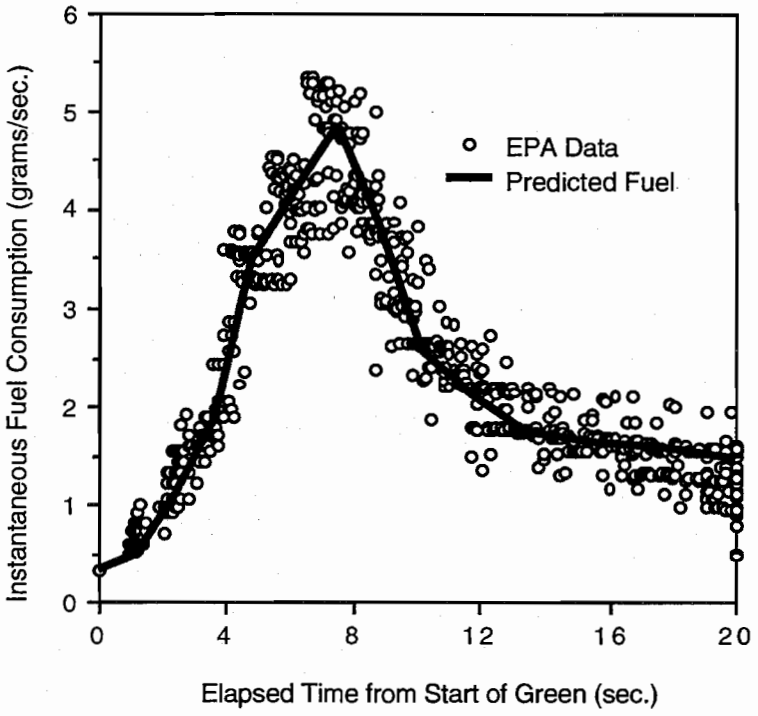

Figure 5.8 Instantaneous fuel consumption rate after the start of green on the outbound leg

Since vehicle speed and acceleration rates expressed in equations 5.4 and 5.9 are functions of time, the fuel consumption rate could also be represented as a function of time. Figure 5.9 shows a cumulative fuel consumption trajectory for vehicles traveling along the outbound leg after the start of green time. The predicted curve is calculated from the cumulative fuel consumption regression model. The adjusted R^2 is 0.992.

$$CF_{acc} = 13 - 9.6935\ t + 24.9251\ t^2 - 1.6140\ t^3 + 0.0305\ t^4 \qquad [5.13]$$

where,

CF_{acc} = cumulative fuel consumption during acceleration at time t, and

t = elapsed time from start of green signal indication.

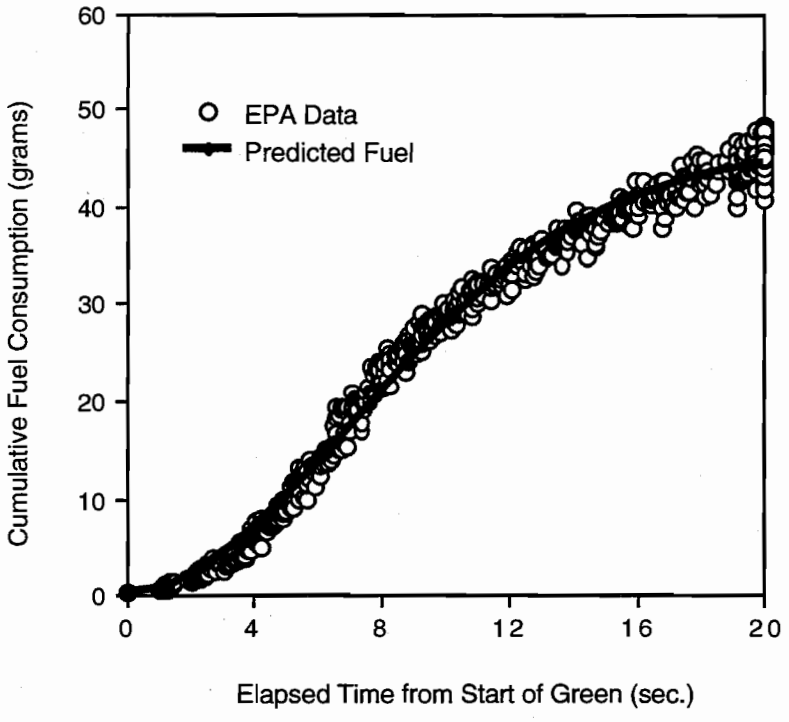

Figure 5.9 Cumulative fuel consumption on the outbound leg as a function of time

Fuel Consumption Profile Model During Deceleration

Vehicle deceleration only slightly affects fuel consumption; therefore, the fuel consumption profile model for deceleration is expressed as a function of vehicle speed:

$$ff_{dec} = \beta_0 + \beta_1 V + \beta_2 V^2 + \beta_3 V^3 \quad [5.14]$$

where,

ff_{dec} = instantaneous fuel consumption during deceleration.

From regression analysis, the fuel consumption profile model is expressed and the adjusted R^2 is 0.952:

$$ff_{dec} = 13.0106 + 0.5215\ V - 0.0160\ V^2 + 0.0001\ V^3 \quad [5.15]$$

Figure 5.10 depicts an instantaneous fuel consumption trajectory obtained from the EPA fuel consumption data base and predicted values from the regression model using inbound

approach observed speeds and decelerations. The instantaneous fuel consumption during acceleration is obviously higher than during deceleration.

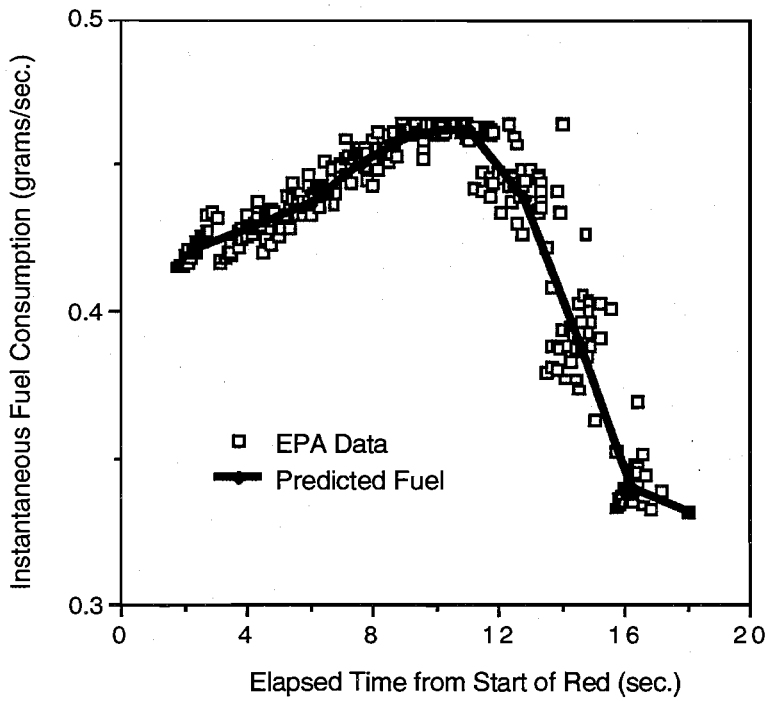

Figure 5.10 Instantaneous fuel consumption rate after the start of red on the inbound approach

Cumulative fuel consumption during deceleration can be likewise expressed as a function of elapsed time. The regression model, expressed in equation 5.16, is a linear function and the results are depicted in Figure 5.11.

$$CF_{dec} = 35.4269 + 16.7202t \ (R^2=0.997) \qquad [5.16]$$

where,

CF_{dec} = cumulative fuel consumption during acceleration at time t, and

t = elapsed time from the start of the red signal indication.

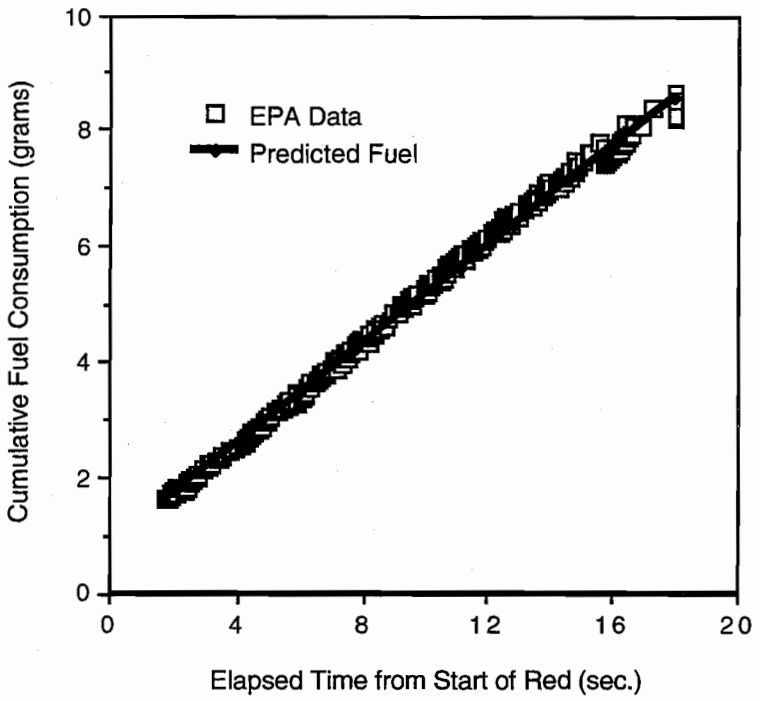

Figure 5.11 Cumulative fuel consumption on the inbound approach as a function of time

FUEL CONSUMPTION BEHAVIOR AT SIGNALIZED INTERSECTIONS

Introduction

As presented in previous sections, vehicle fuel consumption, corresponding to speed and acceleration/deceleration, can be identified as a function of elapsed time from the start of a signal cycle. Since vehicle speed and acceleration/deceleration follow certain patterns along the street segments, the fuel consumption profile can also be differentiated into certain profile sections based on traffic behavior changes. For example, vehicles accelerate rapidly after the start of signal green, continue to accelerate with a lower acceleration rate after the first few seconds, and maintain almost constant speed after they reach desired speeds. Fuel consumption changes, therefore, can also be estimated using speed changes. Thus aggregate fuel consumption rates along street segments or road sections can be estimated and applied to the AFCM aggregate fuel consumption model estimating intersection fuel consumption.

Additionally, intersection fuel consumption behavior and fuel consumption estimation are dependent on the area surrounding the intersection. The size of the intersection surrounding area, termed the "intersection influence area", determines the number of vehicles, speed and acceleration/deceleration changes, and total fuel consumption. The size of the intersection influence area depends on the speed limits which control vehicle speed changes and desired speeds, the upstream and downstream distance to other intersections, and neighboring signal controls which affect vehicle maneuvers. Therefore, the following discussions deal with the intersection influence area and its implication for calibrating the aggregate AFCM fuel consumption rates.

Average Fuel Consumption Rate f_{ij}

The objective of deriving average fuel consumption rates is to develop an aggregate fuel consumption model which is at least as good as instantaneous models and can estimate fuel consumption in a simple and broad way. As described in previous sections, a fuel consumption profile model is a function of a speed and acceleration production term and for vehicle deceleration is a function of speed. Since the fuel consumption profile model includes variable "speed" for both acceleration and deceleration, average fuel consumption rates are calibrated based on speed differentiation.

Average fuel consumption rates f_{ij}, defined as the average fuel consumption rate for a vehicle changing from speed i to speed j, can be estimated from the following equation:

$$f_{ij} = \frac{SF_{ij}}{t_{ij}} \qquad [5.17]$$

where,

$SF_{ij} = CF_j - CF_i$,

f_{ij} = average fuel consumption rate while changing from speed i to j,

SF_{ij} = total fuel consumption for vehicle movement from speed i to j,

t_{ij} = travel time from speed i to speed j, and

CF_j, CF_i = cumulative fuel consumption when vehicle speed reaches i, j.

Seven f_{ij} values are estimated for seven parts of the vehicle speed-time trajectory encompassing zero to desired speed.

f_0 = idle fuel consumption rate,

f_{02} = average vehicle fuel consumption rate from stop to speed V_2, where V_2 is the average speed for stopped vehicles as they cross the stop line,

f_{020} = average vehicle fuel consumption rate from stop to speed V_2, and from speed V_2 to stop,

f_{03} = average vehicle fuel consumption rate from stop to speed V_3, where V_3 is the average speed for arriving vehicles to pass the stop line,

f_{030} = average vehicle fuel consumption rate from stop to speed V_3, and from speed V_3 to stop,

f_{24} = average vehicle fuel consumption rate from speed V_2 to speed V_4, where V_4 is the average speed for stopped vehicles as they cross the intersection,

f_{35} = average vehicle fuel consumption rate from speed V_3 to speed V_5, where V_5 is the average speed for arriving vehicles as they cross the intersection,

f_{4r} = average vehicle fuel consumption rate from speed V_4 to desired speed V_r,

f_{5r} = average vehicle fuel consumption rate from speed V_5 to desired speed V_r, and

f_r = vehicle fuel consumption rate for desired speed V_r.

Therefore, the acceleration fuel consumption rate f_{ij} using observed acceleration data can be estimated from equations 5.12 and 5.13 and the results are shown in Table 5.2.

TABLE 5.2 AVERAGE FUEL CONSUMPTION RATE F_{IJ} FROM SPEED V_I TO V_J DURING ACCELERATION

Variable Name	Definition	Fuel Consumption Rate	
		gallon(10^{-5})/sec	gram/sec
f_0	idle	13.00	0.3310
f_{02}	change speed from V_0 to V_2	19.64	0.5000
f_{020}	change speed from V_0 to V_2, and from V_2 to V_0	19.64	0.5000
f_{03}	change speed from V_0 to V_3	27.88	0.7100
f_{030}	change speed from V_0 to V_3, and from V_3 to V_0	27.88	0.7100
f_{24}	change speed from V_2 to V_4	70.69	1.8000
f_{35}	change speed from V_3 to V_5	39.27	1.0000
f_{4r}	change speed from V_4 to V_r	46.48	1.1837
f_{5r}	change speed from V_5 to V_r	39.27	1.0000
f_r	traveling at a constant speed	32.99	0.8402

Similarly, average fuel consumption f_{ij} for vehicles decelerating to stop can be identified based on speed differentiation. For vehicles that stop, speeds change from V_r to V_0 in front of the stop line. However, some vehicles decelerate but do not stop during the red signal. Assume moving vehicles change speed from V_r to speed V_2 or V_3. Therefore, the fuel consumption rate f_{ij} during deceleration from the collected data can be estimated from equations 5.15 and 5.16 and the results are shown in Table 5.3.

TABLE 5.3 AVERAGE FUEL CONSUMPTION RATE F_{IJ} FROM SPEED V_I TO V_J DURING DECELERATION

Variable Name	Definition	Fuel Consumption Rate	
		gallon(10-5)/sec	gram/sec
f_0	idle	13.00	0.3310
f_{r0}	change speed from V_r to V_0	23.56	0.6000
f_{r2}	change speed from V_r to V_2	27.88	0.7100
f_{r3}	change speed from V_r to V_3	27.88	0.7100

Aggregate Fuel Consumption Estimation at the Intersections

As described in Chapter 4, the AFCM fuel consumption model defined in this study is an aggregate model as opposed to instantaneous fuel consumption models requiring second-by-second data. Average fuel consumption rates f_{ij}, corresponding to individual vehicle speed and acceleration/deceleration profiles, are critical AFCM model parameters. Figure 5.12 depicts the results of average fuel consumption rates f_{ij} for vehicles entering the intersection influence area. Vehicles decelerating to stop for a red signal on the inbound approach will have average fuel consumption f_{r0} which is associated with speed changes from initial speed V_r to final speed V_0 and f_0 after stopping. After the signal changes to green, vehicles accelerate and move to the outbound leg. The average speed for vehicles crossing the stop line is V_2 and average fuel consumption is f_{02}. The average fuel consumption rate for vehicles within the intersection is f_{24} as speed changes from V_2 to speed V_4. The magnitude of f_{4r} is the average fuel consumption rate for vehicles changing from speed V_4 to desired speed V_r. After vehicles reach desired speeds, they will travel at constant speed V_r and have average fuel consumption rate f_r.

However, if vehicles enter the intersection influence area and do not stop, the average fuel consumption rate will be f_r or f_{r3} depending on when they enter the influence area. Furthermore, the average fuel consumption rate for these vehicles crossing the stop line will be f_{24} or f_{4r} because they do not stop.

Total fuel consumption for the intersection; therefore, is estimated by the AFCM incorporating the parameters, vehicle number, average fuel consumption rate, and travel time through the intersection influence area.

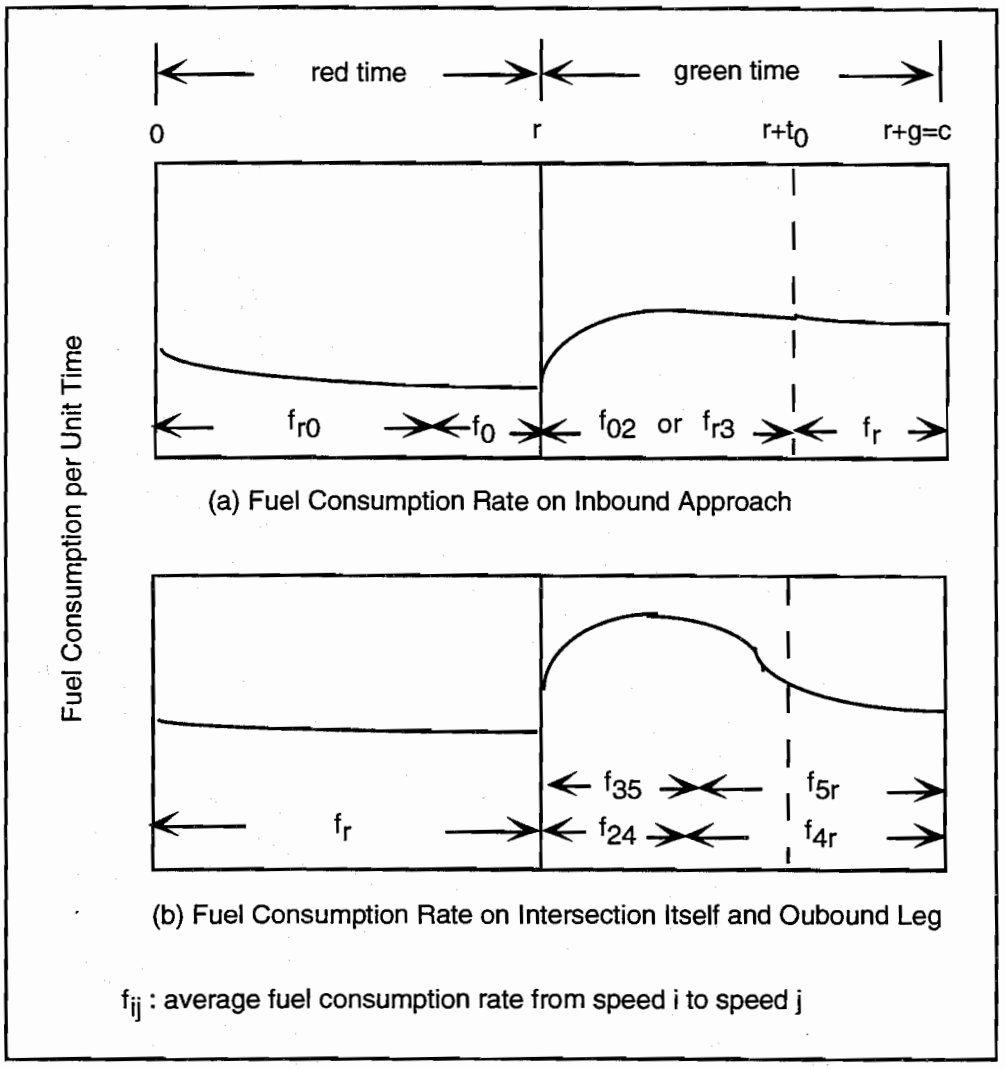

Figure 5.12 Profile of average fuel consumption rate from the analysis and results of aggregate fuel consumption model

SUMMARY

This chapter presents an experimental design, data collection, and data analysis for developing vehicle speed, acceleration/deceleration, and fuel consumption profile models related to traffic signal control in an urban street. The results indicate that a polynomial model is good for describing vehicle speed and acceleration/deceleration trajectories. The polynomial model has different parameters to represent the variety of traffic maneuvers and driver behavior. Furthermore, this model satisfies the real traffic condition that acceleration rate is zero at the start and end of the acceleration and can be used to predict vehicle acceleration distance and determine downstream intersection signal offsets.

Additionally, from the speed, acceleration/deceleration profile models, and fuel consumption data obtained from USEPA, fuel consumption profile models are defined to present fuel consumption behavior at the intersection influence area. The fuel consumption profile model is a function of the combined effect of speed and acceleration during acceleration and is a function of speed during deceleration. The cumulative fuel consumption can be represented as a function of elapsed cycle time.

Another important feature that emerges from the results is that fuel consumption strongly depends on the combined effects of vehicle speed and acceleration/deceleration and thus reveals an effect of signal timing on fuel consumption. Since cumulative fuel consumption is a function of elapsed cycle time, it indicates the effects of signal timing on fuel consumption. Chapters 6 and 7 will discuss detailed descriptions of the relationship between signal timing and fuel consumption and the investigation of an optimal signal control strategy for fuel consumption and delay minimization.

CHAPTER 6. NUMERICAL EXPERIMENTS

INTRODUCTION

As discussed in Chapter 4, fuel consumption at a signalized intersection is estimated using average fuel consumption rates, traffic characteristics, and associated control measures. Due to the system complexity, numerical experiments are conducted to explore the AFCM estimation capability. Two important objectives of these numerical experiments are to establish the credibility of the AFCM and to explore utilization of the model to optimize signal timing.

In the numerical experiments, the intersection influence area is divided into three physical segments: inbound, intersection, and outbound. A signal cycle is divided into three stages: effective red time, green time with saturation flow rate, and remaining green time. Three cases: a two-phase pretimed signal without left turns, a two-phase pretimed signal with left turns on one approach, and a three-phase pretimed signal with a protected left-turn phase are considered to investigate the estimation capability of the AFCM and the different optimization objectives, namely delay and fuel consumption. Also, to establish the model's credibility, results from the AFCM are compared with the TEXAS model. Under the same control measures and traffic characteristics, patterns of elapsed second-by-second fuel consumption along the travel distance and total fuel consumption for the intersection influence area are compared.

Experimental design is described in Section 6.2, and three numerical experiments under a variety of traffic conditions are conducted to investigate the AFCM. Section 6.3 discusses the adjustment factor of left turns and its effects on fuel consumption estimation. The effect of signal timing on fuel consumption estimation is discussed in Section 6.4 and the optimal cycle length from the AFCM and delay are compared in Section 6.5. A brief summary is given in Section 6.6.

NUMERICAL EXPERIMENTS

AFCM Fuel Consumption Estimation

The Analytical Fuel Consumption Model (AFCM) includes detailed sub-models which describe fuel consumption estimation under different traffic conditions in the intersection influence area. Total fuel consumption estimation within a cycle is a summation of fuel consumption on street segments in different cycle stages. From AFCM, total intersection fuel consumption is expressed as:

$$STF = \sum_{n=1}^{N} \sum_{t=1}^{T_n} ff_{nt}(V_{nt}, a_{nt})$$

$$= \sum\sum TF_{ij}$$

$$= TF_{ib\text{-}1}{}^{q} + TF_{ib\text{-}2}{}^{q} + TF_{ib\text{-}3}{}^{q} +$$

$$TF_{int\text{-}1}{}^{q} + TF_{int\text{-}2}{}^{q} + TF_{int\text{-}3}{}^{q} +$$

$$TF_{ib\text{-}1}{}^{q} + TF_{ib\text{-}2}{}^{q} + TF_{ib\text{-}3}{}^{q} \qquad [6.1]$$

where,

STF = total fuel consumption in the intersection influence area during a cycle,

ff_{nt} = fuel consumption rate for vehicle n at time t with speed v_{nt} and acceleration a_{nt},

T_n = travel time for vehicle n in the intersection influence area,

N = number of vehicles, and

TF_{ij} = total fuel consumption for vehicles in street segment i during cycle stage j.

Total fuel consumption for the intersection influence area (STF) is a summation of total fuel consumption (TF_{ij}) for different street segments i in different signal cycle stages j. Since traffic conditions change from time to time, total fuel consumption STF may be different from cycle to cycle. Therefore, to consider fuel consumption as an intersection performance measure, estimation of total fuel consumption may include a series of cycles which include undersaturated and oversaturated traffic conditions.

Experimental Design

Two important objectives of these numerical experiments are to establish the AFCM credibility and to explore utilization of the model for signal timing optimization. In the numerical experiments, the intersection influence area is divided into three physical segments: inbound, intersection, and outbound. A pretimed signal cycle is divided into three stages: effective red time ($0 \le t \le r$), green time with saturation flow rate ($r < t \le r+t_0$), and remaining green time ($r+t_0 < t \le r+g = c$). In the intersection influence area, the inbound approach length is 800 ft and the outbound leg is 800 ft with speed limit 30 mph on each approach. Approach grades and parking in the intersection vicinity are not considered.

Three cases are used to investigate the estimation capability of AFCM by comparing with the results from the TEXAS model: (1) Case I, two-phase pretimed signal without left turns, (2) Case II, two-phase pretimed signal with left turns on one approach, and (3) Case III, three-phase pretimed signal with left turn phase. The geometric configurations and traffic movements of the three cases are depicted in Figures 6.1 to 6.3. Basic information, as shown in Table 6.1, includes cycle lengths, cycle phases, traffic volumes, and saturation flow. The cycle length is assumed to

be 60 seconds for Case I. Case II includes 10% of left turn movements, and the cycle length is assumed to be 70 seconds. Case III is designed to investigate the fuel consumption behavior for exclusive left turn lane with protected phasing, and the cycle length is assumed to be 90 seconds. The green split of cycle length is based on the flow ratio, i.e.,

$$G_i = \frac{y_i}{\sum_i y_i} (C - Lost) \qquad [6.2]$$

where,

C = cycle length,

Lost = nl + R,

n = the number of phases,

l = the average lost time per phase (excluding all-red times),

R = all-red times,

G_i = Green time of phase i, and

y_i = maximum flow ratio of phase i.

In order to appropriately capture the impact of left turns, the saturation flow rate in Cases I and III needs to be adjusted. According to 1994 Highway Capacity Manual (HCM), saturation flow rate is defined as the flow that could be accommodated by the lane group assuming that the green phase was always available to the lane group, i.e., the green ratio is 1.0. An "ideal" saturation flow rate, normally 1900 passenger cars per hour of green time per lane (pcphgpl), is adjusted based on a variety of prevailing conditions. All the adjustment factors are given in 1994 HCM [54]. Then, saturation flow rate can be estimated as:

$$s = s_0 N f_w f_{HV} f_g f_p f_{bb} f_a f_{RT} f_{LT} \qquad [6.3]$$

where:

- s = saturation flow rate for the subject lane group, expressed as a total for all lanes in the lane group under prevailing conditions, in vphg,
- s_0 = ideal saturation flow rate per lane, usually 1,900 pcphgpl,
- N = number of lanes in the lane group,
- f_w = adjustment factor for lane width (12-ft lanes are standard),
- f_{HV} = adjustment factor for heavy vehicles in the traffic stream,
- f_g = adjustment factor for approach grade,
- f_p = adjustment factor for the existence of a parking lane adjacent to the lane group and the parking activity in that lane,

f_{bb} = adjustment factor for the blocking effect of local buses that stop within the intersection area,

f_a = adjustment factor for area type,

f_{RT} = adjustment factor for right turns in the lane group, and

f_{LT} = adjustment factor for left turns in the lane group.

As shown in Table 6.1, the normal saturation flow rate for straight movements in the experiments is assumed to be 1500 veh/hr to reflect different adjustment factors, such as lane width (11ft, 0.967), heavy vehicles (10%, 0.909), and area type (0.95). In Case II, the left turn adjustment factor, based on the calculation from Table 6.2, is 0.782, and the saturation flow rate for the NB which has shared left turn lane with permitted phasing is about 1173 veh/hr. Case III, with an exclusive left turn bay and a protected phase, is adjusted by 0.95, and the saturation flow rate is about 1425 veh/hr.

The results of total fuel consumption and associated trajectories are discussed in the next section according to the three cases.

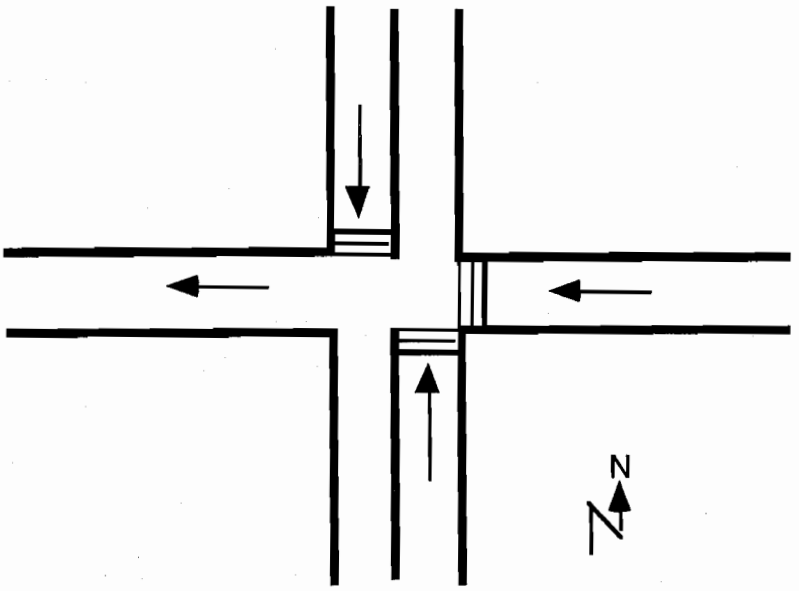

Figure 6.1 Intersection geometric configuration for case I

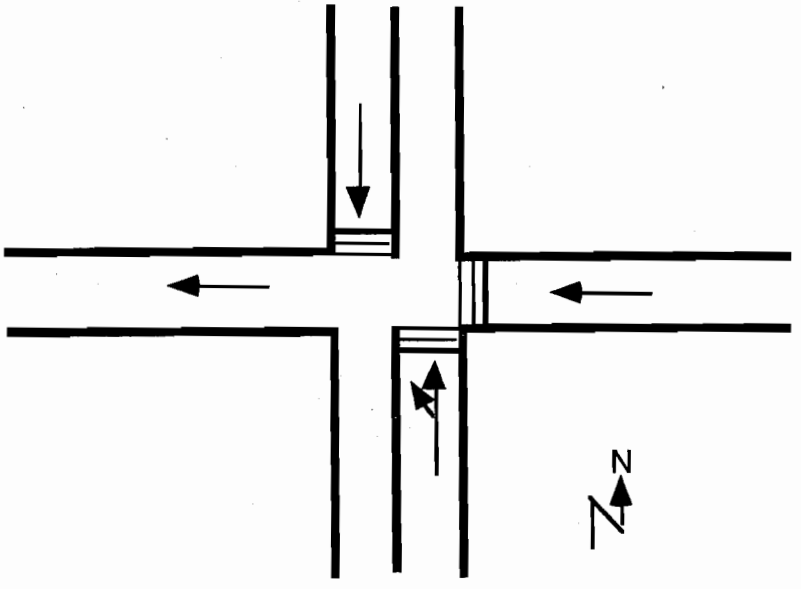

Figure 6.2 Intersection geometric configuration for Case II

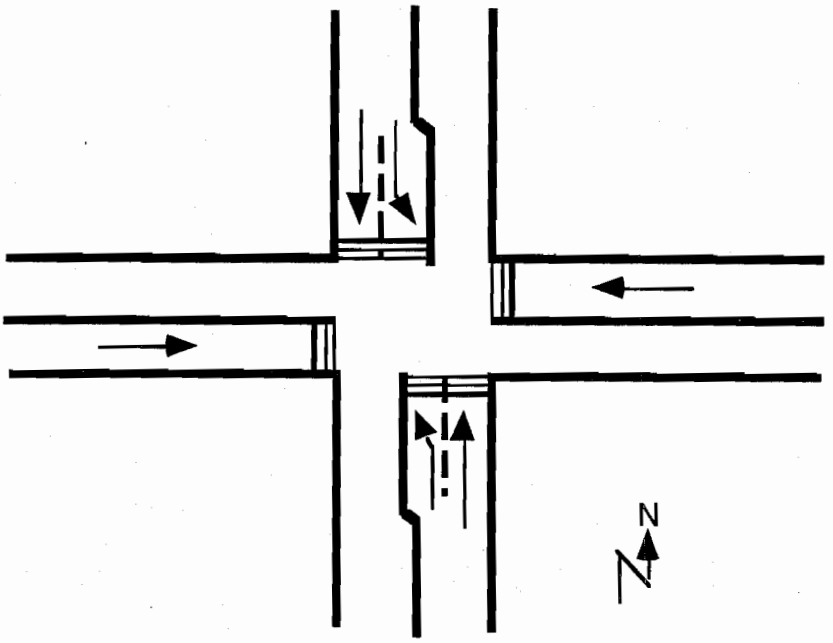

Figure 6.3 Intersection geometric configuration for Case III

TABLE 6.1 BASIC TRAFFIC DATA FOR THE NUMERICAL EXPERIMENTS

Case	Signal Design		Traffic	Traffic Flow	Saturation Flow
	Cycle Length	Phase	Movement	(veh/hr)	(veh/hr)
I	60	I	NB (straight)	650	1500
			SB (straight)	500	1500
		II	WB (straight)	300	1500
II	70	I	NB (with 10% LT)	650	1173
			SB (straight)	500	1500
		II	WB (straight)	300	1500
III	90	I	NB (Straight)	585	1500
			SB (straight)	450	1500
		II	NB (left turn)	65	1425
			SB (left turn)	50	1425
		III	WB (straight)	300	1500
			EB (straight)	300	1500

TABLE 6.2 CALCULATION OF LEFT-TURN ADJUSTMENT FACTOR FOR CASE II [54]

	Westbound	Southbound	Northbound
C, cycle length	70	70	70
G, actual green time for lane group	16	44	44
g, effective green time for lane group	18	47	47
g_o, opposing effective green time	18	47	47
N, number of lanes in lane group	1	1	1
N_o, number of opposing lanes	1	1	1
V_a, volume in lane group	300	500	650
V_{LT}, adjusted left-lane flow rate	0	0	65
P_{LT}, proportion of left turns in lane group	0	0	0.1
V_o, adjusted opposing flow rate	300	650	500
t_L, lost time per phase	5	5	5
COMPUTATION			
LTC = V_{LT} C/3600, left turn per cycle	0.00	0.00	1.26
$V_{olc} = V_o$ C/3600, opposing flow per lane per cycle	5.83	12.64	9.72
R_{po}, opposing platoon ratio	1.00	1.00	1.00
$g_f = G \exp(-0.882\ LTC^{0.717}) - t_L$, $g_f \le g$	11.00	39.00	10.50
$q_{ro} = 1 - R_{po}(g_o/C)$, opposing queue ratio	0.74	0.33	0.33
$g_q = V_{olc}\, q_{ro}/\{0.5-[V_{olc}\,(1-q_{ro})/g_o]\} - t_L$ $V_{olc}\,(1-q_{ro})/g_o \le 0.49$ $0 \le g_q \le g$	5.40	8.00	3.85
$g_u = g - g_q$ if $g_q \ge g_f$ $g_u = g - gf$ if $g_q < g_f$	7.00	8.00	36.50
$f_a = (875-0.625\ V_o)/1000$, $f_a \ge 0$	0.69	0.47	0.56
$P_L = P_{LT}[1+\{(N-1)g/(f_a\, g_u+4.5)\}]$	0.00	0.00	0.10
E_{L1}	4.90	4.90	4.90
$f_{min} = 2(1+P_L)/g$	0.11	0.04	0.05
$f_m = [g_f/g] + [g_u/g][1/\{1+P_L(E_{L1}-1)\}]$ min = f_{min}; max = 1.0	1.00	1.00	0.78
$f_{LT} = [f_m+0.91(N-1)]/N$	1.00	1.00	0.78
$s = 1500\ f_{LT}$, saturation flow rate	1500	1500	1173

Case I - Two-Phase Pretimed Signal without Turning Movements

Total Fuel Consumption Estimation. Total fuel consumption is different for different signal cycle lengths because of different overflow queue likelihood, different traffic movements in per cycle stage, and different queue dissipation times. In Case I, a 60 second cycle length is chosen. Table 6.3 shows the red time, the green time, t_0, and overflow queue Q^s for each phase. Traffic condition depends on several factors including cycle length (c), green time (g), traffic flow rate (q), and saturation flow rate (s). It is an undersaturated condition if $sg \geq qc$, and it is an oversaturated condition if $sg < qc$.

Since sg is greater than qc, the traffic condition for Case I is undersaturated, and overflow queue Q^s is the result of stochastic effects. Total fuel consumption in each cycle stage can be estimated as in Table 4.1.

TABLE 6.3 CASE I SIGNAL TIMING DATA

Cycle (sec.)	Phase		Green Time	Red Time	t_0	Lost Time	Overflow Queue (veh./sec.)
60	I	NB	34	21	20	5	0.4267
		SB	34	21	12		0.0340
	II	WB	16	39	13	5	0.7094

From Equation 4.32, total fuel consumption on the inbound approach during the effective red time is given by

$$TF_{ib\text{-}1} = \int_0^r [N_S f_0 + N_m f_{r0}]\, dt$$

$$TF_{ib\text{-}1} = \int_0^r [(Q^s+qt) f_0 + qT_{11} f_{r0}]\, dt$$

$$= \int_0^r [(Q^s+qt) f_0 + q\,(1 - \frac{N_S \bullet L}{S})\, T_{ib} f_{r0}]\, dt$$

$$= (Q^s r + \frac{1}{2} qr^2) f_0 + [q r (1 - \frac{Q^s + 1/2 \bullet qr}{S} \bullet L)\, T_{ib}]\, f_{r0} \qquad [6.4]$$

where N_S and N_m are the number of vehicles with fuel consumption rates f_0 and f_{r0} on the inbound approach during the effective red time, respectively. The magnitude of f_0, idle fuel consumption, is about 0.3310 grams/sec (13×10^{-5} gallons/sec). Fuel consumption rate, f_{r0}, is the rate for a vehicle decelerating from desired speed V_r to a stopped or an idle state and, from

the collected data is equal to 0.6 grams/sec (23.544×10^{-5} gallons/sec). T_{ib}, used to estimate the number of arriving vehicles that are currently in the deceleration process, is equal to 30 seconds. Therefore, total fuel consumption on the inbound approach during effective red time in a cycle is

$$TF_{ib\text{-}1} = (Q^s r + \frac{1}{2} qr^2) f_0 + [q r (1 - \frac{Q^s + 1/2 \bullet qr}{S} \bullet_L) T_{ib}] f_{r0}$$

$$= 90.402 \text{ grams} \qquad [6.5]$$

By following the same procedure, total fuel consumption for different street segments during different signal cycle stages can be obtained, as shown in Table 6.4. Thus, total fuel consumption, estimated from Equation 6.1, is about 1115.745 grams per cycle (60 seconds) and is 66944.700 grams/hr (26.289 gallons/hr). By comparing with the results from the TEXAS model, the difference between the TEXAS and AFCM is within ±10%, and the results are shown in Table 6.5. It indicates that total fuel consumption estimated from the AFCM is very close to the results from the TEXAS model, which suggests that the mathematical representations of the AFCM might be used to replace the simulation-based model.

Table 6.6 shows the variations of total fuel consumption per hour with respect to the cycle time from 30 to 180 seconds at intervals of 10 seconds. The numerical results shows that the optimal cycle length for minimizing fuel consumption is about 80 seconds.

TABLE 6.4 FUEL CONSUMPTION ESTIMATES FOR STREET SEGMENTS DURING CYCLE STAGES - CASE I (UNIT: GRAMS) (TOTAL ELAPSED TIME = 1 CYCLE 60 SECONDS)

		Effective Red Time	Effective Green Time		Total
			(Before t_0)	(After t_0)	
Northbound	Inbound	90.402	93.573	46.677	230.652
	Intersection	0.000	35.637	7.780	43.417
	Outbound	31.459	82.679	103.707	217.845
Southbound	Inbound	68.550	42.183	52.594	163.327
	Intersection	0.000	22.553	8.732	31.285
	Outbound	23.339	28.982	104.089	156.410
Westbound	Inbound	92.526	31.809	7.226	131.561
	Intersection	0.000	25.740	1.204	26.944
	Outbound	48.671	34.486	31.147	114.304
Total					1115.745

TABLE 6.5 THE DIFFERENCE OF FUEL CONSUMPTION FROM THE TEXAS AND AFCM

		AFCM	TEXAS	Difference (AFCM-TEXAS)/TEXAS
Northbound	Inbound	230.652	233.339	-0.01
	Intersection	43.417	42.227	0.03
	Outbound	217.845	220.302	-0.01
Southbound	Inbound	163.327	175.106	-0.07
	Intersection	31.285	34.414	-0.09
	Outbound	156.410	174.196	-0.10
Westbound	Inbound	131.561	133.739	-0.02
	Intersection	26.944	29.913	-0.10
	Outbound	114.304	113.124	0.01
Total		1115.745	1158.359	-0.04

TABLE 6.6 FUEL CONSUMPTION FOR DIFFERENT CYCLE LENGTH - CASE I

Cycle Length (seconds)	Fuel Consumption / Cycle (grams)	Fuel Consumption / hr (grams)
30	922.637	110716.476
40	880.397	79235.730
50	961.959	69261.019
60	1115.745	66944.700
70	1286.588	66167.383
80	1467.137	66021.165
90	1654.293	66171.720
100	1846.753	66483.108
110	2043.846	66889.505
120	2245.196	67355.880
130	2450.574	67862.049
140	2658.063	68350.191
150	2867.435	68818.440
160	3079.596	69290.910
170	3295.136	69779.351
180	3513.413	70268.260

Fuel Consumption Time History. In order to investigate fuel consumption trajectories within a cycle, average elapsed fuel consumption is compared with TEXAS model results. The TEXAS model (Traffic EXperimental and Analytical Simulation model) is a micro simulation model developed at The University of Texas at Austin. In the TEXAS simulation model, an emissions and fuel consumption processor, EMPRO, provides instantaneous fuel consumption and emissions models [58]. The EMPRO uses instantaneous vehicle speed and acceleration/deceleration with respect to time and location along the road section to estimate instantaneous fuel consumption. Fuel consumption estimation from the AFCM; therefore, is compared with results from the TEXAS model.

The same observed speed-time histories are used in both the AFCM and the TEXAS model. Trajectories of fuel consumption variation on the northbound and westbound approach are shown in Figures 6.4 and 6.5. Traffic volume is 650 vph for the northbound approach (NB), 300 vph for the westbound approach (WB), and the signal cycle time is 60 seconds. In Figure 6.4, data points represent second-by-second fuel consumption from the AFCM and the curve represents instantaneous fuel consumption from the TEXAS model. Elapsed time from 0 to 24 seconds is the effective red time, from 24 to 60 seconds is the effective green time, and t_0 is 20 seconds. During the effective red time, because of the increasing number of inbound approach vehicles, fuel consumption increases as the elapsed time increases as shown in Figure 6.4(a). When the signal changes to green, vehicles accelerate to reach a desired speed traveling on the outbound leg. The highest fuel consumption rate during a cycle occurs during acceleration. This means that fuel consumption per unit time reaches a maximum during time t_0 and then decreases. This situation can be observed clearly from elapsed time 24 to 44 seconds in Figure 6.4(c), in which the fuel consumption increases dramatically due to high acceleration rates. Note that in Figure 6.4(c), fuel consumption exists in the first few seconds of the effective red time because some vehicles on the outbound leg have not been discharged.

Instantaneous fuel consumption, obtained from the TEXAS model, is the average second-by-second fuel consumption from simulation periods of 20 minutes. The pattern is similar and consistent with results from the AFCM. For instance, fuel consumption increases in the effective red time on the inbound approach, increases dramatically in t_0 as vehicles accelerate into the intersection and the outbound leg, decreases at the end of t_0, and remains stable when vehicles travel on the outbound leg.

Similar results can be found in Figure 6.5 in which the elapsed time from 0 to 42 seconds is the effective red time, from 42 to 60 seconds is the effective green time, and t_0 is 13 seconds.

Table 6.7 shows the correlation of elapsed fuel consumption from the AFCM and the TEXAS model. It indicates that the elapsed fuel consumption is highly correlated although the inbound approach has the smallest correlation coefficients. The main reason is the assumption of fuel consumption rate f_{02} for all queued vehicles to move from the stop line. Practically, the first few vehicles should have lower fuel consumption rates than those vehicles at the end of queues. However, to simplify the AFCM, only one fuel consumption rate f_{02} is used to represent queued vehicle fuel consumption.

The AFCM is acceptable when compared with the TEXAS model. One can investigate the impact of different traffic volumes on fuel consumption and the variation of average fuel consumption for different cycle lengths, and thus derive an optimal cycle length for fuel consumption minimization.

TABLE 6.7 CORRELATION OF ELAPSED FUEL CONSUMPTION FOR THE AFCM AND THE TEXAS MODEL - CASE I

		Correlation
Northbound	Inbound	0.80
	Intersection	0.91
	Outbound	0.96
Southbound	Inbound	0.74
	Intersection	0.78
	Outbound	0.90
Westbound	Inbound	0.73
	Intersection	0.90
	Outbound	0.94

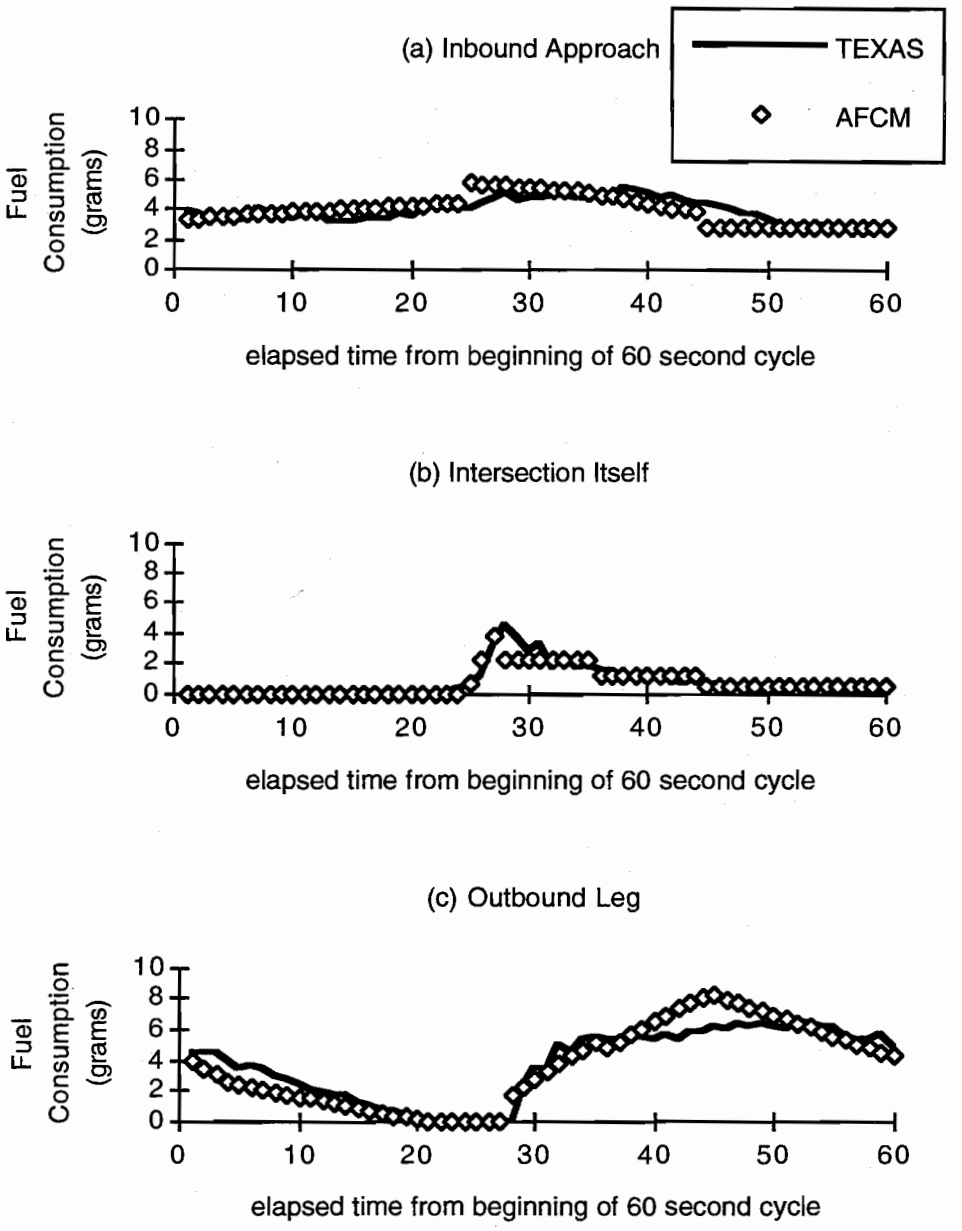

Figure 6.4 Fuel consumption versus elapsed time on the northbound approach for the AFCM and the TEXAS model - Case I

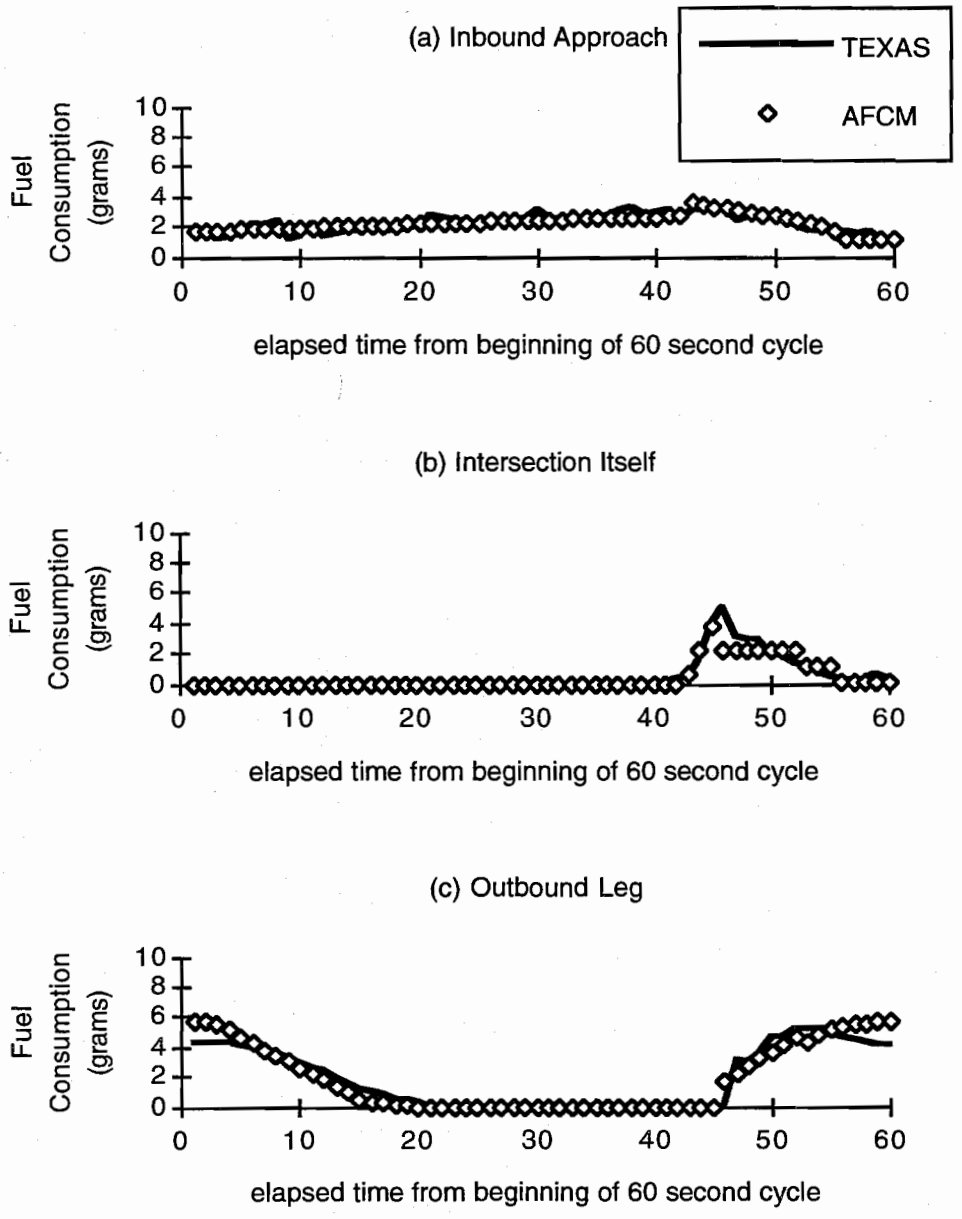

Figure 6.5 Fuel consumption versus elapsed time on the westbound approach for the AFCM and the TEXAS model - Case I

Case II - Two Phase Pretimed Signal with Turning Movements

Numerical analyses and tests of Case I indicate that AFCM is an accurate fuel consumption technique. Since Case I does not include traffic conflicts in the intersection influence area, another example, Case II with a two-way street, including 10% left turns from the northbound approach, is used to further investigate fuel consumption behavior. The traffic data and geometric configuration of Case II are shown in Table 6.1 and Figure 6.2.

Total Fuel Consumption Estimation. Table 6.8 shows the signal timing data for Case II. The northbound approach has a shared left turn lane and permitted left turn phase. Since Case II includes 10% of left turns on the northbound approach, a longer cycle length is used, and larger green time ratio is given to cycle phase I. Traffic situations are undersaturated and the overflow queue Q^S is the result of stochastic effects.

The procedure of fuel consumption estimation is the same as for Case I and the estimation results are shown in Table 6.9. For fuel consumption estimation, there are three traffic movement groups: northbound, southbound, and westbound. Since the northbound approach has 10% left turns, the saturation flow rate is adjusted to 1173 vph. In order to consistently estimate fuel consumption within a signal cycle, left turn movement after the stop line is included in the northbound calculation although its direction is toward the west. Generally, the main concept of the AFCM development is to predict how vehicles consume fuel in the intersection influence area. Therefore, fuel consumption due to left turn movements in either direction can be treated similarly.

TABLE 6.8 CASE II SIGNAL TIMING DATA

Cycle (sec.)	Phase		Green Time	Red Time	t_0	Lost Time	Overflow Queue (veh./sec.)
70	I	NB	44	21	43	5	2.0214
		SB	44	21	12		0.0068
	II	WB	16	49	20	5	2.5330

TABLE 6.9 FUEL CONSUMPTION ESTIMATES FOR STREET SEGMENTS DURING CYCLE STAGES - CASE II (UNITS: GRAMS) (TOTAL ELAPSED TIME = 1 CYCLE 70 SECONDS)

		Effective Red Time	Effective Green Time		Total
			(Before t_0)	(After t_0)	
Northbound	Inbound	100.669	228.328	8.478	337.475
	Intersection	0.000	57.666	1.413	59.079
	Outbound	55.193	227.710	19.394	302.297
Southbound	Inbound	68.793	42.028	73.218	184.039
	Intersection	0.000	22.483	12.203	34.686
	Outbound	23.339	28.787	127.100	179.226
Westbound	Inbound	149.387	59.017	0.000	208.404
	Intersection	0.000	39.588	0.000	39.588
	Outbound	153.436	78.919	0.000	232.355
Total					1577.149

By varying the cycle time from 40 to 180 seconds at intervals of 10 seconds, variations of fuel consumption can be examined, as shown in Table 6.10. The fuel consumption for an hour is obtained to depict the optimal cycle length for fuel consumption minimization. By comparing with Case I, the optimal cycle length (130 seconds) of Case II is much higher than that of Case I (80 seconds) due to the 10% of left turns.

TABLE 6.10 FUEL CONSUMPTION FOR DIFFERENT CYCLE LENGTHS - CASE II

Cycle Length (seconds)	Fuel Consumption / Cycle (grams)	Fuel Consumption / hr (grams)
40	14195.87	1277628.300
50	1275.539	91838.808
60	1420.65	85239.000
70	1577.149	81110.520
80	1656.171	74527.695
90	1814.551	72582.040
100	1988.047	71569.692
110	2170.899	71047.604
120	2361.002	70830.060
130	2555.584	70770.018
140	2755.292	70850.366
150	2959.624	71030.976
160	3168.242	71285.445
170	3380.913	71595.805
180	3597.471	71949.420

In order to observe the results with 10% left turns, the difference of total fuel consumption between the TEXAS model and the AFCM is compared and shown in Table 6.11. The results indicate that fuel consumption for some directions are not quite agreed, and the results for the northbound and westbound from the AFCM are much higher than those from the TEXAS. One possible reason might be the interaction between let-turn vehicles and opposing vehicles. Since the TEXAS can capture such interactions by simulating gaps, vehicle interactions can be modeled more accurately than the AFCM. To avoid the overestimation, the saturation flow rates might need to be adjusted to reflect vehicle interactions in the AFCM. This issue is discussed in more detail in Section 6.3.

The results of fuel consumption from the northbound and westbound are overestimated. Since the cycle length and traffic flow rates are fixed, the only way to improve the results is to change the saturation flow rate. It seems that the left turn adjustment factor might be too small in terms of fuel consumption estimation. Due to the small adjustment factor, the saturation flow rate is underestimated, and the overflow queues and the time t_0 are overestimated.

TABLE 6.11 THE COMPARISON OF FUEL CONSUMPTION FROM THE AFCM AND THE TEXAS MODEL - CASE II

		AFCM	TEXAS	Difference (AFCM-TEXAS)/TEXAS
Northbound	Inbound	337.475	277.582	0.22
	Intersection	59.079	49.603	0.19
	Outbound	302.297	261.752	0.15
Southbound	Inbound	184.039	197.271	-0.07
	Intersection	34.686	35.923	-0.03
	Outbound	179.226	195.682	-0.08
Westbound	Inbound	208.404	195.656	0.07
	Intersection	39.588	34.271	0.16
	Outbound	232.355	132.747	0.75
Total		1577.149	1380.485	0.14

Fuel Consumption Time History. Fuel consumption time histories on the northbound, southbound, and westbound approaches are shown in Figures 6.6, 6.7, and 6.8. The data points represent second-by-second fuel consumption from the AFCM and the curve represents instantaneous fuel consumption from the TEXAS model. In Figures 6.6 and 6.7, the elapsed time from 0 to 23 seconds is the effective red time, from 23 to 70 seconds is the effective green time, and t_0 is 43 seconds in Figure 6.6 and 12 seconds in Figure 6.7. In Figure 6.8, the elapsed time from 0 to 52 seconds is the effective red time, from 52 to 70 seconds is the effective green time, and t_0 is greater than the effective green time. Table 6.12 shows the results of correlation analysis from the TEXAS model and the AFCM. It indicates that the two fuel consumption estimate sets are correlated although the southbound inbound approach is poorest. The main reason is the 10% left turn movements and how they are treated.

TABLE 6.12 CORRELATION OF ELAPSED FUEL CONSUMPTION FOR THE AFCM AND THE TEXAS MODEL - CASE II

		Correlation
Northbound	Inbound	0.89
	Intersection	0.76
	Outbound	0.96
Southbound	Inbound	0.64
	Intersection	0.79
	Outbound	0.89
Westbound	Inbound	0.87
	Intersection	0.82
	Outbound	0.97

From the above AFCM results, total fuel consumption is overestimated, and elapsed fuel consumption on the southbound inbound approach is not highly correlated to that of the TEXAS model. In order to improve the results, the effect of left turn on fuel consumption will be discussed more detail in the following sections.

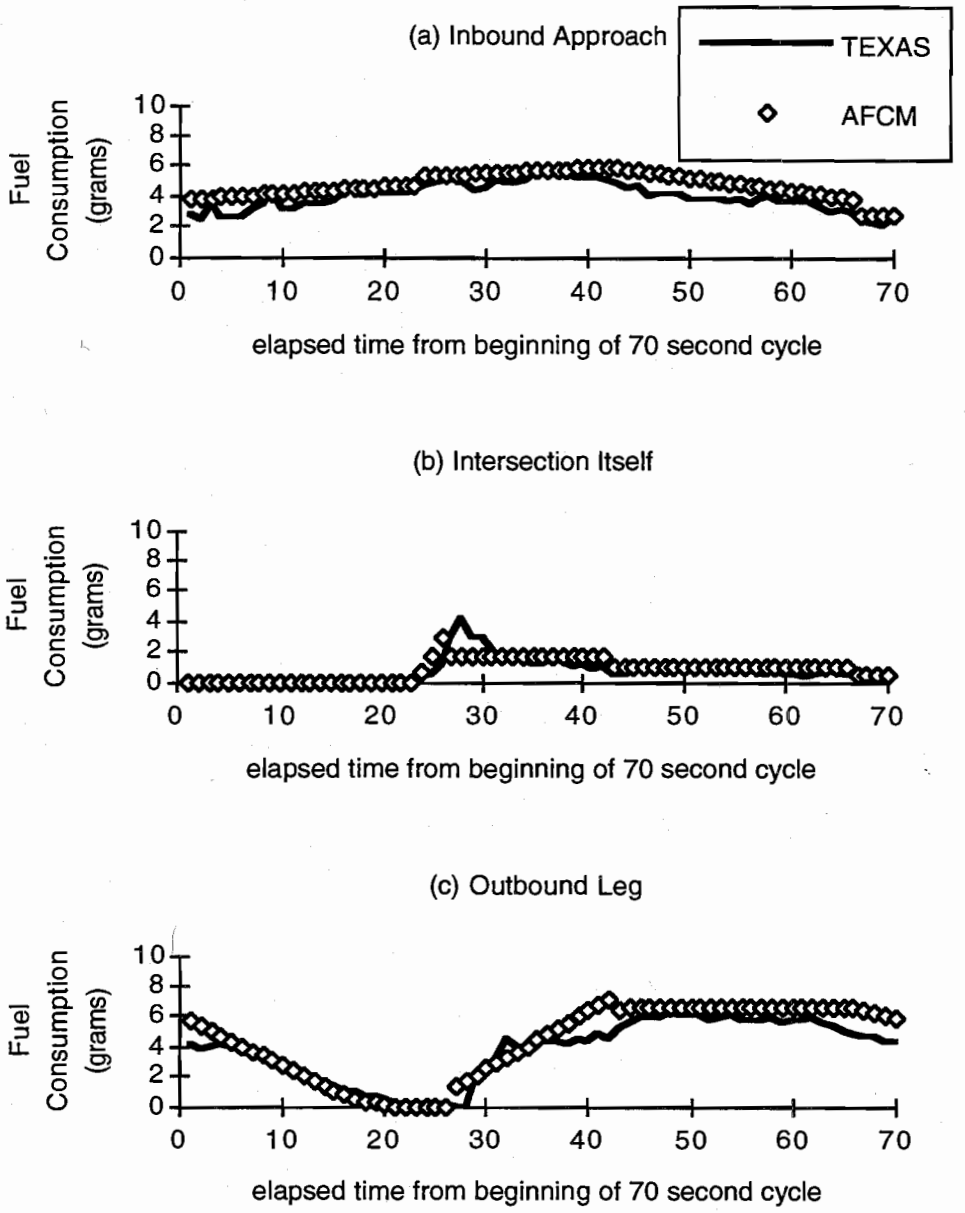

Figure 6.6 Fuel consumption versus elapsed time on the northbound approach for the AFCM and the TEXAS model - Case II

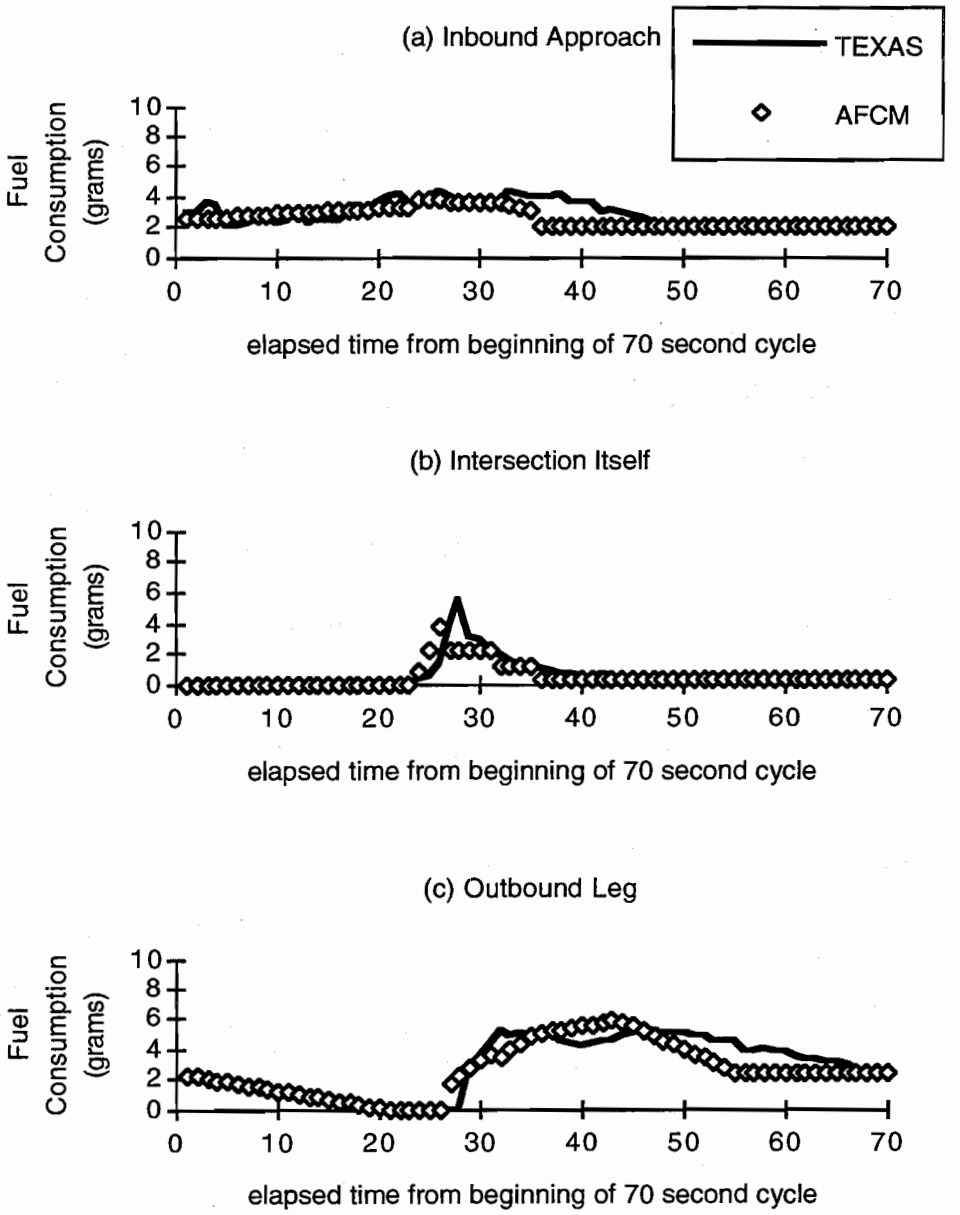

Figure 6.7 Fuel consumption versus elapsed time on the southbound approach for the AFCM and the TEXAS model - Case II

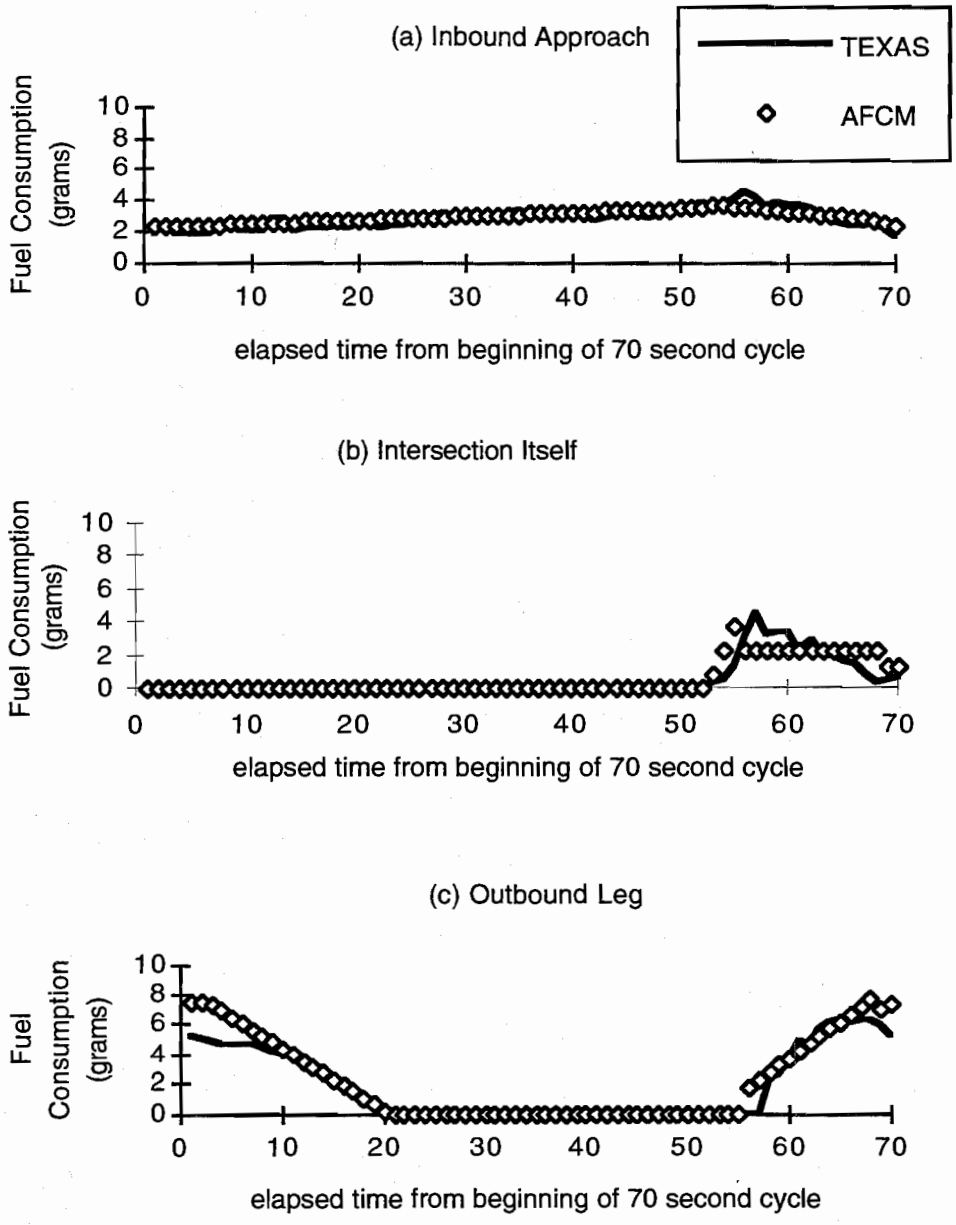

Figure 6.8 Fuel consumption versus elapsed time on the westbound approach for the AFCM and the TEXAS model - Case II

Case III - Three Phase Pretimed Signal with a Left Turn Phase

From Case II, the AFCM does not accurately estimate fuel consumption for left turns with a shared left turn lane and permitted phase. In this section, an exclusive left turn and protected phase are provided to investigate the left turn movement effects on fuel consumption. The left turn bay is assumed long enough for all left turn vehicles. There are three phases with the phase sequence designated as: (1) northbound and southbound straight, (2) northbound and southbound left turn, and (3) westbound and eastbound straight. Detailed geometric configuration, traffic flow data and signal phase design are depicted in Figure 6.3 and Table 6.1. The traffic flow rate and left turn percentage are the same as in Case II.

Total Fuel Consumption Estimation. Total fuel consumption is calibrated using the phase design and traffic data given in Tables 6.1 and 6.13. As described in the previous sections, total fuel consumption includes all approaches and all traffic movements. The total fuel consumption is estimated for a 90 second cycle and the difference from the AFCM and TEXAS is compared in Table 6.14. The results show a highly agreement between the TEXAS and the AFCM although the differences of fuel consumption for both left turn movements on NB and SB are larger than other approaches. One possible reason might be that the numbers of vehicles for left turns are much less than other approaches and thus create these fluctuations.

Table 6.15 shows the fuel consumption per cycle and per hour by varying cycle lengths from 50 to 180 seconds at 10-second intervals. It shows that the optimal cycle length for fuel consumption minimization is 120 seconds.

TABLE 6.13 SIGNAL TIMING DATA FOR CASE III

Cycle (sec.)	Phase		Green Time	Red Time	t_0	Lost Time	Overflow Queue (veh./sec.)
90	I	NB	43	42	32	5	0.8270
		SB					0.1552
	II	NB	10	75	14	5	1.6744
		SB					0.5807
	III	EB	22	63	20	5	1.1692
		WB					1.1692

TABLE 6.14 FUEL CONSUMPTION ESTIMATES FOR STREET SEGMENTS DURING CYCLE STAGES - CASE III (UNITS: GRAMS) (TOTAL ELAPSED TIME = 1 CYCLE 90 SECONDS)

Phase	Traffic Movement	Intersection Segment	AFCM	TEXAS	Difference (AFCM-TEXAS)/TEXAS
I	NB Straight	IB	347.023	367.796	-0.06
		INT+OB	357.816	382.099	-0.06
	SB Straight	IB	246.173	248.816	-0.01
		INT+OB	261.364	286.571	-0.09
II	NB Left Turn	IB	78.877	92.621	-0.15
		INT+OB	69.638	52.139	0.34
	SB Left Turn	IB	45.450	39.928	0.14
		INT+OB	37.485	45.515	-0.18
III	WB	IB	217.521	223.731	-0.03
		INT+OB	202.791	209.218	-0.03
	EB	IB	217.521	225.969	-0.04
		INT+OB	202.791	210.417	-0.04
	Total		2284.45	2384.82	-0.04

TABLE 6.15 FUEL CONSUMPTION FOR DIFFERENT CYCLE LENGTHS - CASE III

Cycle Length (seconds)	Fuel Consumption / Cycle (grams)	Fuel Consumption / hr (grams)
50	3504.416	252317.952
60	2305.465	138327.900
70	2449.595	125979.171
80	2499.276	112467.420
90	2727.666	109106.640
100	2992.760	107739.360
110	3240.457	106051.320
120	3533.482	106004.460
130	3839.657	106328.963
140	4154.308	106825.063
150	4480.095	107522.280
160	4816.219	108364.928
170	5162.133	109315.758
180	5517.459	110349.180

Fuel Consumption Time History. Fuel consumption time histories from the AFCM and the TEXAS model are compared using correlation analysis. From Table 6.16, the fuel consumption estimates are highly correlated although the inbound approaches show the lowest correlation values. The main reason is the assumption of fuel consumption rate f_{02} for all queued vehicles. Practically, the first few vehicles should consume less fuel on the inbound approach than those vehicles at the end of the queue. Moreover, the first few vehicles making left turns versus straight movements have different traffic behaviors. However, to simplify AFCM development, only one fuel consumption rate f_{02} is used to represent the queued vehicle fuel consumption.

Due to exclusive left turn lanes and protected phases in Case III, the trajectories of elapsed fuel consumption for both straight and left turn movements are better matched. Figures 6.9 to 6.11 depict the trajectories of elapsed fuel consumption for the northbound straight, northbound left turn, and westbound approaches. They represent the variation of fuel consumption within the 90 second cycle time. In Figure 6.9, the effective red time is from 0 to the 45th second, and the effective green time is from the 45th to the 90th second. In Figure 6.10, the effective red time is very long at 78 seconds, and the effective green time is 12 seconds which is less than time t_0. The effective red time is 65 seconds and the effective green time is 24 seconds in Figure 6.11.

TABLE 6.16 CORRELATION OF ELAPSED FUEL CONSUMPTION FOR THE AFCM AND THE TEXAS MODEL - CASE III

		Correlation
Northbound Straight	Inbound	0.93
	Intersection	0.82
	Outbound	0.96
Southbound Straight	Inbound	0.83
	Intersection	0.88
	Outbound	0.96
Northbound Left Turn	Inbound	0.96
	Intersection	0.82
	Outbound	0.80
Southbound Left Turn	Inbound	0.80
	Intersection	0.76
	Outbound	0.79
Westbound	Inbound	0.91
	Intersection	0.78
	Outbound	0.96
Eastbound	Inbound	0.83
	Intersection	0.76
	Outbound	0.96

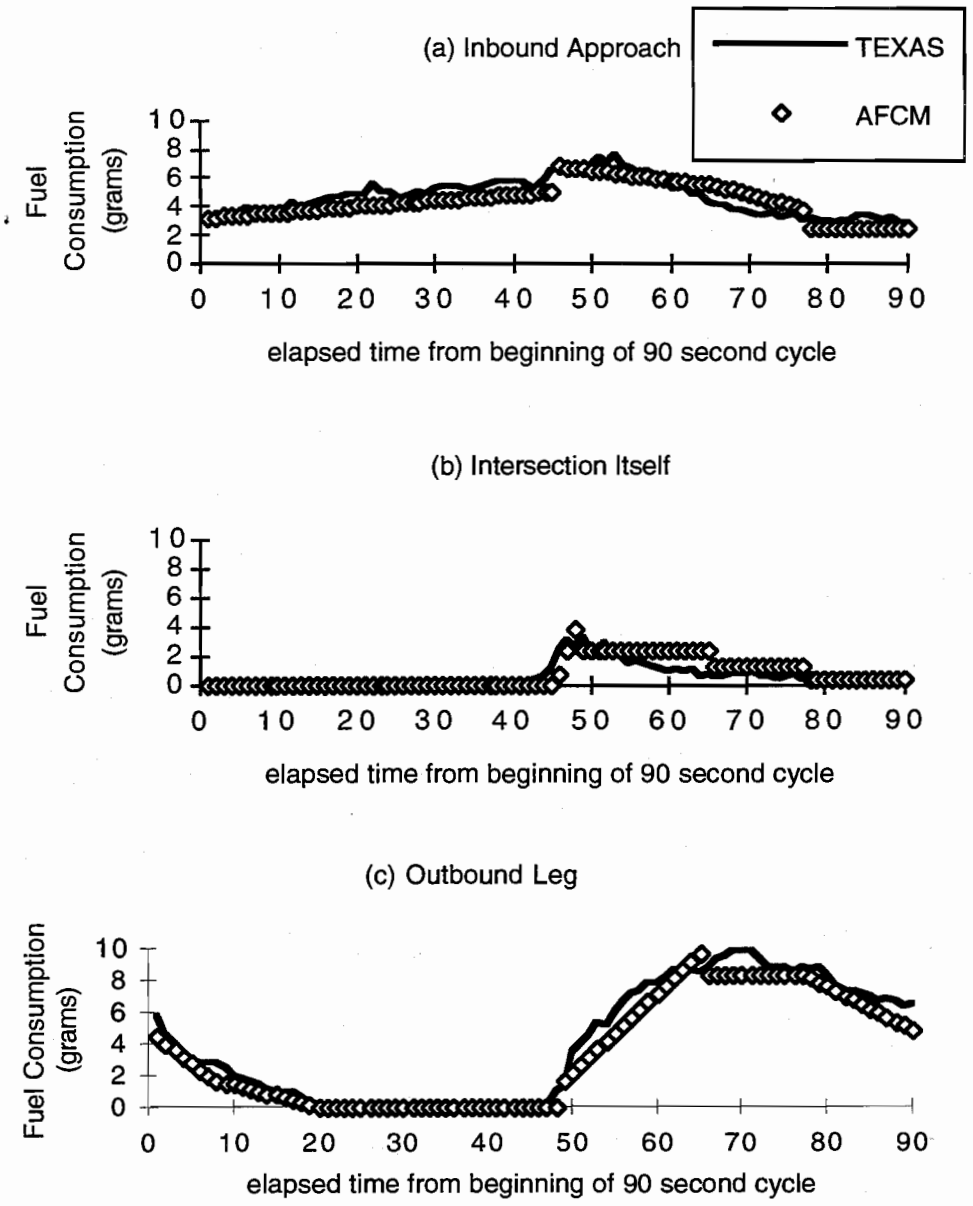

Figure 6.9 Fuel consumption versus elapsed time on the northbound approach (straight) from the AFCM and the TEXAS model - Case III

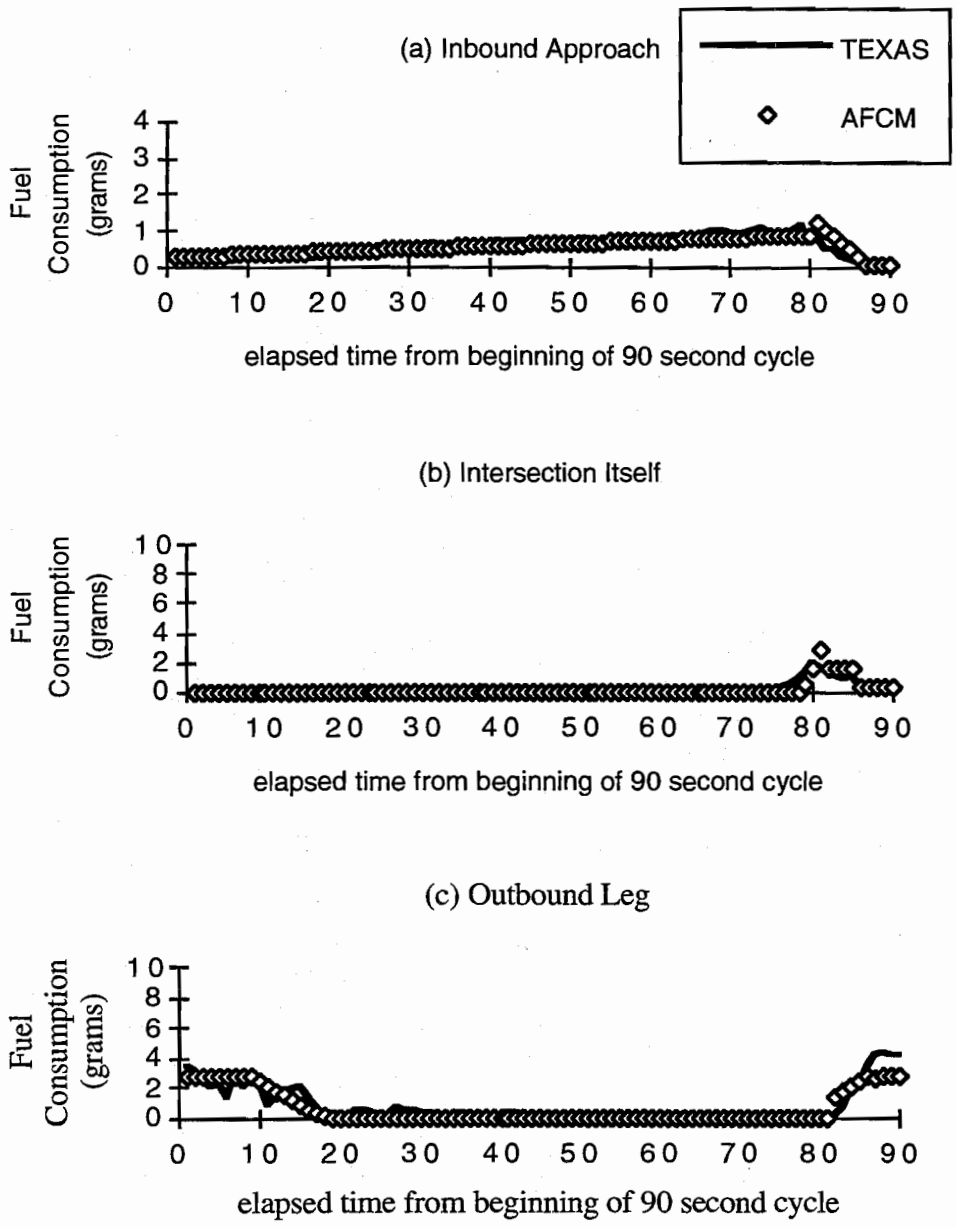

Figure 6.10 Fuel consumption versus elapsed time on the northbound approach (left turn) from the AFCM and the TEXAS model - Case III

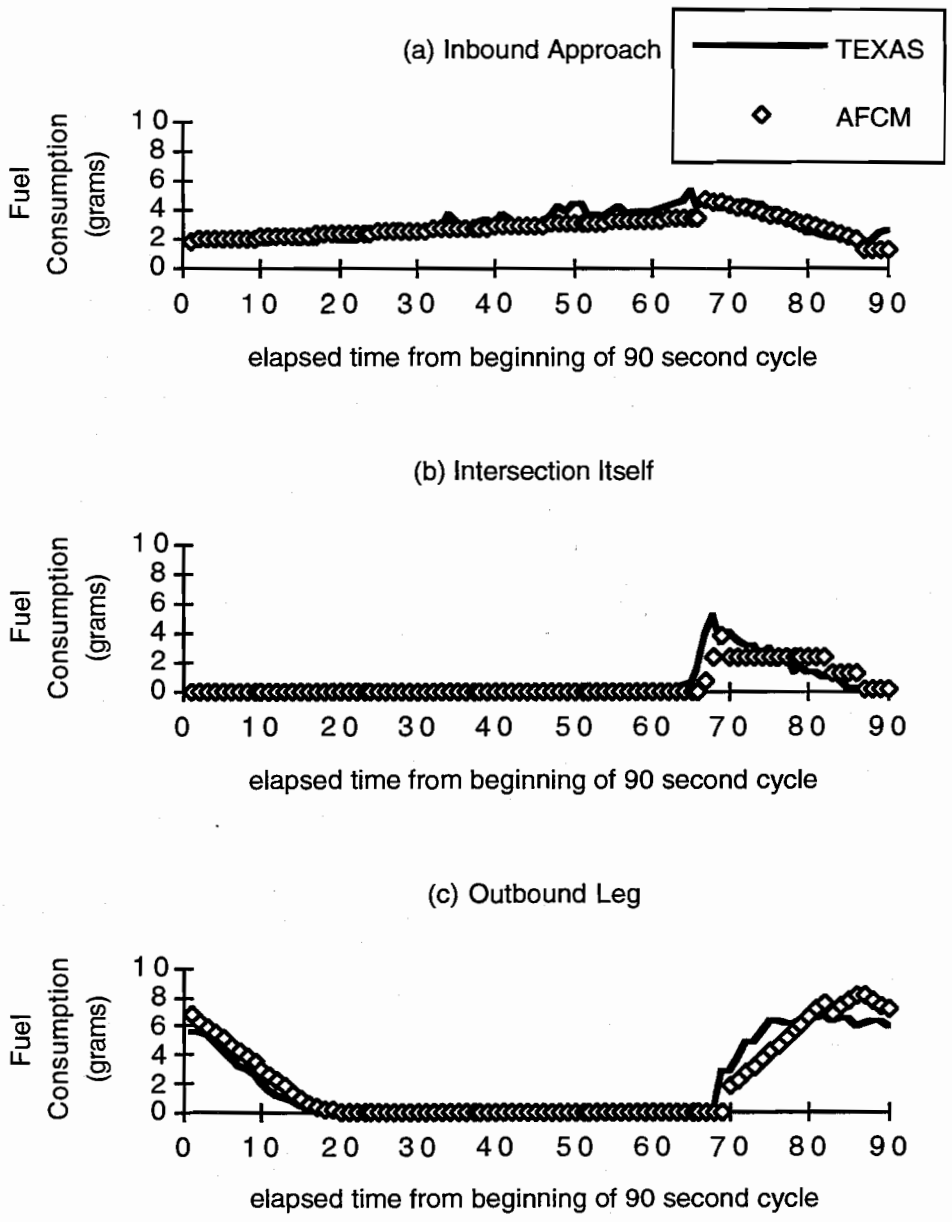

Figure 6.11 Fuel consumption versus elapsed time on the westbound approach from the AFCM and the TEXAS model - Case III

EFFECTS OF LEFT TURNS ON FUEL CONSUMPTION

Introduction

From the discussions in Section 6.2, left turns have major effects on fuel consumption estimation when left turns have a shared left turn lane with a permitted phase. The results of fuel consumption from the AFCM are much higher than those from the TEXAS model. One possible reason discussed in Section 6.2 might be the interactions between left-turn vehicles and opposing vehicles. One way to improve the AFCM estimation is to adjust saturation flow rate according to left turns. Since the saturation flow rate calibrated from the 1994 HCM is underestimated for the purpose of fuel consumption estimation, the adjustment is further investigated to reflect left turns on fuel consumption. In this Section, two possible alternatives, termed as the second and the third, are proposed and the numerical experiments are conducted. The second alternative uses the adjustment process according to 1985 HCM, and the third alternative is proposed based on 1985 and 1994 HCMs.

Left Turn Adjustment Factor and Fuel Consumption Estimation

From the numerical results shown in Section 6.2, the saturation flow rate calibrated from 1994 HCM might be too small for Case II; therefore, fuel consumption from the AFCM is overestimated. The second alternative is to apply the adjustment process according to 1985 HCM. The left-turn adjustment factor, as shown in Table 6.17, is calculated based on the supplemental worksheet of 1985 HCM. A new saturation flow rate, 1384 vph, is obtained instead of 1173 vph.

The saturation flow rate is then applied to the AFCM. Table 6.18 shows the comparison of fuel consumption between the AFCM and the TEXAS model. The difference of total fuel consumption is much smaller than that from the 1994 HCM; however, the correlation of the inbound approach on the northbound is still very low. Although the new saturation flow rate has improved upon fuel consumption estimation, the differences for certain approaches might still too large.

TABLE 6.17 CALCULATION OF LEFT-TURN ADJUSTMENT FACTOR FOR CASE II (THE SECOND ALTERNATIVE) [53]

	Westbound	Southbound	Northbound
C, cycle length	70	70	70
G, effective green	20	45	45
N, number of lanes	1	1	1
V_a, approach flow rate	300	500	650
V_m, mainline flow rate	300	500	585
V_{LT}, left turn flow rate	0	0	65
P_{LT}, proportion of left turn	0	0	0.1
N_o, opposing lanes	1	1	1
V_o, opposing flow rate	300	585	500
P_{LTo}, proportion of left turn in opposing volume	0	0.1	0
COMPUTATION			
$S_{op} = 1800\ N_o/[1+P_{LTo}((400+V_m)/(1400-V_m))]$	1800.00	1636.36	1800.00
$Y_o = V_o/S_{op}$	0.17	0.36	0.28
$g_u = (g-CY_o)/(1-Y_o)$	10.00	31.09	35.38
$f_s = (875-0.625V_o)/1000$	0.69	0.51	0.56
$P_L = P_{LT}[1+(N-1)g/(f_s g_u+4.5)]$	0.00	0.00	0.10
$g_q = g - g_u$	10.00	13.91	9.62
$P_T = 1 - P_L$	1.00	1.00	0.90
$g_f = 2\ (P_T/P_L)\ [1-P_T^{0.5gq}]$			7.15
$E_L = 1800/(1400-V_o)$	1.64	2.21	2.00
$f_m = g_f/g + (g_u/g)\ [1/(1+P_L(E_L-1))]+(2/g)(1+P_L)$	1.00	1.00	0.92
$f_{LT} = (f_m+N-1)/N$	1.00	1.00	0.92
$s = 1500\ f_{LT}$, saturation flow rate	1500	1500	1384

TABLE 6.18 THE COMPARISON OF FUEL CONSUMPTION FROM THE RESULTS OF THE AFCM AND TEXAS MODEL (THE SECOND ALTERNATIVE)

		Correlation	Difference of Fuel Consumption (AFCM-TEXAS)/TEXAS
Northbound	Inbound	0.57	-0.10
	Intersection	0.76	-0.07
	Outbound	0.82	-0.03
Southbound	Inbound	0.72	-0.06
	Intersection	0.79	-0.05
	Outbound	0.91	-0.08
Eastbound	Inbound	0.77	-0.08
	Intersection	0.85	-0.04
	Outbound	0.97	0.03

One major change in left-turn adjustment factor from 1985 HCM and 1994 HCM is the estimation of f_m. In 1994 HCM, f_m is expressed:

$$f_m(1994) = g_f/g + (g_u/g)\,[1/(1+P_L\,(E_L-1))] \qquad [6.6]$$

However, 1n 1985, f_m is expressed as:

$$f_m(1985) = g_f/g + (g_u/g)\,[1/(1+P_L\,(E_L-1))] + (2/g)\,(1+P_L) \qquad [6.7]$$

Moreover, the supplemental worksheets for computation of left-turn factor are different. Since the saturation flow rate calibrated from 1994 HCM is underestimated and from 1985 might be overestimated, the third alternative is proposed based on empirical results. In this alternative, f_m from 1994 HCM is used in the 1985 HCM worksheet. As a result, a left-turn adjustment factor, 0.87, is obtained and the saturation flow rate is about 1311 vph.

The results based on the new saturation flow rate are shown in Table 6.19. The results show that the correlation of elapsed fuel consumption is over 70% and the difference of fuel consumption is within 10%. Figures 6.12 to 6.14 show fuel consumption time histories on the northbound, southbound, westbound approaches from results of the third alternative. From the results shown in Table 6.19 and Figures 6.12 to 6.14, the third alternative performs better and might be more appropriate in the AFCM. Variations of total fuel consumption with respect to the cycle length is shown in Table 6.20. The optimal cycle length for fuel consumption minimization is 100 seconds.

TABLE 6.19 THE COMPARISON OF FUEL CONSUMPTION FROM THE RESULTS OF THE AFCM AND TEXAS MODEL (THE THIRD ALTERNATIVE)

		Correlation	Difference of Fuel Consumption (AFCM-TEXAS)/TEXAS
Southbound	Inbound	0.72	-0.02
	Intersection	0.75	0.02
	Outbound	0.90	0.01
Northbound	Inbound	0.72	-0.02
	Intersection	0.79	0.02
	Outbound	0.91	-0.04
Eastbound	Inbound	0.81	-0.08
	Intersection	0.85	0.00
	Outbound	0.97	0.08

TABLE 6.20 FUEL CONSUMPTION FOR DIFFERENT CYCLE LENGTHS - CASE II (THE THIRD ALTERNATIVE)

Cycle Length (seconds)	Fuel Consumption / Cycle (grams)	Fuel Consumption / hr (grams)
40	1035.352	93181.680
50	1138.479	81970.488
60	1221.946	73316.760
70	1366.529	70278.634
80	1532.552	68964.840
90	1710.460	68418.400
100	1896.478	68273.208
110	2088.811	68361.087
120	2286.210	68586.300
130	2486.868	68867.114
140	2690.185	69176.186
150	2896.958	69526.992
160	3107.458	69917.805
170	3321.575	70339.235
180	3539.228	70784.560

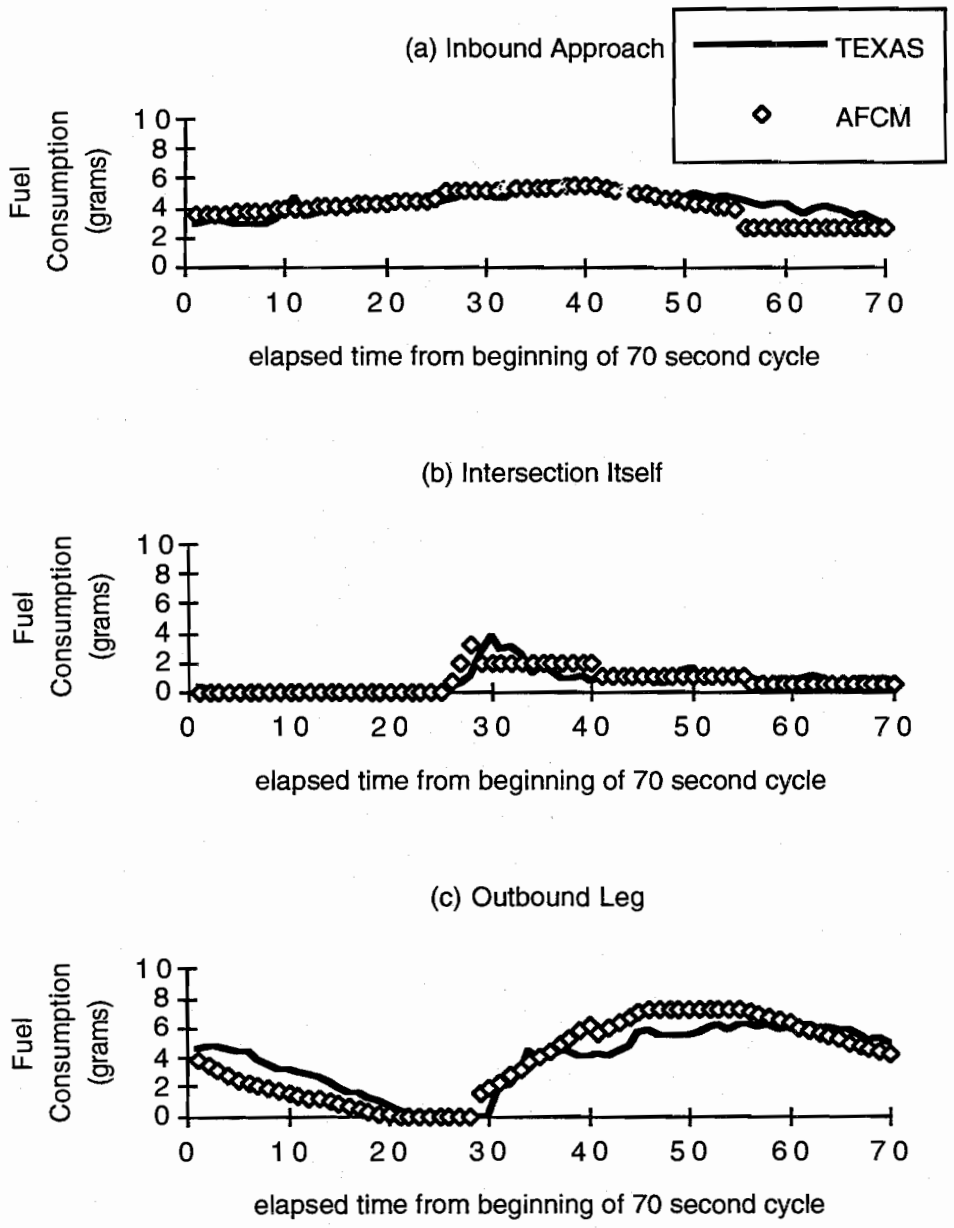

Figure 6.12 Fuel consumption versus elapsed time on the northbound approach for the AFCM and the TEXAS model - Case II (the third alternative)

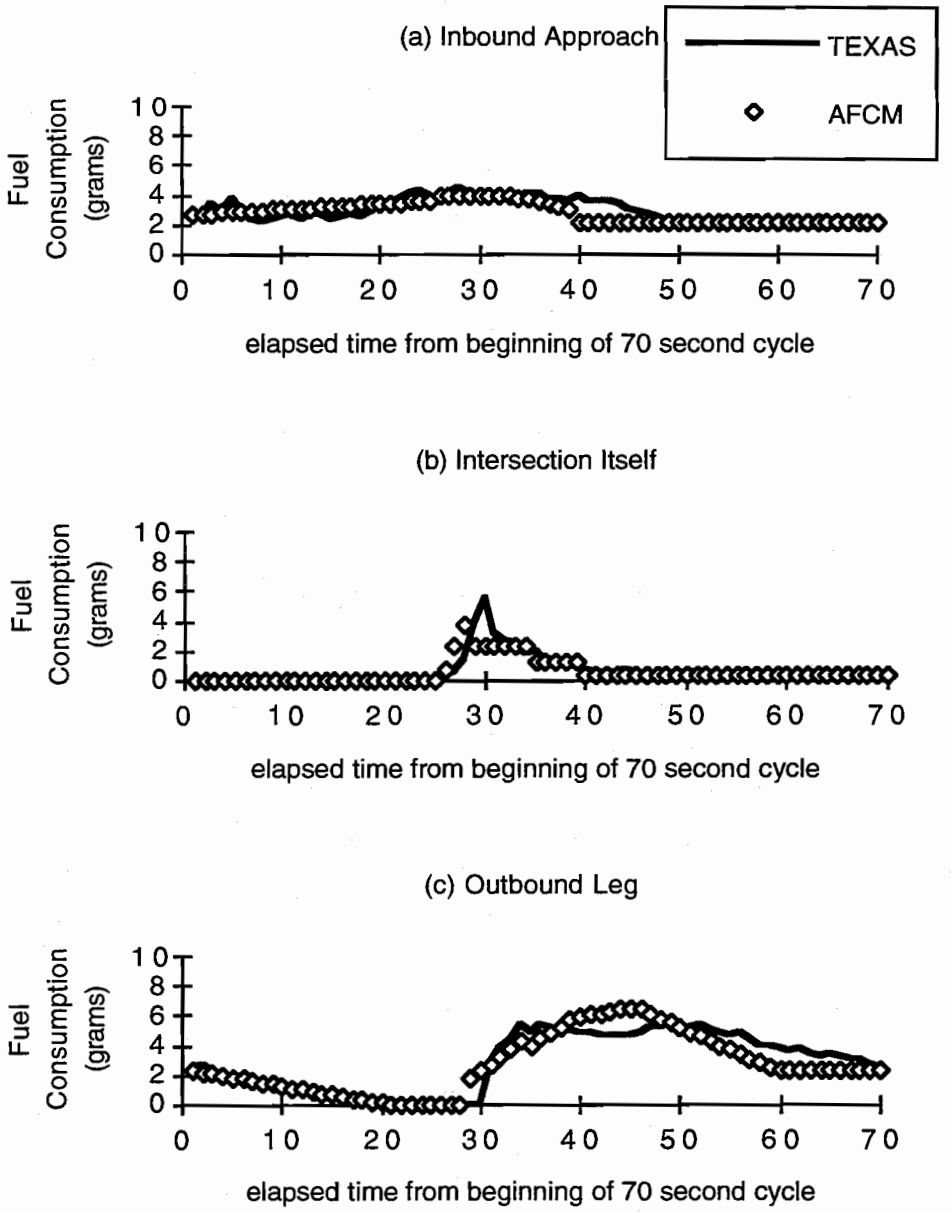

Figure 6.13 Fuel consumption versus elapsed time on the southbound approach for the AFCM and the TEXAS model - Case II (the third alternative)

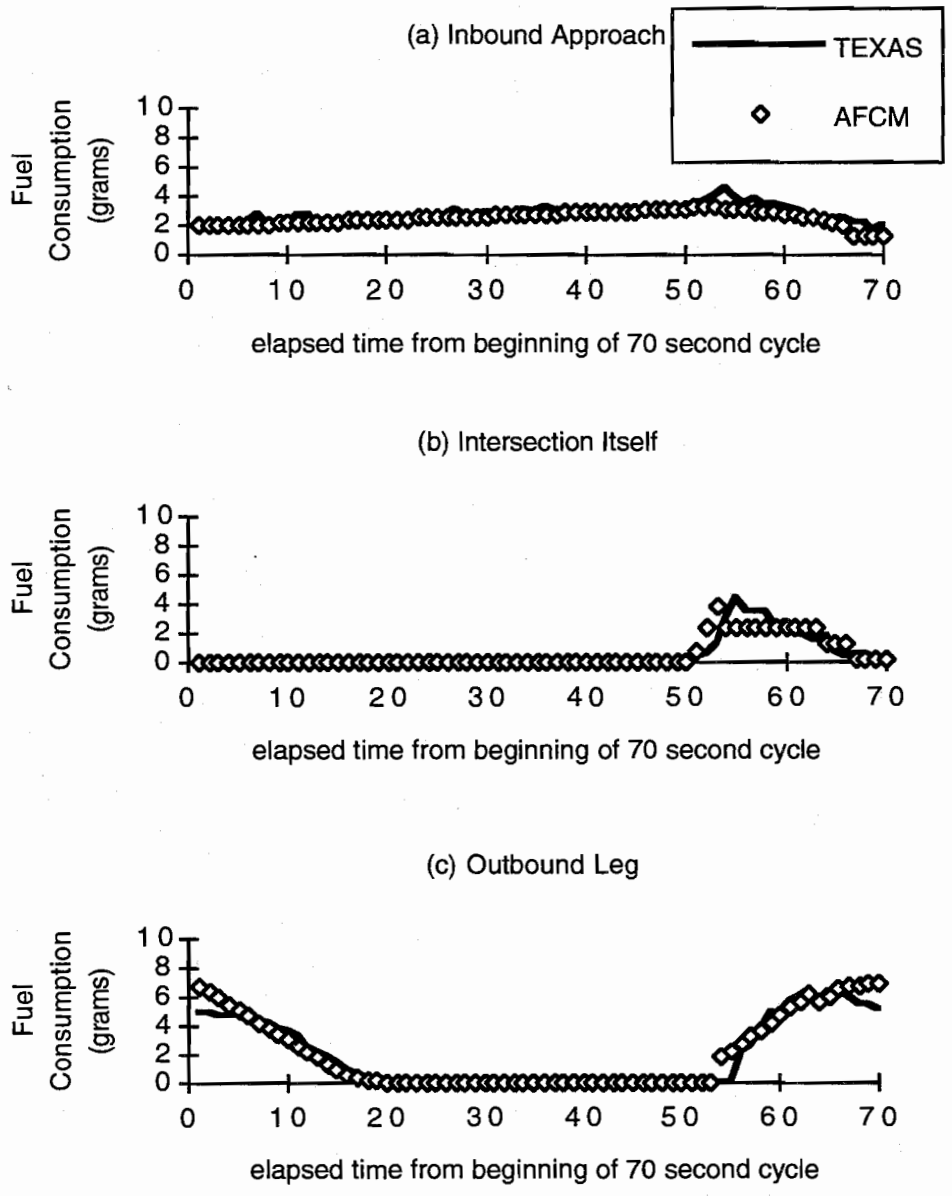

Figure 6.14 Fuel consumption versus elapsed time on the westbound approach for the AFCM and the TEXAS model - Case II (the third alternative)

EFFECTS OF SIGNAL TIMING ON FUEL CONSUMPTION

Optimal Cycle Lengths for Fuel Consumption Minimization

Since it is difficult to derive an optimal cycle length for minimizing fuel consumption by mathematical optimization techniques, numerical analysis is applied to find an approximate optimal result by varying cycle lengths from 20 to 180 seconds at 10 second increments. By following the description of Case I in Section 6.2, there are only two approaches westbound and northbound without turning movements in the intersection. The flow rate on the westbound approach is assumed to be 300 vph and the flow rates on the northbound approach are varied for peak/non-peak traffic conditions. Fuel consumption variations with respect to cycle lengths for volumes from 400 to 950 vph on the northbound approach are illustrated in Figure 6.15. In this figure, changes of cycle length have a significant impact on fuel consumption in the high volume case, but not in the low volume 400 vph case. Although the 400 vph curve is rather flat, one can still find an optimal fuel consumption minimization cycle length. In the 950 vph case, fuel consumption for the long cycle length is less than that for the short cycle length.

Generally, all curves shown in Figure 6.15 are convex, and an optimal cycle length can be expected for each case. Numerical results of the optimal cycle lengths based on fuel consumption minimization are listed in Table 6.21, which shows longer cycle lengths are expected for high volume cases because of more acceleration and deceleration maneuvers.

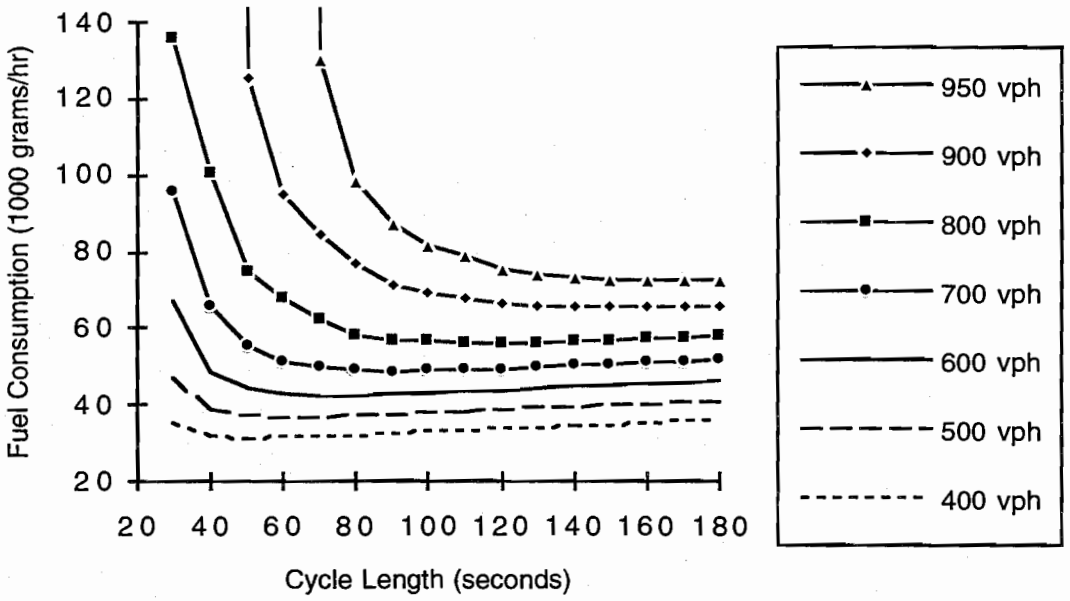

Figure 6.15. Optimal cycle lengths vs. traffic volumes from the AFCM

TABLE 6.21 OPTIMAL CYCLE LENGTHS VS. TRAFFIC VOLUMES

Critical Flow (veh./hr)		Optimal Cycle Length for Min. Fuel (sec.)
Northbound	Westbound	
400	300	50
500	300	60
600	300	70
700	300	90
800	300	120
900	300	150
950	300	170

For an intersection with pretimed traffic signals, fuel consumption changes during the 24 hours of a day due to changing traffic demands. These changing demands are sometimes described as three generically different conditions. These are sometimes considered as low volume during late night, medium volume in off-peak hours, and high volume in peak hours. In

order to minimize fuel consumption, the cycle length should be adjusted for the different time periods according to traffic volume changes. For instance, if flow rates for an intersection are 800 vph in the morning and afternoon peak hours, 400 vph at night, and 600 vph for the rest of a day, the optimal cycle length should be 120 seconds in the peak hours, 50 seconds at night, and 70 seconds in the off-peak hours.

Signal Timing and Fuel Savings

AFCM can be practically applied to undersaturated and oversaturated conditions. Since optimal cycle lengths for fuel consumption minimization can be analytically estimated, fuel savings are obtainable using optimal cycle lengths for various traffic demands. For example, an intersection with a fixed cycle length of 60 seconds and fixed green split might have traffic demand on the northbound approach increase from 500 vph in the non-peak hour to 950 vph in the peak hour, and decrease back to 500 vph after the peak hour, all within a 165-minute period. The traffic conditions range from undersaturated to oversaturated, and back to undersaturated conditions. Since the cycle length is fixed, overflow queues are increase due to the oversaturated condition and thus more delay is incurred and more excess fuel is consumed.

Table 6.22 shows the detailed traffic demand for the 165-minute period. In order to compare the fuel consumption between the fixed 60 seconds cycle length and various optimal cycle lengths for various traffic demands, the traffic demand is assumed to increase from low volume of 500 vph to the highest volume of 950 vph, and then to decrease to 500 vph.

Since the traffic demand is variable for the 165-minute period, overflow queues increase as the traffic flow increases for the fixed cycle length. However, the overflow queues will be dissipated gradually after the traffic flow decreases to undersaturated conditions. Figure 6.16 depicts the overflow queue growing with increasing traffic demands and dissipating with decreasing traffic demands when the cycle length is fixed. The overflow queues increase dramatically after the degree of saturation becomes greater than 1.0 (traffic volume is greater than 900 vph) and continue to grow with the higher traffic flow rates. However, the highest overflow queue length appears in the 105th minute of the 165-minute period when the traffic flow is 900 vph which is 15 minutes after the highest traffic flow of 950 vph.

TABLE 6.22 TRAFFIC DEMANDS FOR THE 165-MINUTE PERIOD

Elapsed Time within 165 Minutes (min.)	Period (min.)	Flow (veh./hr)		Fixed Cycle Length (sec.)	Optimal Cycle Length for Min. Fuel (sec.)
		NB	WB		
1 - 15	15	500	300	60	60
16 - 30	15	600	300	60	60*
31 - 42	12	700	300	60	90
43 - 60	18	800	300	60	120
61 -75	15	900	300	60	150
76 - 90	15	950	300	60	180**
91 -105	15	900	300	60	150
106 -123	18	800	300	60	120
124 -135	12	700	300	60	90
135 -150	15	600	300	60	60*
151 -165	15	500	300	60	60

* Use 60 seconds instead of 70 seconds.

** Use 180 seconds instead of 170 seconds.

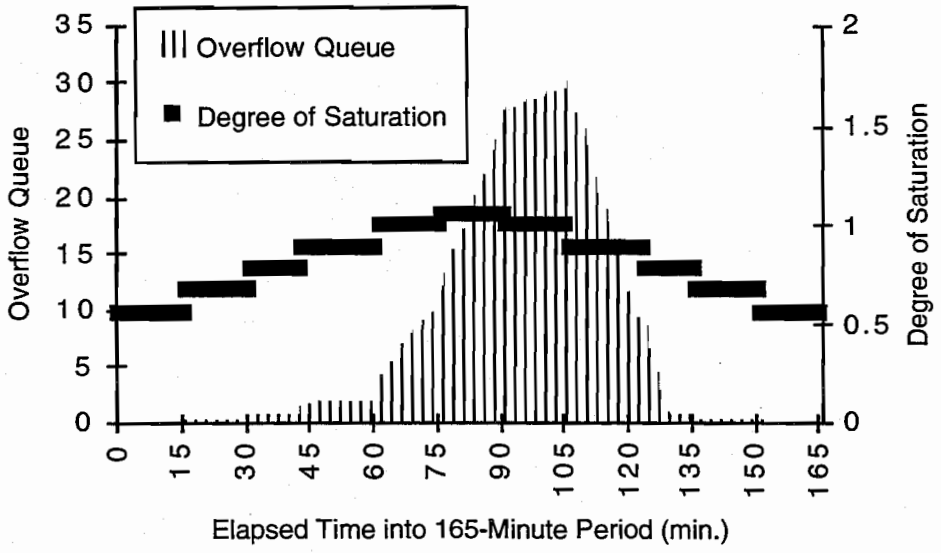

Figure 6.16 Overflow queue growth and dissipation with increasing and decreasing traffic demand on the northbound

In order to improve the performance of individual traffic signals and traffic system management, traffic signal timing should be dependent on traffic demand. Total fuel consumption can be minimized by using optimal cycle lengths shown in Table 6.21. However, for simplification of the fuel consumption calibration and comparison between fixed cycle lengths and optimal cycle lengths, the optimal cycle length for a volume of 600 vph is 60 seconds instead of 70 seconds, and for a volume of 950 vph is 180 seconds instead of 170 seconds (as shown in Table 6.22). Certainly, total fuel consumption is expected to be less if the signal timing used is exactly the optimal cycle length.

Figure 6.17 depicts fuel consumption at each elapsed minute of the 165-minute period. Fuel consumption of the fixed 60 second cycle is higher than that of varying near optimal cycle lengths. Moreover, from Table 6.23, using the optimal cycle length could save at least 34200 grams (13.5 gallons) during the 165 minute analysis period.

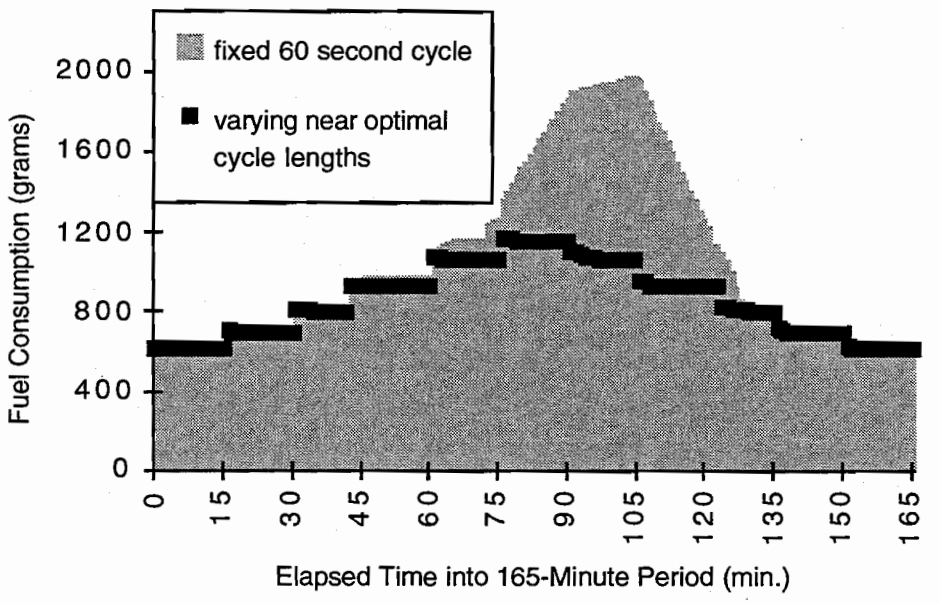

Figure 6.17 Fuel consumption within the elapsed time of 165-minute period on the northbound

TABLE 6.23 TOTAL FUEL CONSUMPTION FOR FIXED 60 SECOND CYCLE AND VARYING NEAR OPTIMAL CYCLE LENGTHS FOR THE 165-MINUTE PERIOD

	Fuel Consumption within the 165 Minutes	
	Fixed 60 Second Cycle	Varying Near Optimal Cycle Lengths
Northbound	133046.156	93461.802
Westbound	41650.455	46986.381
Total (grams)	174696.611	140448.183
(gallons)	68.603	55.154

OPTIMAL CYCLE LENGTHS FOR FUEL CONSUMPTION AND DELAY

Delay is the most popular performance index for evaluating traffic system management. Several studies have investigated the optimal signal cycle length for delay minimization and have been applied to traffic control systems. However, due to the increasing attention on energy conservation and environmental concerns, fuel consumption has become an important objective of traffic system management. The mathematical models of the AFCM can be used not only to estimate fuel consumption, but also to obtain the optimal cycle length for fuel consumption minimization. Webster's delay minimization relationship is compared with the AFCM fuel consumption minimization technique. From Webster's study, the optimal cycle length for delay minimization can be estimated from Equation 6.8 [84]:

$$C_0 = \frac{1.5L + 5}{1 - Y} \qquad [6.8]$$

where,

Y: the sum for all signal phases of the highest ratios of flow to saturation flow,

L: nl + R,

n: the number of phases,

l: the average lost time per phase (excluding all-red times), and

R: all-red times.

Table 6.24 shows the optimal cycle lengths for fuel consumption and delay minimization for Cases I, II, and III discussed in Section 6.2. For Cases I and II, optimal cycle lengths for delay minimization are 60 and 70 seconds and for fuel consumption are 80 and 100 seconds, respectively. For Case III, the optimal cycle length for fuel consumption minimization is 120

seconds and for delay minimization is 80 seconds. Figures 6.18 to 6.20 depict fuel consumption and delay as functions of the signal cycle length from Cases I, II, and III. For the same traffic conditions, the optimal cycle lengths for minimizing fuel consumption are higher than for minimizing delay. Moreover, the difference between optimal cycle lengths for fuel consumption and delay is greater when the summation of flow ratios is larger. This indicates some relationship between flow ratio and optimal cycle length for fuel consumption minimization.

TABLE 6.24 OPTIMAL CYCLE LENGTHS FOR FUEL CONSUMPTION AND DELAY MINIMIZATION

Case	Traffic Movement	Critical Lane Flow q (veh./hr)	Signal Phase	Flow Ratio (q/s)	Optimal Cycle Length For: Fuel Consumption (sec.)	Delay (sec.)
I	NB	650	I	0.43	80	60
	WB	300	II	0.20		
II	NB (ST)	585	I	0.46	100	70
	NB (LT)	65				
	WB	300	II	0.20		
III	NB (ST)	585	I	0.39	120	80
	NB (LT)	65	II	0.06		
	WB	300	III	0.20		

Since the optimal cycle lengths for fuel consumption and delay are different, the trade-off between fuel consumption and delay must be considered in the context of overall traffic system management. The results of trade-off should be between the values of optimal cycle lengths for delay and fuel consumption, i.e., the optimal cycle lengths for considering both delay and fuel consumption are higher than the optimal cycle lengths for delay minimization and lower than the optimal cycle lengths for fuel consumption minimization.

From Figures 6.18 to 6.20, all curves are convex and optimal cycle lengths can be expected for each case. Since the optimal cycle length for delay minimization can be obtained from a simple function derived by Webster Webster, 1958), the optimal cycle length for fuel consumption minimization should also be derived from a simple formulation. A detailed description of deriving an expression for the optimal cycle length to minimize fuel consumption is discussed in Chapter 7.

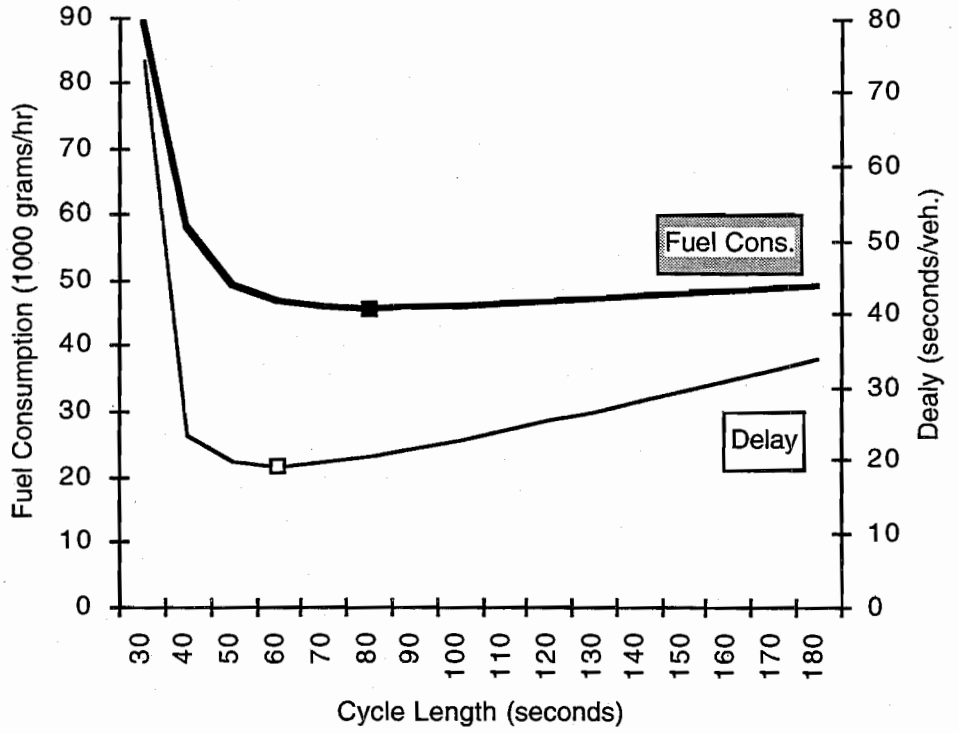

Figure 6.18 Fuel consumption and delay as functions of signal cycle length - Case I

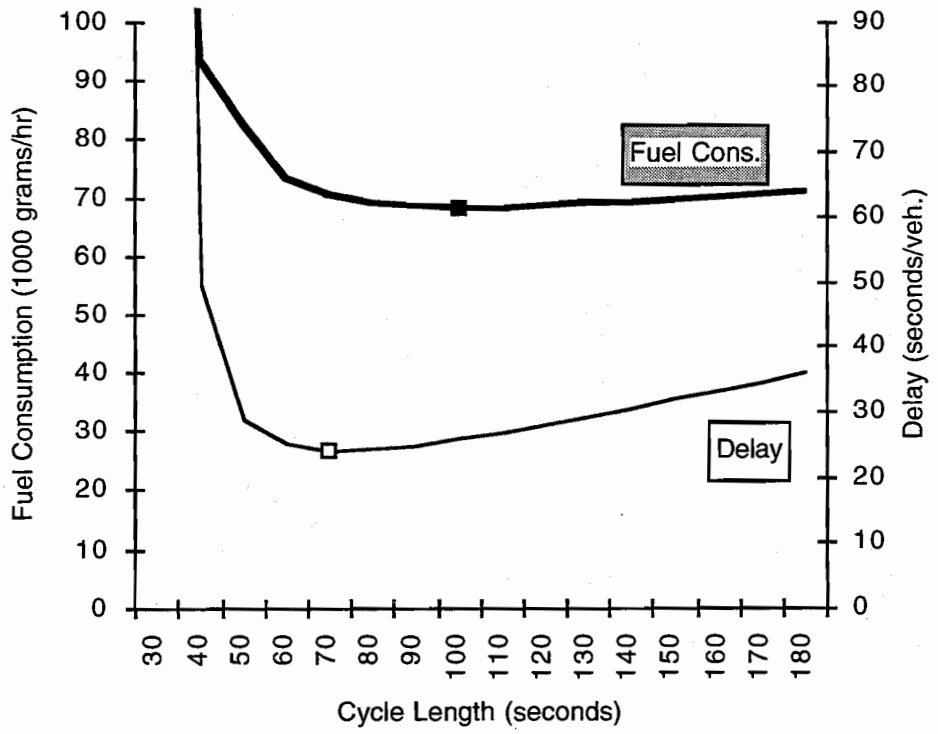

Figure 6.19 Fuel consumption and delay as functions of signal cycle length - Case II

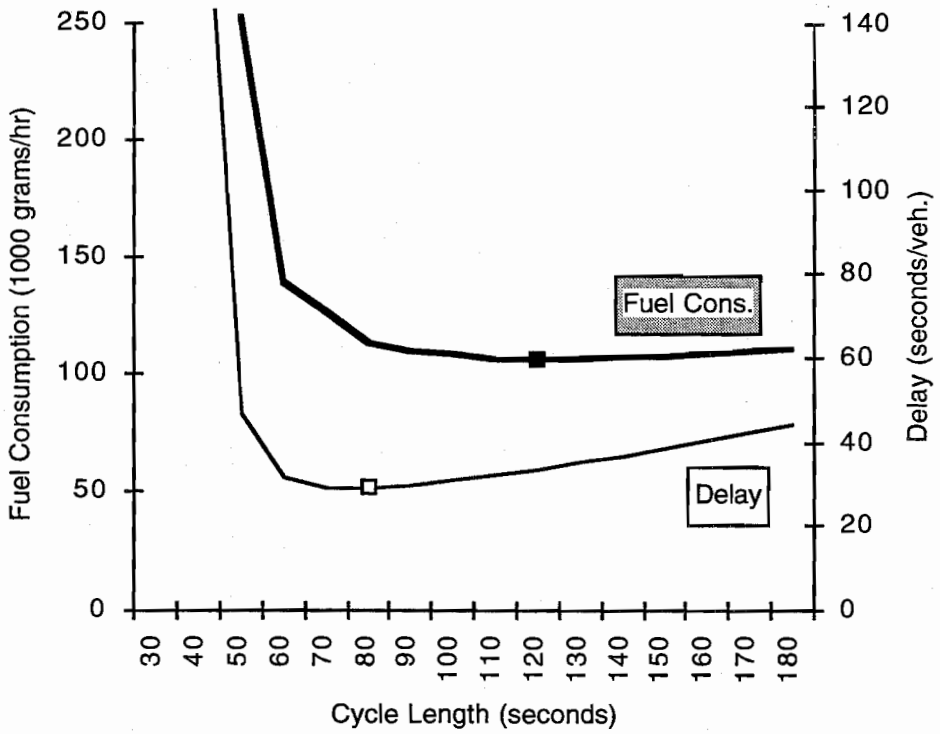

Figure 6.20 Fuel consumption and delay as functions of signal cycle length - Case III

SUMMARY

In this chapter, three cases of numerical experiments: Case I, a two-phase pretimed signal without left turns; Case II, a two-phase pretimed signal with left turns on one approach; and Case III, a three-phase pretimed signal with a protected left-turn phase, are conducted to explore the AFCM estimation capability and to investigate the effect of signal timing on fuel consumption and delay.

In order to establish the model's credibility, results from the AFCM are compared with the TEXAS model. Under the same traffic control measures and traffic characteristics, patterns of elapsed second-by-second fuel consumption along the travel distance are similar from the AFCM and the TEXAS model. The value of correlation coefficients show that second-by-second fuel consumption from the two methods is correlated which indicates that fuel consumption is strongly dependent on instantaneous traffic behavior. Also, total fuel consumption as a function of signal cycle length can be obtained from the numerical analysis. The relationship between fuel consumption and signal cycle length is convex which reveals that the optimal cycle length for fuel consumption minimization is obtainable.

Since the left turn movements on a shared left turn lane with a permitted phase have significant effects on traffic movement, the adjustment factor for left turns is investigated numerically to reflect the effects of left turns on fuel consumption. From the numerical experiments, the best procedure to estimate left-turn factors used in the AFCM is the combination of the procedure in 1985 HCM and the f_m in 1994.

Moreover, the optimal cycle length for fuel consumption minimization is higher than for delay minimization. Since the optimal cycle length for delay minimization is a function of the flow ratio, the optimal cycle length for fuel consumption minimization could also be related to the flow ratio. In the following chapter, the relationship between signal timing and fuel consumption will be discussed in detail.

CHAPTER 7. OPTIMUM CYCLE LENGTHS FOR FUEL CONSUMPTION MINIMIZATION

INTRODUCTION

Through the previous chapters, effects of signal timing on fuel consumption has been examined using hypothetical intersections. Using the AFCM and varying cycle time from 30 to 180 seconds at intervals of 10 seconds, fuel consumption as a function of cycle length was investigated. Since all the functions were convex curves and optimal cycle lengths for fuel consumption minimization could be identified.

However, a simple expression for determining optimal cycle lengths to minimize fuel consumption is strongly desired. The objective of deriving such an expression is very similar to that for delay based optimal cycle time expressions. However, since the types of delay effect fuel consumption differently, optimum cycle lengths for fuel consumption and delay minimization might be different. For instance, idling vehicles (stopped delay) consume fuel at an idle fuel consumption rate, but decelerating vehicles (non-stopped delay) have a different fuel consumption rate.

This chapter describes a simple expression reduced from the AFCM for deriving optimal cycle lengths. The expression includes three terms: the first term describes fuel consumption by stopped vehicles which have idle fuel consumption rates, the second term describes fuel consumption by vehicles accelerating from a stopped status until they pass the stop line, and the third term represents stochastic effects of vehicle movements which consume excess fuel. Section 7.2 discusses the optimal cycle length expression derivation. Section 7.3 tests the expression and compares results to the AFCM. Based on these comparisons, the expression is improved providing more accurate results. A brief summary is given in Section 7.4.

DERIVATION OF EXPRESSIONS FOR OPTIMAL CYCLE LENGTH

The Traffic Engineers Handbook suggests that the ratios of signal phase green time to total green time ($\frac{g_i}{\Sigma g_i}$) should be the same as the corresponding ratios y_i to the sum of y_i ($\frac{y_i}{\Sigma y_i}$), where y_i is the maximum ratio of flow to saturation flow served by the green indication [78]. In deriving an expression for the optimum cycle time for fuel consumption minimization, it is assumed that the effective phase green times have this relationship to their respective y values. For a

particular intersection, optimum conditions are obtained by minimizing the fuel consumption with respect to cycle time. The effect of cycle time on fuel consumption will now be investigated.

From the previous discussions, deriving an expression for optimal cycle time from the original AFCM forms is complicated because the AFCM includes several submodels for three street segments (inbound approach, intersection itself, and outbound leg) in three cycle stages (the effective red time, time from green onset to t_0, and time from t_0 to the end of green). A reduced form which represents critical items for the effect of cycle time on fuel consumption is expressed as:

$$TF = \sum_{i=1}^{n} \{\frac{1}{2} q_i r_i (\frac{r_i}{C}) f_a + \frac{1}{2} q_i r_i (\frac{t0_i}{C}) f_b + \frac{x_i^2}{2(1-x_i)} f_c\} \qquad [7.1]$$

where,

q_i = critical lane flow of phase i,

r_i = effective red time of phase i,

$t0_i$ = time t0 of phase i,

$x_i = q_i C/g_i S$ (degree of approach saturation),

f_a, f_b, and f_c = fuel consumption rates,

n = number of signal phases, and

TF = average fuel consumption for critical lanes during one signal cycle.

The term $1/2[q_i r_i (r_i/C)]$ represents idle fuel consumption, $1/2[q_i r_i (t0_i/C)]$ represents fuel consumption by vehicles accelerating from a stopped condition, and $x_i^2/2(1-x_i)$ represents fuel consumption due to random vehicle arrivals.

Since the green phase durations are proportional to the corresponding ratios of flow to saturation flow (y_i), let $Y = \sum_{i=1}^{n} y_i$ and $k_i = y_i/Y$, then

$$g_i = k_i C - k_i L \qquad [7.2]$$

$$r_i = C - k_i C - k_i L \qquad [7.3]$$

$$y_i = k_i Y \qquad [7.4]$$

$$q_i = k_i s_i Y \qquad [7.5]$$

$$x_i = \frac{q_i C}{g_i S} = y_i \frac{C}{g_i} = \frac{YC}{(C-L)} \qquad [7.6]$$

where L = total lost time for a cycle.

Rearranging Equation 7.1 we have

$$TF = \sum_{i=1}^{n} \{\frac{1}{2}[k_i s_i Y f_a + k_i s_i Y \frac{k_i Y}{1-k_i Y} f_b][\frac{(C-k_i C+k_i L)^2}{C}]+$$

$$\frac{1}{2}\frac{C^2 Y^2}{(C-L)(C-L-CY)} f_c\} \qquad [7.7]$$

Differentiating with respect to the cycle time C gives

$$\frac{dTF}{dC} = \sum_{i=1}^{n} \{\frac{1}{2}[k_i s_i Y f_a + k_i s_i Y \frac{k_i Y}{1-k_i Y} f_b][\frac{2(C-k_i C+k_i L)(1-k_i)}{C} - \frac{(C-k_i C+k_i L)^2}{C^2}]$$

$$+ \frac{1}{2} Y^2 f_c [\frac{2C}{(C-L)(C-L-CY)} - \frac{C^2}{(C-L)^2(C-L-CY)} - \frac{C^2(1-Y)}{(C-L)(C-L-CY)^2}]\} \qquad [7.8]$$

= 0 for minimum fuel consumption.

According to Webster's derivation, the optimal cycle length for delay minimization is approximately equal to twice of the minimum cycle ($2C_m$) [84]. A pre-selected optimum cycle length, $2C_m$, is chosen to simplify the term C-L-CY in Equation 7.8 since this term does not have major effect on the optimum cycle length for fuel consumption minimization. Due to the substitution, a corrected term is developed and discussed in Section 7.3.2. The minimum cycle (C_m) is the shortest cycle which allows all the traffic which arrives in one cycle (assuming uniform flow) to pass through the intersection in the same cycle. It is the sum of the lost time per cycle and the time necessary to pass all traffic through the intersection at the maximum possible rate, i.e.

$$C_m = L + \sum_{i=1}^{n} C_m \frac{q_i}{s_i} \qquad [7.9]$$

where $\frac{q_i}{s_i}$ is the highest ratio of flow to saturation flow for the i^{th} phase. Therefore,

$$C_m = L + C_m \sum_{i=1}^{n} y_i$$

$$= L + C_m Y$$

$$= \frac{L}{1-Y} \qquad [7.10]$$

Since the pre-selected optimum cycle C_o is $2C_m = 2L/(1-Y)$, thus L can be replaced by $C_o(1-Y)/2$ for the term "C-L-CY"; thus,

$$C\text{-}L\text{-}CY = C - \frac{C(1-Y)}{2} - CY = \frac{C(1-Y)}{2} \qquad [7.11]$$

Equation 7.8 can be reduced to

$$\frac{dTF}{dC} = \sum_{i=1}^{n} \{\frac{1}{2}[k_i s_i Y f_a + k_i s_i Y \frac{k_i Y}{1-k_i Y} f_b][\frac{2(C-k_i C+k_i L)(1-k_i)}{C} - \frac{(C-k_i C+k_i L)^2}{C^2}] + \frac{1}{2} Y^2 f_c [\frac{-2C}{(C-L)^2(1-Y)}]\} \quad [7.12]$$

$$= 0$$

Let

$$M = \frac{1}{2}(1\text{-}Y)[k_i s_i Y f_a + k_i s_i Y \frac{k_i Y}{1-k_i Y} f_b] \quad [7.13]$$

$$N = Y^2 f_c \quad [7.14]$$

By multiplying $C^2(C\text{-}L)^2(1\text{-}Y)$ into the above equation, the Equation 7.12 becomes

$$\frac{dTF}{dC} = \sum_{i=1}^{n} \{M[(1-k_i)^2C^4 - (1-k_i)^2LC^3 - NC^3 + (1-2k_i)L^2C^2 + 2k_i^2L^3C - k_i^2L^4]\} \quad [7.15]$$

$$= 0$$

It is obvious that Equation 7.15 is a nonlinear function of a single variable, f(C). It can be solved using one-dimensional optimization methods such as interval reduction and quadratic curve fitting methods. A common and widely used approach to single-dimensional minimization is known as interval reduction including the golden section and the bisection methods. In order to ensure the existence of a finite minimum of f(C) for some C in the interval of interest, it is assumed that C lies within some finite interval [a, b] and that f(C) is continuous and uniquely defined [73]. Detailed procedures and algorithms of one-dimensional optimization methods are described in Chapter 4 of Sheffi's "Urban Transportation Networks". The bisection method is used here to derive the optimal cycle time for fuel consumption minimization.

The bisection method involves iterative procedures in which each iteration is focused on a current interval. Figure 7.1 depicts a flowchart of the bisection method. The input f(C) is Equation 7.15 given the flow rate, saturation flow rate, degree of saturation, lost time, and fuel consumption parameters on phase i. The interval [a, b] is the possible cycle time from 20 to 180 seconds. The optimal cycle time can be obtained using this procedure.

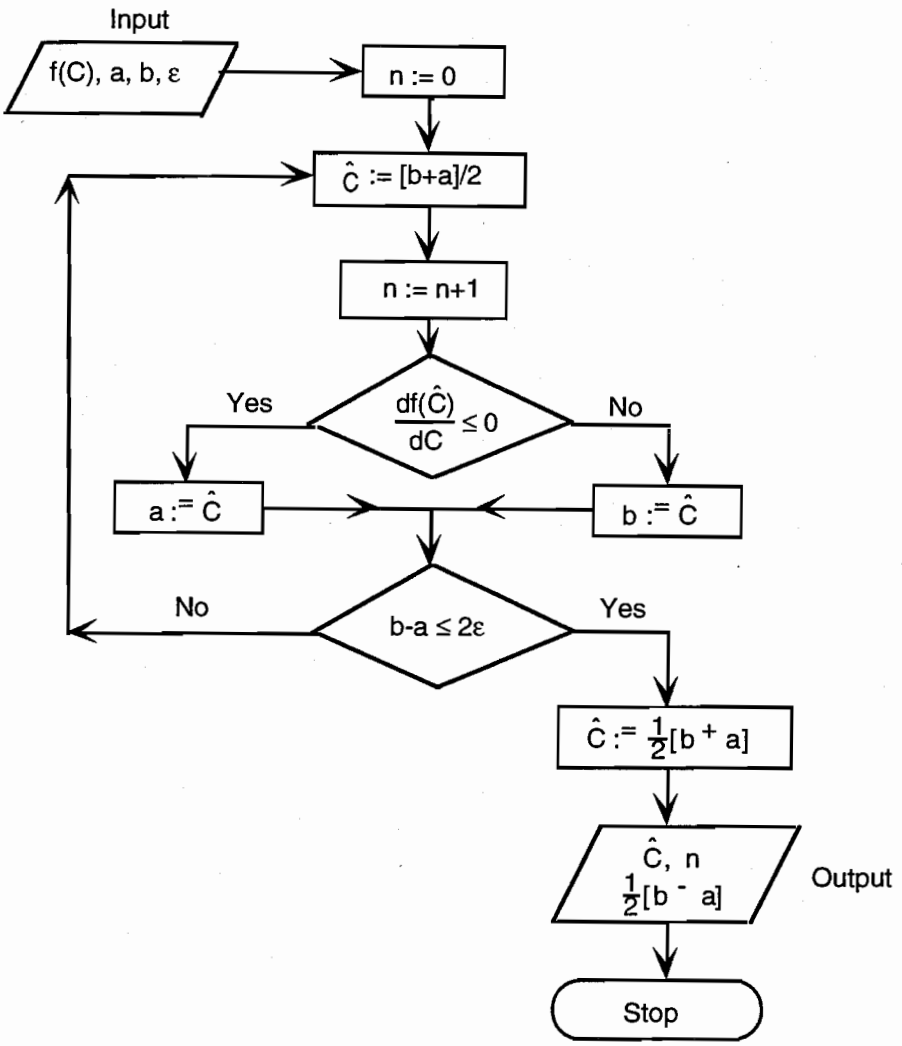

Figure 7.1 Flowchart of the bisection algorithm [73]

NUMERICAL ANALYSIS AND VERIFICATION OF THE EXPRESSIONS

Optimal cycle lengths for fuel consumption minimization can be obtained from expression Equation 7.15 given the flow rate q, saturation flow rate s, and degree of saturation y on each approach, and total lost time L and fuel consumption parameters f_a, f_b, and f_c. The magnitudes of f_a, f_b, and f_c are defined according to the traffic characteristics of the three terms in the expression. Since the first term represents vehicles contributing to idle fuel consumption, the value of f_a is idle fuel consumption rate f_0 (0.3310 grams/second). The value of f_b is equal to f_{02} (0.5 grams/second) because the second term describes the fuel consumption by vehicles

accelerating from stopped status to pass the stop line at speed V_2. The value of f_c is higher than those of f_a and f_b since the third term represents stochastic effects of vehicle movement which consume excess fuel. The value of f_c is assumed to be equal to f_{r2} (0.71 grams/second) which is the average fuel consumption rate for vehicles moving from their desired speed to speed V_2.

Table 7.1 shows the optimal cycle lengths for the case I (described in Chapter 6) by varying flow rates from 300 to 1000 vph on the northbound approach. The optimal cycle lengths from the expression tend to be greater than those from the original AFCM forms.

TABLE 7.1 OPTIMAL CYCLE LENGTHS FROM THE AFCM AND THE OPTIMIZATION EXPRESSION

Flow (veh./hr)		Optimal Cycle Length for Min. Fuel Consumption	
Northbound	Eastbound	From the AFCM (sec.)	From the Optimization Expression (sec.)
300	300	40	71
400	300	50	71
500	300	60	87
600	300	70	108
700	300	90	139
800	300	120	185
900	300	150	259
1000	300	180	xxx*

* The optimal cycle length is beyond plausible limitation.

The optimal cycle lengths from the optimization expression tend to be overestimated due to the reduced forms, the replacement of L by $C_o(1-Y)/2L$ in the third term, and the assumed value of the fuel consumption parameter f_c. Therefore, adjustment factors need to be added to improve the expression.

The Relationship Between Lost Time and Optimal Cycle Length

Equation 7.15 is derived assuming the optimal cycle is approximately equal to twice the minimum cycle, i.e., minimum cycle $C_m = L/(1-Y)$ and optimal cycle $C_o = 2L/(1-Y)$. However, the optimal cycle lengths for fuel consumption minimization are higher than for delay minimization from the previous discussions in Chapter 6. Table 7.2 summarizes the optimal cycle lengths for fuel consumption and delay minimization for various traffic flow rates. One-way street operations with a

two phase pretimed traffic signal and saturation flow rate of 1500 vph for critical lanes are assumed. The average ratio of optimal cycle lengths for fuel consumption minimization to those for delay minimization is close to 1.4; therefore, the optimal cycle C_o is approximately equal to

$$C_o = 2.8L/(1-Y) \qquad [7.16]$$

Equation 7.15 can be modified to give $C_o = 2.8L/(1-Y)$, thus

$$\frac{dTF}{dC} = \sum_{i=1}^{n} \{ M [(1-k_i)^2C^4 - 2(1-k_i)^2LC^3 - \frac{70}{81}NC^3 + (1-2k_i)L^2C^2 - \frac{56}{81}NLC^2 + 2k_i^2L^3C - k_i^2L^4] \} \qquad [7.17]$$

$$= 0$$

The optimal cycle length C_o; therefore, can be obtained using the bisection method to solve

$$\sum_{i=1}^{n} \{ M [(1-k_i)^2C_o^4 - 2(1-k_i)^2LC_o^3 - \frac{70}{81}NC_o^3 + (1-2k_i)L^2C_o^2 - \frac{56}{81}NLC_o^2 + 2k_i^2L^3C_o - k_i^2L^4] \}$$

$$= \quad 0 \qquad [7.18]$$

TABLE 7.2 OPTIMAL CYCLE LENGTHS FOR FUEL CONSUMPTION AND DELAY MINIMIZATION FROM VARIOUS TRAFFIC FLOW RATES

Flow Phase I (veh/hr)	Phase II (veh/hr)	Optimal Cycle Length for Min. Fuel Consumption From AFCM A (seconds)	Delay B (seconds)	Ratio A/B
200	200	30	27	1.10
300	200	40	30	1.33
400	200	50	33	1.50
500	200	60	38	1.60
600	200	70	43	1.63
700	200	80	50	1.59
800	200	100	60	1.66
900	200	130	76	1.72
300	300	40	33	1.21
400	300	50	38	1.32
500	300	60	43	1.40
600	300	70	50	1.40
700	300	90	60	1.50
800	300	120	75	1.60
900	300	150	101	1.49
400	400	60	43	1.40
500	400	70	50	1.40
600	400	80	60	1.33
700	400	110	75	1.47
800	400	140	101	1.39
500	500	80	60	1.33
600	500	100	75	1.33
700	500	130	101	1.29
600	600	130	101	1.29

Table 7.1 is updated using Equation 7.18 and the results are shown in Table 7.3. The optimal cycle lengths are closer to those from the original AFCM comparing with Table 7.1; however, they are underestimated. Especially, the differences become larger as the flow rate increases. Since the expression has already been reduced, a possible way to improve the optimal cycle length estimates is to correct the estimates using an adjustment factor, and the discussion is described as follows.

TABLE 7.3 OPTIMAL CYCLE LENGTHS FROM THE AFCM AND THE OPTIMIZATION EXPRESSION (AFTER THE MODIFICATION OF RELATIONSHIP BETWEEN LOST TIME AND OPTIMAL CYCLE)

Flow (veh./hr)		Optimal Cycle Length for Min. Fuel Consumption	
Northbound	Eastbound	From the AFCM (sec.)	From the Optimization Expression (sec.)
200	300	40	38
300	300	40	41
400	300	50	46
500	300	60	54
600	300	70	64
700	300	90	78
800	300	110	99
900	300	150	131
1000	300	180*	180*

* The maximum optimal cycle length.

Optimal Cycle Length Correction Term

Since the optimal cycle lengths from the optimization expression are underestimated, a correction term needs to be added. The correction term is obtained using regression analysis, and the tentatively entertained regression model is

$$Co_{AFCM} - Co = \alpha + \beta \prod_{i=1}^{n} k_i Y \qquad i \neq j \qquad [7.19]$$

where Co_{AFCM} is the optimal cycle length from the original AFCM form, and Co is the optimal cycle length from Equation 7.18. Thus, the corrected optimal cycle length can be approximately equal to:

$$Co_{corrected} = Co + (\alpha + \beta \prod_{i=1}^{n} k_i Y) \qquad [7.20]$$

From regression analysis, α and β are -4 and 202, respectively and the adjusted R^2 value is 0.72, i.e.,

$$Co_{corrected} = Co - 4 + 202 \prod_{i=1}^{n} k_i Y \ (R^2 = 0.72) \qquad [7.21]$$

Table 7.4 shows optimal cycle lengths from the AFCM and the corrected optimization expression. It indicates the corrected optimal cycle lengths are more accurate and compared to the AFCM the corrected results are within 10%.

TABLE 7.4 OPTIMAL CYCLE LENGTHS FROM THE AFCM AND THE CORRECTED OPTIMIZATION EXPRESSION

Flow (veh./hr)		Optimal Cycle Length for Min. Fuel Consumption	
Northbound	Eastbound	From the AFCM (sec.)	From Corrected Results of the Optimization Expression (sec.)
200	300	40	43
300	300	45	46
400	300	50	53
500	300	60	62
600	300	70	75
700	300	90	93
800	300	110	119
900	300	150	160
1000	300	180*	180*

* The maximum optimal cycle length.

In order to examine the sensitivity of the corrected optimization expression to traffic flow rates for Case I (described in Chapter 6), optimal cycle lengths were computed using AFCM, the original and corrected estimation expressions, and the results are shown in Table 7.5. Although there are differences between the AFCM results and the corrected expression, magnitudes of the differences are less than 10%. Practically, the corrected expression is appropriate for deriving optimal cycle lengths, and is rather simple and precise compared to the original AFCM form.

TABLE 7.5 OPTIMAL CYCLE LENGTHS FROM THE AFCM AND THE CORRECTED OPTIMIZATION EXPRESSION FOR VARIOUS TRAFFIC FLOW RATES

Flow		Optimal Cycle Length for Min. Fuel Consumption		
Phase I (veh/hr)	Phase II (veh/hr)	From the AFCM (second)	From the Optimization Expression (second)	Corrected Results For the Optimal Cycle Length (second)
200	200	31	33	33
300	200	38	38	39
400	200	46	45	48
500	200	57	54	59
600	200	66	66	73
700	200	84	82	91
800	200	103	103	113
900	200	130	134	146
1000	200	180*	180*	180*
300	300	44	41	45
400	300	51	46	53
500	300	61	54	63
600	300	74	64	76
700	300	90	78	93
800	300	116	99	117
900	300	155	131	151
1000	300	180*	180*	180*
400	400	59	50	60
500	400	70	58	72
600	400	84	68	86
700	400	111	84	105
800	400	143	109	134
900	400	180*	158	180*
500	500	83	66	84
600	500	108	78	101
700	500	138	100	127
600	600	136	97	125
700	600	161	135	169
700	700	180*	180*	180*

* The maximum optimal cycle length.

SUMMARY

This chapter presents development of a simplified fuel consumption based signal timing relationship. The simple form is reduced from the AFCM described in previous chapters, and it describes the major effects of vehicle characteristics, traffic behavior, and fuel consumption parameters on optimal cycle length. The expression includes three terms: the first term represents fuel consumed by stopped vehicles which have idle fuel consumption, the second term describes the fuel quantity consumed by vehicles accelerating after stopping, and the third term represents stochastic fuel consumption effects of vehicle movements which consume excess fuel. The expression is:

$$TF = \sum_{i=1}^{n} \{\frac{1}{2} q_i r_i (\frac{r_i}{C}) f_a + \frac{1}{2} q_i r_i (\frac{t0_i}{C}) f_b + \frac{x_i^2}{2(1-x_i)} f_c\}$$

The term $1/2[q_i r_i \ (r_i/C)]$ represents idle fuel consumption, $1/2[q_i r_i (t0_i/C)]$ represents fuel consumption by vehicles accelerating from a stopped condition, and $x_i^2/2(1-x_i)$ represents fuel consumption due to random vehicle arrivals.

In order to derive the expression for optimal cycle lengths, they are assumed to be equal to 2.8L/(1-Y) and a correction term is added improving the expression. The test results and the comparisons between the original AFCM form and the expression indicate that optimal cycle lengths from the expression are very close to those from the AFCM. Under this scenario, optimal cycle lengths for fuel consumption minimization can be easily estimated using the simplified expression.

The expression is appropriate for deriving the optimal cycle lengths for intersection fuel consumption minimization; however, the original AFCM described in Chapter 4 is needed for the total intersection fuel consumption estimation.

CHAPTER 8. CONCLUSION

This chapter presents concluding comments on this research and suggests future research directions. Overall conclusions are summarized and discussed in Section 8.1. Section 8.2 presents the author's perspective on the contributions of various aspects of the work to the state of the art of fuel consumption modeling in urban areas. Section 8.3 discusses future avenues and directions for research in this area.

OVERALL CONCLUSIONS

This section first presents general conclusions, followed by a more detailed summary of conclusions from the research undertaken in this research.

The objectives of this research are to develop a fuel consumption model for signalized intersections, and to explore the effects of signal timing on fuel consumption. In order to achieve these objectives, a conceptual framework, which considers interrelationships among several elements, including three major elements traffic characteristics, signal control strategies, and roadway geometric conditions, are proposed. Based on these processes, a fuel consumption model, AFCM, is developed for estimating fuel consumption in the intersection influence area. This is the first attempt to tackle the problem by considering the three elements simultaneously.

The AFCM, permitting application in undersaturated and oversaturated traffic conditions, includes basic model development and model extensions considering queue probability and overflow queues. The AFCM describes different vehicle operating conditions consuming fuel on the inbound approach, the intersection itself, and the outbound leg for three signal cycle stages (the effective red time, queue discharge green time t_0, and time from t_0 to the effective green time end). The basic model development assumes that vehicle arrivals are uniform and deterministic, and the model extension has included stochastic effects and overflow conditions. The overflow conditions have major impacts on fuel consumption for the inbound approach. The analysis of queue probability and overflow queues proposed by Cronje has been applied to characterize queue probability and overflow queue sizes in the AFCM [33, 34, 35].

As previously mentioned, the AFCM aims to analyze impacts of three elements: traffic characteristics, signal control strategies, and roadway geometric configurations. Traffic characteristics such as traffic flow rates, vehicle movements, and overflow queues have major impacts on fuel consumption. Pretimed signal control is assumed, and fuel consumption is affected by signal cycle time and green split. Geometric configurations are basic elements in describing the conditions of the intersection influence area. The three elements, therefore, are

investigated comprehensively by conducting experimental, data collection, and numerical tests to enrich the AFCM capability.

Experimental data collection is conducted to develop vehicle speed, acceleration/deceleration profile models which are then used to establish fuel consumption profile models and associated parameters. Data was collected by videotaping traffic on the Congress Avenue between 1st Street and Barton Springs Blvd. in Austin, TX. Vehicle speed and acceleration/deceleration rates, calibrated from the data reduction and analysis, are used to establish speed and acceleration/deceleration profile models. The speed, acceleration/deceleration profile models are polynomials of elapsed cycle time which satisfy the real traffic conditions that acceleration rate is zero at the start and end of acceleration. From the speed, acceleration/deceleration profile models, and corresponding fuel consumption data obtained from USEPA which describe fuel consumption in terms of vehicle speed and acceleration/deceleration rates, fuel consumption profile models are calibrated to capture fuel consumption behavior in the intersection influence area. The acceleration fuel consumption profile model is a function of vehicle speed and acceleration, and the deceleration profile model is a function of vehicle speed. Since speed and acceleration/deceleration profile models are functions of elapsed cycle time, and fuel consumption profile models are functions of speed and acceleration, the cumulative fuel consumption models are functions of elapsed cycle time. Therefore, average vehicular fuel consumption rates are estimated from cumulative fuel consumption differences divided by elapsed travel time.

The objective of deriving average fuel consumption rates integrated into the three major AFCM elements is to develop an aggregate fuel consumption model which is at least as good as instantaneous models and can estimate fuel consumption in a simple and broad way. The average fuel consumption rates are then included as AFCM fuel consumption parameters.

The AFCM is implemented and tested through hypothetical intersection configurations, various traffic conditions, and signal cycle times to explore AFCM estimation capability and to investigate the effects of signal timing on fuel consumption. Results from the AFCM are compared with the results from the TEXAS model. The comparisons show that elapsed fuel consumption from the two models are highly correlated and that the elapsed fuel consumption estimated from the AFCM provides representative trajectories of fuel consumption variation along the intersection influence area. Moreover, total fuel consumption can be represented as a convex function of signal cycle time, revealing that the optimal cycle length is obtainable for fuel consumption minimization.

In addition, numerical experiments are conducted to compare optimal cycle lengths for fuel consumption and delay minimization. Various cases are analyzed and compared, indicating optimal cycle lengths for fuel consumption minimization are generally higher than for delay minimization.

Through these experiments, it has been shown that signal timing could be optimized by minimizing fuel consumption. Due to the complicated forms of the AFCM, a simple form reduced from the AFCM is used to derive an expression to estimate optimal cycle lengths. The reduced form describes the major effects of vehicle characteristics, traffic behavior, and fuel consumption parameters on optimal cycle length. It includes three terms: the first term represents stopped vehicles with idle fuel consumption rates, the second term describes fuel consumption for vehicles accelerating from a stop, and the third term represents stochastic effects of vehicle movements which consume excess fuel. The test results and the comparisons between the original AFCM form and the streamlined expression indicate that optimal cycle lengths from the expression are rather close to those from the AFCM. Optimal cycle lengths for fuel consumption minimization can be easily predicting using the reduced form.

RESEARCH CONTRIBUTIONS

The most significant contribution of this research is development of the analytical fuel consumption model AFCM. Unlike traditional fuel consumption models, the AFCM integrates traffic characteristics, signal control strategies, and roadway geometric configurations. In addition, the AFCM allows the specification of randomness of vehicle arrivals and overflow queues, which are important factors in describing traffic characteristics and vehicle movement.

Another significant contribution is the derivation of an expression for optimal cycle time based on fuel consumption minimization. The derived expression, reduced from the original AFCM form and simplified using certain assumptions, represents one of the first attempts at developing fuel consumption based optimal signal timing methodology. The resulting simple expression is applied and tested, and the results indicate close agreement with optimal cycle lengths determined numerically using the AFCM.

Another contribution is identifying vehicle speed, acceleration, and deceleration profile models, based on field experiments. These models, corresponding to USEPA fuel consumption test specifications, are used to investigate fuel consumption trajectories, develop cumulative fuel consumption models, and derive fuel consumption parameters. The derived fuel consumption parameters are empirically applied to the AFCM, and the AFCM is successfully implemented.

FUTURE RESEARCH

One of the most difficult problems associated with the AFCM is trying to determine whether it is a reasonable approximation of the actual system being studied. The model presented in this research includes several elements that might need more validation from field experiments, especially determination of fuel consumption rates and application at different types of intersections.

The AFCM fuel consumption parameters might be not suitable for some cases. Further research may improve the AFCM by obtaining extensive field fuel consumption data to estimate more general values of fuel consumption parameters. Moreover, the adjustment factor for fuel consumption effects of left turns needs more investigation.

In addition, since the AFCM is an aggregate fuel consumption model, and the trajectories of vehicles and fuel consumption along the intersection segments are continuous and have similar patterns at neighboring intersections, the AFCM could be extended to be a general model in predicting fuel consumption for an arterial street or a network. While arterial or network-wide aggregate estimation provides more information for evaluating traffic system management objectives, advanced development of the AFCM is recommended.

REFERENCES

1. A Policy on Geometric Design of Highways and Streets (1990). American Association of State Highway and Transportation Offices, Washington, D.C.
2. Akcelik, R. (1981). "Fuel Efficiency and Other Objectives in Traffic System Management", Traffic Engineering and Control, Vol. 22, pp. 54-65.
3. Akcelik, R., Bayley, C., Bowyer, D.P. and Biggs, D.C. (1983). "A Hierarchy of Vehicle Fuel Consumption Models", Traffic Engineering and Control, Vol. 24, No. 10, pp. 491-495.
4. Akcelik, R. and Biggs, D.C. (1987). "Acceleration Profile Models for Vehicles in Road Traffic", Transportation Science, Vol. 21, No. 1, Feb. 1987, pp. 36-54.
5. Akcelik, R. (1980). Time-Dependent Expressions for Delay, Stop Rate and Queue Length at Traffic Signals. Internal Report AIR 367-1, Australian Road Research Board, Nunawadig.
6. Akcelik, R. And Rouphail, N.M. (1994). "Overflow Queues and Delays with Random and Platooned Arrivals at Signalized Intersections", Journal of Advanced Transportation, Vol. 28, No. 3, pp. 227-251.
7. Al-Khalili, A.J. (1985)."The Optimum Green Split of a Cycle Time", 1985 IEEE Transactions on Systems, Man, and Cybernetics, Vol. SMC-15, No. 15, September/October 1985.
8. Al-Khalili, A.J. and El-Hakeem, A.K. (1984). "Computer Control System for Minimization of Fuel Consumption in Urban Traffic Network", IEEE, New York, NY. USA Available from IEEE Service Cent, Piscataway, NJ, USA pp. 249-254.
9. Al-Omishy, H.K., Fayad, E.M. and Ibrahim, R.R. (1993). "The Influence of Various Factors on the Fuel Consumption of Petrol-Powered Vehicles Using a Computer-Simulation Model", Energy, Vol. 18, No. 1, pp. 63-68, 1993.
10. Ang, B.W. and Oh, S.T. (1988). "Transport and Traffic Management Schemes and Energy Saving in Singapore", Energy, Vol. 13, No. 2, pp. 141-148, 1988.
11. Ang, B.W., Fwa, T.F. and Poh, C.K. (1991)."A Statistical Study on Automobile Fuel Consumption", Energy, Vol. 16, No. 8, pp. 1067-1077, 1991.
12. Ang, B.W., NG, T.T. and Fwa, T.F. (1992). "A Factorization Analysis of Automobile Fuel Consumption in Actual Traffic", Energy, Vol. 17, No. 7, pp. 629-634.
13. Badin, F. and Maillard, P. (1990). "Forecasting by Simulation of a Passenger Car Consumption", Proceedings - Society of Automotive Engineers, SAE, Warrendale, PA, USA, pp. 823-835.

14. Bauer, C.S. (1975). "Some Energy Considerations in Traffic Signal Timing", Traffic Engineering, 45(2), pp. 19-25.

15. Bayley, C. (1980). "Energy Implications of Co-ordinated Traffic Signals", Australian Road Research, Vol. 10, No. 2, pp. 16-24, 1980.

16. Bester, C. J. (1981). "Fuel Consumption on Congested Freeways", Transportation Research Record, No. 801, pp. 51-54.

17. Bester, C.J. (1984). "Effect of Pavement Type and Condition on the Fuel Consumption of Vehicles", Transportation Research Record, No. 1000, pp. 28-32.

18. Biggs, D.C. (1988). ARFCOM - Models for Estimating Light to Heavy Vehicle Fuel Consumption, Australian Road Research Board, Research Report ARR No. 152, September, 1988.

19. Biggs, D.C. and Akcelik, R. (1985). Further Work on Modelling Car Fuel Consumption, Australian Road Research Board, Internal Report AIR 390-10, 1985.

20. Biggs, D.C. and Akcelik, R. (1986). "Estimation of Car Fuel Consumption", Proceedings of 13th Australian Road Research Board / 5th Road Engineering Association of Asia and Australasia Conference, Part 7, August 1986, pp. 123-132.

21. Biggs, D.C. and Akcelik, R. (1986). "Models for Estimation of Car Fuel Consumption in Urban Traffic", ITE Journal, Vol. 56, No. 7, July 1986, pp. 29-32.

22. Biggs, D.C. and Akcelik, R. (1987). "Estimating Effect of Vehicle Characteristics on Fuel Consumption", Journal of Transportation Engineering, Vol. 113, No. 1, January, 1987.

23. Bowyer, D.P., Akcelik, R. and Biggs, D.C. (1985). Guide to Fuel Consumption Analyses for Urban Traffic Management, Special Report, SR No. 32, Nunawading, Victoria, Australia: Australian Road Research Board, 1985.

24. Bowyer, D.P., Akcelik, R. and Biggs, D.C. (1986). "Fuel Consumption Analyses for Urban Traffic Management", ITE Journal, Vol. 56, No. 12, December 1986, pp. 31-34.

25. Bowyer, D.P.and Biggs, D.C. (1987). Towards More Fuel Efficient Control Practices at Isolated Urban Intersections, Research Report ARR 147, Australian Road Research Board.

26. Brohard, T. (1986). "Signal Improvements Save Time and Fuel", Public Works, Vol. 117, No. 2, February 1986, pp. 52-53.

27. Chang, M.F. and Herman, R. (1980). "Driver Response to Different Driving Instructions: Effect on Speed, Acceleration and Fuel Consumption", Traffic Engineering and Control, 21, 545.

28. Chang, M.F. and Herman, R. (1981). "Trip Time Versus Stop Time and Fuel Consumption Characteristics in Cities", Transportation Science, Vol. 15, No. 3, pp. 183- 209.

29. Chang, M.F., Evans, L., Herman, R. and Wasielewski, P. (1976). "Gasoline Consumption in Urban Traffic", Transportation Research Record, No. 599, pp. 25-30.

30. Chang, M.F., Evans, L., Herman, R. and Wasielewski, P. (1977). "Observations of Fuel Savings due to the Introduction of Right-Turn-On-Red", Traffic Engineering and Control, Vol. 18, No. 2, pp. 475-477.

31. Cohen, S.L. and Euler, G. (1978). "Signal Cycle Length and Fuel Consumption and Emissions", Transportation Research Record, No 667, pp. 41-48.

32. Courage, K.G. and Parapar, S.M. (1975). "Delay and Fuel Consumption at Traffic Signals", Traffic Engineering, 45(11), pp. 23-27.

33. Cronje, W.B. (1983). "Analysis of Existing Formulas for Delay, Overflow and Stops", Transportation Research Record 905, Transportation Research Board, Washington, D.C.

34. Cronje, W.B. (1983). "Derivation of Equations for Queue Length, Stops and Delay for Fixed-Time Traffic Signals", Transportation Research Record 905, Transportation Research Board, Washington, D.C.

35. Cronje, W.B. (1983). "Optimization Model for Isolated Signalized Traffic Intersections", Transportation Research Record 905, Transportation Research Board, Washington, D.C.

36. Cronje, W.B. (1986). "Comparative Analysis of Models for Estimating Delay for Oversaturated Conditions at Fixed-Time Traffic Signals", Transportation Research Record 1091, Transportation Research Board, Washington.

37. Davis, S.C. and Strang, S.G. (1994). Transportation Energy Data Book: Edition 14, ORNL-6798, Oak Ridge National Laboratory, Oak Ridge, Tennessee.

38. DeCicco, J.M. (1995). "Projected Fuel Savings and Emissions Reductions from Light-Vehicle Fuel Economy Standards", Transportation Research - A, Vol. 29A, No. 3, pp. 205-228.

39. DeLuchi, M., Greene, D., and Wang, Q. (1993). Motor-Vehicle Fuel-Economy: the Forgotten Hydrocarbon Control Strategy? Research Report UCD-ITS-RR-93-3, Institute of Transportation Studies, Univ. Of California Davis, Davis, California.

40. Evans, L. (1978). "Urban Traffic, Fuel Economy and Emissions - Consistency of Various Measurements", Soc. Auto. Eng. SAE Tech. Paper No. 780934.

41. Evans, L. and Herman, R. (1978). "Automobile Fuel Economy on Fixed Urban Driving Schedules", Transportation Science, Vol. 12, No. 2, pp. 137-152.

42. Evans, L. and Herman, R. (1978). "Urban Fuel Economy: An Alternate Interpretation of Recent Computer Simulation Calculations", Transportation Research, Vol. 12, pp. 163-165.

43. Evans, L., Herman, R. and Lam, T. (1976). "Gasoline Consumption in Urban Traffic", Society of Automotive Engineers, SAE Paper 760048, 1976.

44. Evans, L., Herman, R. and Lam, T. (1976). "Multivariate Analysis of Traffic Factors Related to Fuel Consumption in Urban Driving", Transportation Science, Vol. 10, No. 2, pp. 205-215.

45. Evans, Leonard and Herman, R. (1977). "A Simplified Approach to Calculations of Fuel Consumption in Urban Traffic Systems", Traffic Engineering Control 17 (8. 9), pp. 352-354.

46. Everall, P.F. (1968). The Effect of Road and Traffic Conditions on Fuel Consumption, Ministry of Transport, RRL Report LR226.

47. Fwa, T.F. and Ang, B.W. (1992). "Estimating Automobile Fuel Consumption in Urban Traffic", Transportation Research Record, No. 1366, pp. 3-10.

48. Gassmann, S. (1990). "Influence of Driver, Vehicle and Traffic on Fuel Consumption in Real Urban Traffic", Proceedings - Society of Automotive Engineers, Published by SAE, Warrendale, PA, USA, pp. 811-815.

49. Greene, D.L. (1993). "Transportation and Energy: the Global Environmental Challenge", Transportation Research - A, Vol. 27A, No. 3, pp. 163-166.

50. Haskew, Harold, Cullen, Kevin, Liberty, Thomas F., and Langhorst, William K. (1995). The Execution of a Cooperative Industry/Government Exhaust Emission Test Program, General Motors Powertrain Group, 1995.

51. Herman, R. and Ardekani, S. (1985). "The Influence of Stops on Vehicle Fuel Consumption in Urban Traffic", Transportation Science, Vol. 19, No. 1, pp. 1-12.

52. Herman, R., Rule, R.G., and Hackson, M.W. (1978). "Fuel Economy and Exhaust Emissions Under Two Conditions of Traffic Smoothness", Passenger Car Meeting, Troy Hilton, Troy, Michigan, June 5-9, 1978, SAE Paper No. 780614.

53. Highway Capacity Manual (1985). Special Report 209, Transportation Research Board, National Research Council, Washington, D.C.

54. Highway Capacity Manual (1994). Transportation Research Board, National Research Council, Washington, D.C.

55. Hippel, F.V. (1987). "Automobile fuel Economy", Energy, Vol. 12, No. 10/11, pp. 1063-1071, 1987.

56. Johns, L.S. and Blair, P.D. (1991). Improving Automobile Fuel Economy: New Standard, New Approaches, U.S. Congress, Office of Technology Assessment, OTA-E-504 (Washington, DC: U.S. Government Printing Office).

57. Lam, T.N. (1985). "Estimating Fuel Consumption from Engine Size", Journal of Transportation Engineering, V. 111, No. TE4, July, 1985, pp. 339-357.

58. Lee, F.P., Lee, C.E., Machemehl, R.B., and Copeland, C.R. (1983). Simulation of Vehicle Emissions at Intersections, research report 250-1, Center for Transportation Research, the University of Texas at Austin.

59. Luk, J.Y.K. and Akcelik, R. (1984). "Predicting Area Traffic Control Performance with Transyt/8 and an Elemental Model of Fuel Consumption", Proceedings - Conference of the Australian Road Research Board, Vol. 12, Part 4, pp. 87-101, 1984.

60. Matsuura, Y. and Liu, X. (1985). "Improvement of Fuel Consumption by Controlled Passage Through Traffic Signals", Proceedings - Society of Automotive Engineers, pp. 45-56, 1985.

61. Messenger, G.S., Richardson, D.B., Graefe, P.W.U. and Mufti, I.H. (1980). Urban Traffic Signal Control for Fuel Economy, Mechanical Engineering Report ME-247, January 1980, National Research Council, Canada.

62. Moore, S.E. and Nairn, R.J. (1982). "An Analysis of Fuel Consumption Models", Proceedings of the Joint SAE-A/AARB Second Conference on Traffic, Energy and Emissions, Melbourne, Australia, May 19-21, 1982.

63. Myers, P.S. (1992). "Reducing Transportation Fuel Consumption - How Far Should We Go?", Proceedings - Society of Automotive Engineers, Published by SAE, Warrendale, PA, USA, pp. 225-234, 1992.

64. Newell, G.F. (1989). Theory of Highway Traffic Signals, Course Notes UCB-ITS-CN-89-1, Institute of Transportation Studies, University of California at Berkeley, Chapter 2.

65. Newman, P.W.G. and Kenworthy, J.R. (1988). "The Transport Energy Trade-off: Fuel-Efficient Traffic Versus Fuel-Efficient Cities", Transportation Research - A, Vol. 22A, No. 3, May 1988, pp. 163-174.

66. Olszewski, P.S. (1990). "Modelling of Queue Probability Distribution at Traffic Signals", Proc 11th International Symposium on Transportation and Traffic Theory.

67. Pelensky, E., Blunden, W.R., Munro, R.D. (1968). "Operating Costs of Cars in Urban Areas", Proceedings of Fourth Conference of the Australian Road Research Board, Vol. 4, Part 1, pp. 475-504, 1968

68. Pienaar, W.J. (1982). "Car Fuel Consumption Under Urban Travel Conditions", Civil Engr. S. Afr. 24, pp. 309-314.

69. Pitt, D.R. Lyons, T.J., Newman, P.W.G. and Kenworthy, J.R. (1987). "Fuel Consumption Models: An Evaluation Based on a Study of Perth's Traffic Patterns", Traffic Engineering and Control, Vol. 28, No. 2, pp. 60-68.

70. Polanis, S.F. (1984). "Signal Coordination and Fuel Efficiency: Winston-Salem's Experience", Transportation Quarterly, Vol. 38, April 1984.

71. Post, K., Kent, J.H., Tomlin, J. and Carruthers, N. (1984). "Fuel Consumption and Emission Modelling by Power Demand and a Comparison with Other Models", Transportation Research - A, Vol. 18A, No. 3, pp. 191-213.

72. Reljic, S., Kamhi-Barna, M. and Stojanovic, S. (1992). "Multicriteria Signal Plan Choice at an Isolated Intersection", Mathematics in Transport Planning and Control (Institute of Mathematics & its Applications Conference Series 38), 1992, pp. 81-93.

73. Sheffi, Y. (1985). Urban Transportation Network: Equilibrium Analysis with Mathematical Programming Methods, Prentice-Hall, Inc., Englewood Cliffs, New Jersey.

74. Site, P.D. and Filippi, F. (1995). "Bus Service Optimization and Car Pricing Policies to Save Fuel in Urban Areas", Transportation Research A, Vol. 29A, No. 5, pp. 345-358.

75. Taylor, M.A.P. and Young, T.M. (1993). "A Macro for Analysing Fuel Consumption and Travel Time Data", Road and Transport Research, Vol. 2, No. 3, pp. 62-69.

76. Taylor, M.A.P. and Young, T.M. (1996). "Fuel Consumption and Emissions Models for Traffic Engineering and Transport Planning Applications: Some New Results", Proceedings of 18th Australian Road Research Board Conference, Part 6, pp. 189-204.

77. Taylor, M.A.P. and Young, T.M. (1996). "Developing a Set of Fuel Consumption and Emissions Models for Use in Traffic Network Modelling", Proceedings of 13th International Symposium on Transportation and Traffic Theory, Lyon, pp. 289-314.

78. Transportation and Traffic Engineering Handbook (1982). 2nd Edition, ITE, Prentice-Hall., Englewood Cliffs, New Jersey.

79. TRANSYT-7F User's Manual, USDOT, FHWA, Washington, D.C.

80. Velikanov, D.P., Stavrov, O.A. and Zamyatin, M.L. (1987). "Energy Conservation in Transportation", Energy, Vol. 12, No. 10/11, pp. 1047-1055, 1987.

81. Watanatada, T. and Harral, C.G. (1987). The Highway Design and Maintenance Standards Model, Vol. 1, the John Hopkins University Press, Baltimore, Maryland.

82. Watson, H.C., Milkins, E.E. and Marshall, G.A. (1979). "Controlling Traffic Flow for Minimum Energy Consumption and Emissions", Transportation Conference 1979, The national Committee on Transportation of the Institution of Engineers, Australia.

83. Watson, H.C., Milkins, E.E. and Marshall, G.A. (1980). "A Simplified Method for Quantifying Fuel Consumption of Vehicles in Urban Traffic", SAE-Aust 40(1), pp. 6-13.

84. Webster, F. V. (1958). Traffic Signal Setting, Road Research Technical Paper No. 39, Her Majesty's Stationery Office, London.

85. Wilson, S.C. and Smith, R.L. (1988). "Impact of Urban Development Alternatives on Transportation Fuel Consumption", Transportation Research Record 1155, pp. 1-11.

86. Wortman, R.H. and Fox, T.C. (1994). "An Evaluation of Vehicle Deceleration Profiles", Journal of Advanced Transportation, Vol. 28, No. 3, pp. 203-215.